Spring 2014

Selected durability studies of geopolymer concrete with respect to carbonation, elevated temperature, and microbial induced corrosion

Mohammad Sufian Badar
Louisiana Tech University

SELECTED DURABILITY STUDIES OF GEOPOLYMER

CONCRETE WITH RESPECT TO CARBONATION,

ELEVATED TEMPERATURE, AND

MICROBIAL INDUCED

CORROSION

by

Mohammad Sufian Badar, B.Sc., M.Sc., M.S.

A Dissertation Presented in Partial Fulfillment
of the Requirements for the Degree
Doctor of Philosophy

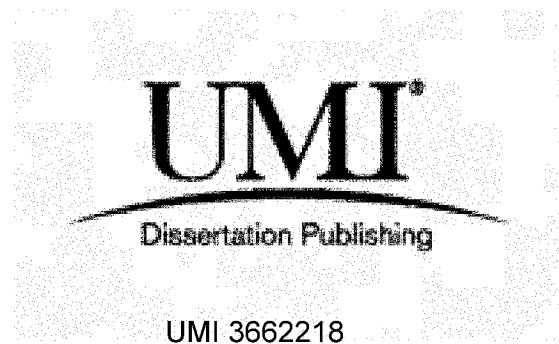COLLEGE OF ENGINEERING AND SCIENCE
LOUISIANA TECH UNIVERSITY

May 2014

UMI Number: 3662218

UMI

Dissertation Publishing

UMI 3662218

ProQuest

LOUISIANA TECH UNIVERSITY

THE GRADUATE SCHOOL

JANUARY 21, 2014
_____
Date

We hereby recommend that the thesis prepared under our supervision

by___Mohammad Sufian Badar, M.S._____

entitled_____

SELECTED DURABILITY STUDIES OF GEOPOLYMER CONCRETE

WITH RESPECT TO CARBONATION, ELEVATED TEMPERATURE,

AND MICROBIAL INDUCED CORROSION

_____

be accepted in partial fulfillment of the requirements for the Degree of

Doctor of Philosophy

_____
Supervisor of Thesis Research

_____
Head of Department

Civil Engineering
_____
Department

Recommendation concurred in:

_____

_____

_____   Advisory Committee

_____

Approved: Approved:

_____   _____
Director of Graduate Studies   Dean of the Graduate School
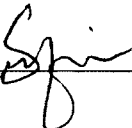
_____
Dean of the College

APPROVAL FOR SCHOLARLY DISSEMINATION

The author grants to the Prescott Memorial Library of Louisiana Tech University the right to reproduce, by appropriate methods, upon request, any or all portions of this Thesis. It is understood that "proper request" consists of the agreement, on the part of the requesting party, that said reproduction is for his personal use and that subsequent reproduction will not occur without written approval of the author of this Thesis. Further, any portions of the Thesis used in books, papers, and other works must be appropriately referenced to this Thesis.

Finally, the author of this Thesis reserves the right to publish freely, in the literature, at any time, any or all portions of this Thesis.

Author _____

Date _01/21/2014_____

DEDICATION

This dissertation is lovingly dedicated to my mother (late Nurunnisa), father (late Mohd. Badre Alam), wife (Rana Kamal Sufian), daughters (Sarah and Aisha), and my brothers and sister. Their support, encouragement, guidance, and constant love have sustained me throughout my life.

TABLE OF CONTENTS

LIST OF TABLES

LIST OF FIGURES

ACKNOWLEDGMENTS

First and foremost, I would like to praise and thank Allah SWT, the almighty, who has granted me countless blessings, knowledge, and opportunities so that I can complete my Ph.D. This duration of the degree program has completely changed my thinking, approach, personality and created a stronger belief that all of this was possible with his help.

It gives me great pleasure to express my deep sense of gratitude to Dr. Erez Allouche, Associate Professor of Civil Engineering, Director of the Alternative Cementitious Binders Laboratory (ACBL), College of Engineering and Science, and Louisiana Tech University for giving me wonderful opportunities to work under his competent guidance and supervision in the emerging area of new cementitious binder, Geopolymer Concrete (GPC). I am highly grateful to him for providing all necessary facilities, continuous encouragement, full cooperation, invaluable guidance, and the freedom he has allowed me all throughout my Ph.D. tenure.

I would like to thank Dr. Kunal Kupwade-Patil who encouraged and helped me during the entire period of the Ph.D. program. I would also like to thank Dr. Carlos Montes, Dr. Shaurav Alam, and all colleagues of the South campus. I really appreciate the help and guidance provided by my advisory committee members Dr. Sven Eklund, Dr. Patrick Hindmarsh, Dr. David Mills, Dr. Naziuddin Wasiuddin, and the late Dr. Robert McKim.

My friends at the Islamic Center of North Louisiana, Dr. Ali Darrat's family, Mr. Awan Malik's family, Mr. Nasri El-Awadi's family, Dr. Jawed, Dr. Arfa, Dr. Wajihuddin, Ahmed, Assad, Zain, Dr. Elshad, Ehsan, and Hatwib for all their great support during these five years. They were with me emotionally, socially, and financially all the time. Their

ABSTRACT

This thesis reports a comprehensive study related to the experimental evaluation of carbonation in reinforced geopolymer concrete, the evaluation of geopolymer concretes at elevated temperature, and the resistance of geopolymer concrete to microbial induced corrosion (MIC).

Carbonation: Reinforced concretes, made of geopolymer, prepared from two class F fly ashes and one class C fly ash, were subjected to accelerated carbonation treatment for a period of 450 days. Electrochemical, microstructure and pore structure examinations were performed to evaluate the effect of corrosion caused due to carbonation. GPC specimens prepared from class F fly ash exhibited lower corrosion rates by a factor of 21, and higher pH values (pH>12) when compared with concrete specimens prepared from class C Fly ash (GPC-MN). Microstructure and pore characterization of GPC prepared using class F fly ash revealed lower porosity by a factor of 2.5 as compared with thier counterparts made using GPC-MN. The superior performace of GPC prepared with the class F fly ash could be attributed to the dense pore structure and formation of the protective layer of calcium and sodium alumino silicate hydrates (C/N-A-S-H) geopolymeric gels around the steel reinforcement.

Elevated Temperature: Geopolymers are an emerging class of cementitious binders which possess a potential for high temperature resistance that could possibly be utilized in applications such as nozzles, aspirators and refractory linings. This study reports on the results of an investigation into the performance of a fly ash based geopolymer binder in high

temperature environments. Geopolymer concrete (GPC) was prepared using eleven types of fly ashes obtained from four countries. High content alumina and silica sand was used in the mix for preparing GPC. GPC was subjected to thermal shock tests following ASTM C 1100-88. The GPC samples prepared with tabular alumina were kept at 1093° C and immediately quenched in water. GPC specimens prepared with certain fly ashes exhibited signs of expansion along with cracking and spalling, while GPC prepared with specific class F fly ash showed superior resistance to thermal shock. Microstructural analysis revealed that the resistance of GPC at elevated temperatures was dependent on the type of fly ash used, its particle size distribution, formation of zeolitic phases such as sodalite, analcime and nepheline, and the overall pore structure of the geopolymer concrete. The work indicates that the chemical composition and particle size distribution of the fly ash, type of fly ash (Class C & F) and the geopolymerization process that took place a vital role in the performance of geopolymer concretes in high temperature applications.

Microbial Induced Corrosion: Corrosion is a major form of deterioration in concrete structures. According to a report published by the U.S. FHWA 2002, the cost of corrosion in water and wastewater conveyance, and storage and treatment facilities in the U.S. is about $138 billions.

A main form of corrosion in wastewater collection systems is Microbial Induced Corrosion (MIC). However, the conditions present in industrial or municipal wastewater pipes, or storage facility are induced by the production of sulfuric acid by biological processes, which cannot be fully mimicked by simple acid corrosion.

The present study intends to provide similar conditions inside pipe specimens that mimic a true sewer atmosphere. The experimental setup consisted of three 12" diameter and 30" long concrete pipe specimens, 2 specimens were coated with different formulations of

GPC while the third was a control. Both ends of each pipe specimen were sealed to prevent hydrogen sulfide gas from escaping. One pipe was coated with GPC that had a biocide agent entrained. Another pipe specimen was coated with OPC and the 3rd pipe was used as a control and was not coated.

Parameters measured can be divided into three groups: general environmental parameters like pH and temperature: pH is measured at regular intervals. Substrates and products that include Chemical Oxygen Demand (COD) and sulfide concentrations: COD is measured using the Hach Method (APHA, 5220D).Temperature (65 - 70° F) and humidity (50 - 60%) were maintained throughout the experiment. Sulfide concentration was measured by the methylene blue method (APHA, 4500-S-2D). Bacterial count was measured by Spectrophotometer (APHA, 9215B).

In addition, the thickness of the slime layer was measured and the end of the 16-week test. Test data revealed that the use of the antibacteria agent has initial input on the rate of pH reduction, but that effect were out after 6 weeks, The slime lyer band on the wall of the geopolymer coated pipes was to be 1/4 of that found on the non-coated pipe, suggesting the geopolymer matrices provide a less suitable substrate for sulfate reducing bacteria (Desulfovibrio desulfuricans) compound with a standard OPC substate.

CHAPTER 1

INTRODUCTION

Geopolymer concrete is an emerging class of cementitious binder, which exhibits superior chemical and mechanical properties such as higher mechanical strength along with minimum energy consumption and negligible carbon footprint [1–3]. The field of geopolymer cements provides various scientific challenges in terms of understanding its durability mechanisms at the microstructural level when subjected to severe environments.

This study deals with durability evaluation of geopolymer concrete for elevated temperature resistance, carbonation, and microbial induced corrosion. The aim of this investigation was to analyze the chemical resistance of geopolymer concrete when subjected to various durability tests, followed by chemical, microstructure and pore structure analysis.

1.1 Problem

Ordinary Portland cement has been known for 150 years, and the durability mechanisms of OPC's such as resistance to chemicals, sulfates, sulfate reducing bacteria, and CO_2 were extensively studied [4,5]. The shortcoming of OPC based cements led to the introduction of alternative cementitious binders.

The growing demand for concretes with higher performance, lower cost and reduced environmental impact when compared to those produced with conventional Portland cements has promoted the development of clinker-free alternative cementitious materials including alkali-activated cements, also referred to as geopolymers, whose use can contribute to the reduction of the carbon footprint of construction projects [2]. Geopolymer binders are

1

produced via the chemical reaction of a reactive aluminosilicate source, mainly fly ash derived from the coal burning process, with an alkaline activator, to produce a hardened monolith that can develop high mechanical strength [1–3]. This reaction can result in the formation of zeolite type phases along with a highly disordered aluminosilicate geopolymer gel [69].

Geopolymer concretes are an emerging class of cementitious "green" binders. Although this family of cementitious binder has been known for nearly 25 years, their durability mechanisms at a microstructure level are not completely understood. This lack of knowledge has hindered researchers and practitioners from predicting the service life of structures constructed using geopolymer binders. The current study examines three durability mechanisms with environments with an emphasis on changes of the micro-structural levels. Figure 1.1 shows the major problems in different types of cements.
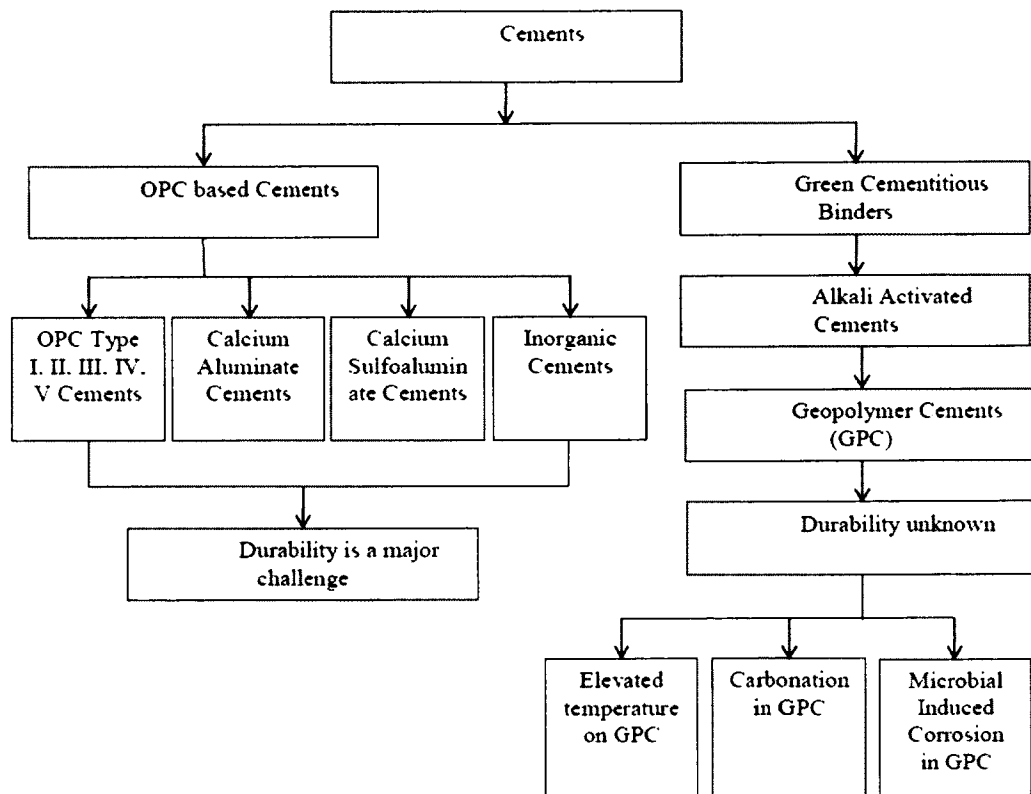
Figure 1.1: Graphical representation of the problem statement guiding this work.

1.2 Objective

The objective of this study was to investigate selected durability mechanisms of GPC when subjected to carbonation, high temperature, and microbial induced corrosion. Extensive microstructural analysis was conducted using Scanning Electron Microscopy (SEM), Fourier Transform Infrared Spectroscopy (FTIR), X-Ray Diffraction (XRD), and Energy dispersive X-ray fluorescence (ED-XRF). Pore structure studies were examined via Mercury Intrusion Porosimetry (MIP), and X-Ray microtomography (X-Ray μCT). Electrochemical studies were performed using half-cell potential method and the corrosion rates were measured using linear polarization resistance (LPR) method.

Analytical analysis was performed to measure the growth of bacteria. Temperature, and humidity were maintained to optimize the concentration of bacteria. This aspect of the study was used to evaluate the durability resistance of geopolymer when subjected to microbial induced corrosion. Figure 1.2 shows the durability mechanism of geopolymer concrete.
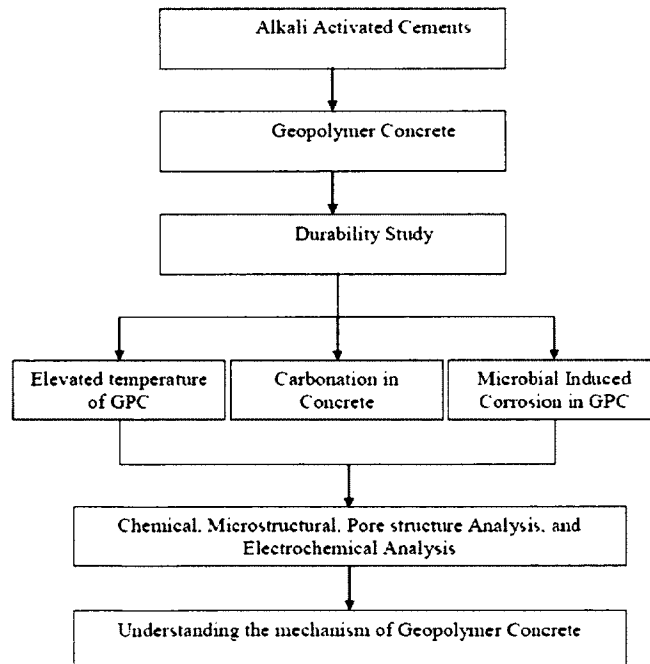
Figure 1.2: Approach for the analysis of the durability mechanisms of geopolymer concretes.

1.3 Approach

Durability mechanism of GPC at the microstructural level was examined when subjected to carbonation, elevated temperature resistance and microbial induced corrosion. GPC specimens prepared with silica sand and alumina as a filler were subjected to thermoshock resistance. Specimens were subjected to 2000° F and immediately quenched and analyzed for mechanical failure as well as microstructural damages. In addition, reinforced GPC specimens were exposed to carbonation and compared with the untreated controls. Electrochemical measurements (corrosion potential and corrosion rates) were taken during the entire duration of the study (450 days). This was followed by chemical, microstructure and pore structure studies in order to examine the effect of carbonation on reinforced geopolymer concretes.

In addition, we examined GPC to determine the influence of microbial induced corrosion. MIC was evaluated in terms of bacterial growth. Substrates and products including Chemical Oxygen Demand (COD), sulfate and sulfide concentrations were considered periodically. COD was measured using the Hach Method (APHA, 5220D). Sulfate content was measured by liquid chromatography (ASTM D4327-03) and sulfide concentration was measured by the methylene blue method (APHA, 4500-S-2D). Bacterial counts were measured by spectrophotometer (APHA, 9215B).

1.4 Overview

Chapter two provides a literature review of the durability mechanisms of geopolymer concretes. In addition, this section also deals with the fundamentals of geopolymer technology, synthesis, characterization, and mix design of geopolymer concretes, followed by various durability studies such as alkali silica reaction, sulfates, chloride attack, and the effect of elevated temperature on geopolymer concretes. Chapters three, four and five present the

experimental procedure, results, and discussion of carbonation, elevated temperature, and microbial induced corrosion of the geopolymer concretes. This thesis consists of a compodium of several technical papers by the author, which are published or accepted for publications. These are listed in Table 1.1.

Table 1.1: List of publications incorporated into the dissertation.

Section	Title	Publication	Place/Year
3.1	Evaluation of Geopolymer Concretes at Elevated Temperature	37th International and exposition on advanced ceramics and composites, American Ceramic Society	Daytona Beach, FL/ 2013
3.2	Selected studies on durability of geopolymer concrete	ASTM, Special Technical Publication (STP 1566) Geopolymer binder systems	San Diego, CA, 2012
3.3	Resistance of Geopolymer to Microbial Induced Corrosion	113th General Meeting, American Society of Microbiology, 2013	Denver, CO, 2013
3.4	The Evaluation of Geopolymer Concrete against Microbial Induced Corrosion (MIC	UCT (Underground Construction Technology) 2014	Houston, TX, Jan. 28 – 30, 2014

CHAPTER 2

BACKGROUND

2.1 Ordinary Portland Cement

Portland cements are hydraulic cements composed primarily of hydraulic calcium silicates [4, 6]. Portland cement is prepared mainly from limestone and clay. It is heated in a kiln between 2550 to 2900° F, thus allowing the raw materials to interact and form calcium silicates. To maintain the quality of cement with maximum utilization of heat and low CO_2 emission, special care is taken at different stages of processing. The quality of the cement also depends on the purity of raw materials, clay, one of the raw materials, is mostly composed of oxides of aluminum and silicon. The primary source of silica is iron-bearing aluminosilicates [7, 8]. Silica, derived from aluminosilicates, provide limited contribution to the strength of the cement [7]. It is a major concern in terms of durability and setting time. Pure silica is found abundantly in quartz. However, it is not commonly used due to its unreactive form, and more importantly, a mixture of lime and silica has high fusion temperatures (>3600° F). Due to high temperature, the mixture can only react at a slow process called sintering. Aluminum and iron oxide are used to lower the fusion temperature. To maintain the need amount of SiO_2 and Fe_2O_3, quartz and iron oxides are added in small quantities. Table 2.1 designates the different constituents of oxides of different metals and non-metals. Table 2.2 describes the hydration reaction and its different products. Table 2.3 lists the different hydration products of OPC.

6

Table 2.1: Constituents of cement [7].

Oxide	Standard symbol	Abbreviated symbol
Aluminum oxide	Al_2O_3	A
Calcium oxide	CaO	C
Carbon dioxide	CO_2	$\bar{C}$
Iron oxide	Fe_2O_3	F
Calcium fluoride	CaF_2	$\bar{F}$
Water	H_2O	H
Potassium oxide	K_2O	K
Magnesium oxide	MgO	M
Sodium oxide	Na_2O	N
Phosphorous oxide	P_2O_5	P
Silicon oxide	SiO_2	S
Sulfur oxide	SO_3	$\bar{S}$
Titanium oxide	TiO_2	T

Table 2.2: Hydration reactions of Portland (Oxide Notation) [7].

$2(3Cao.SiO_2)$ Tricalcium silicate	$+11H_2O$	$=3CaO.2SiO_2.8$ H_2O Calcium silicate hydrate (C-S-H)	$+(CaO.H_2O)$ Calcium hydroxide
$2(2Cao.SiO_2)$ Dicalcium silicate	$+9H_2O$	$=3CaO.2SiO_2.8$ H_2O Calcium silicate hydrate (C-S-H)	$+CaO.H_2O$ Calcium hydroxide
$3Cao.Al_2O_3)$ Tricalcium aluminate	$+3(CaO.SO_3.2H_2O)$ Gypsum	$+26H_2O$	$=6CaO.Al_2O_3.3SO_3.3$ $2H_2O$ Ettringite
$2(3Cao.Al_2O_3)$ Tricalcium aluminate	$+6CaO.Al_2O_3.3SO_3.3$ $2H_2O$ Ettringite	$+4H_2O$	$=3(4CaO.Al_2O_3.SO_3.1$ $2H_2O$ Calcium monosulfoaluminate
$3Cao.Al_2O_3$ Tricalcium aluminate	$+CaO.H_2O$ Calcium hydroxide	$+12H_2O$	$=4CaO.Al_2O_3.13H_2O$ Tetracalcium aluminate hydrate
$4Cao.Al_2O_3.Fe$ $_2O_3$ Tetracalcium aluminoferrite	$+10H_2O$	$+2(CaO.H_2O)$ Calcium hydroxide	$=6CaO.Al_2O_3.$ $Fe_2O_3.12H_2O$ Calcium aluminoferrite hydrate

Table 2.3: Hydration products of Portland cement [7].

Name of compound	Oxide composition	Abbreviation
Tricalcium silicate	$3CaO.SiO_2$	C_3S
Dicalcium silicate	$2CaO.SiO_2$	C_2S
Tricalcium aluminate	$3CaO.Al_2O_3$	C_3A
Tetracalcium aluminoferrite	$4CaO.Al_2O_3.Fe_2O_3$	C_4AF

2.2 Types of Portland Cement

Type I is used for general construction purposes. Type II is used when moderate sulfate resistance is desired. It can be used against sulfate attack since C_3A (tricalcium aluminate) content is limited. This type of cement can also be used when moderate heat of hydration is desired. Type III can be used when high early strength is desired. It is chemically similar to Type I, except the particles have been grounded finer. It can be used in cold weather conditions also. Type IV containing a higher percentage of C_2S is used when low heat of hydration is needed. It develops strength at a slower rate compared with other cement types and used in mass concrete structures, such as large gravity dams. Type V is used when high sulfate resistance is required. The specification calls for a maximum of 5% on C_3A to be applied when subjected to sulfate rich environments. A hydration product of cements with more than 5% C_3A, contains monosulfate hydrate which is unstable when exposed to a sulfate solution.

Conversion of monosulfate to ettringite is generally associated with expansion and cracking. Type V cements, like other Portland cements, is not resistant to acids and other highly corrosive substances. Concrete durability has been defined by the American Concrete Institute as its resistance to weathering action, chemical attack, abrasion, and other degradation processes [9]. Deterioration of concrete is usually caused by chemical, and

mechanical damage. The physical causes include freezing and thawing, wetting and drying along with the extreme changes that could influence the concrete. The chemical agents that deteriorate concrete, are leached and efflorescence, susceptible to sulfate attack, alkali-silica reaction, and corrosion of concrete. The external chemical attack includes the ingress of carbon dioxide and other natural or industrial liquids and gases. The degradation of the concrete matrix decreases the service life of concrete structures and may lead to catastrophic failure [1].

The lack of sufficient durability of OPC structures has led to the development of alternative cementitious binders. These binders were introduced targeting specific durability applications, such as sulfate resisting cements and refractory cements. Common alternative cements used by the industry are calcium sulfoaluminate cements, calcium aluminate cements, artificial and natural pozzolan cements, composite cements, and alkali activated cements. A large number of alternative cementitious binders have been available for some of time, yet they have not been extensively used due to limited durability data, workalability issues and cost implications.

2.2.1 Calcium Aluminate Cement (CAC)

Calcium aluminate cements are manufactured from limestone or bauxite with low SiO_2. It has unique properties like early strength, and elevated sulfate resistance. It is used in preparing refractory materials due to its high temperature resistance. The setting time of CACs could be increased by mixing it with Portland cement. It has a relatively high heat of hydration, which is useful for low-temperature application. To optimize its strength and durability, it is essential to maintain certain conditions like a low ratio of w/c (<0.4), higher cement content in the concrete (400 Kgm^{-3}), and no alkaline contaminants [13]. Table 2.4 shows the composition of calcium aluminate cements

Table 2.4: Typical compositions of calcium aluminate cements (mass percentage) [7].

Type of cement	Al_2O_3	CaO	Fe_2O_3 +FeO	FeO	SiO_2	TiO_2	MgO	K_2O+ Na_2O	SO_3
Ciment Fondu	38-40	37-39	15-18	3-6	3-5	2-4	<1.5	<0.4	<0.2
40% Alumina	40-45	42-48	<10	<5	5-8	~2	<1.5	<0.4	<0.2
50% Alumina	49-55	34-39	<3.5	<1.5	4-6	~2	~1	<0.4	<0.3
50% Al_2O_3 (low Fe)	50-55	36-38	<2	<1	4-6	~2	~1	<0.4	<0.3
70% Alumina	69-72	27-29	<0.3	<0.2	<0.8	<0.1	<0.3	<0.5	<0.3
80% Alumina	79-82	17-20	<0.25	<0.2	<0.4	<0.1	<0.2	<0.7	<0.2

The ideal temperature for the setting time of CACs is in the range of 25-30° C. The length of the induction period is directly related to the C/A ratio in the solution. The duration of the setting time is 6-12 hours if the ratio is 1.06. However, it sets fast if the ratio is more than 1.2. The hydration reaction of CACs accelerared with an increase in temperature. Also, it depends on the time of mixing when it starts setting in the mixer, it also causes the formation of progressive thickening [13].

Formation of CAH_{10} from CA increases the volume by more than 3.64. However, the porosity increase and the compressive strength decrease. CACs are more resistant to a sulfate attack, to sea water, and to an acid solution provided pH is more than 4. Resistance is increased until pH 3 if the newly formed salt is of low solubility. The low w/c ratio increases the resistance of CACs. This is due to a blockage of ingress of chlorides, sulfate ions, and other aggressive species. Alkaline hydrolysis, which is a combination of CO_2 and alkali, is detrimental to hydrated calcium aluminates and the hydrous alumina [13].

2.2.2 Calcium Sulfoaluminate Cement (CSA)

Calcium sulfoaluminate cement was developed in China in the 1970s by the China Building Materials Academy. The objective was to develop self-stressed concrete pipes by utilizing the expansive nature of the cement. It is produced by the mixing gypsum into a

clinker. The optimum setting time and strength are achieved by adding 15 to 25% by weight of gypsum. CSA is a low-CO_2 emission cement compared to the Portland cement. CSA requires only 1200 to 1300° C temperature to produce a clinker, while the Portland cement clinker needs 1400 to 1500° C. Compared to Portland cement, CSA needs a low limestone and fuel consumption, which facilitates a significantly low CO_2 emission. However, the SO_2 emissions are higher. The product of CSA after hydration is:

$$C_4A_3 + 2C\bar{S}H_2 + 34H \longrightarrow C_3AS_3H_{32} + 2AH \tag{2.1}$$

$$C_4A_3S + 8C\bar{S}H_2 + 6CH_2 + 74H \longrightarrow 3C_3AS_3H_{32} + 2AH. \tag{2.2}$$
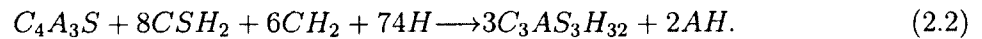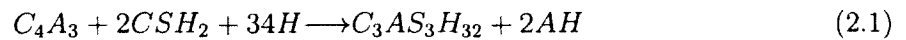
The ettringite is formed in reaction 1, which expands the structure. To exploit this expansiveness, it is used as a shrinkage-resistant and self-stressing cement [14, 15]. Ettringite is formed in the presence of lime and helps in gaining early strength if it is not expansive [16].

The rapid hardening of this cement increases impermeability and chemical resistance. However, it decreases drying shrinkage and alkalinity. The impact is minimal on performance even in very hot and dry environments. However, this cement is sensitive to temperature and water/cement ratios. The setting time of the non-retarded calcium sulfoaluminate cement (CSA) concrete in the summer time (27-29° C) is 5 min with the water/cement ratio of 0.35. It can be increased up to 15-20 min with the suitable retarder. The pH of CSA is 10.5-11, while the pH of Portland cement is 13, which makes the latter up to 300 times more alkaline. The low alkalinity of CSA hinders the onset of the alkali silica reaction (ASR). The raw material of CSA is bauxite (oxide/hydroxide of Al, Fe), limestone, and gypsum. The scientists are trying to replace this cement with the industrial waste and byproduct of the blast furnace slag and fly ash. The replacement of costly raw materials by by-product, like fly ash, is the challenging objective.

2.3 Alkaline Cements

Kuhl was the first scientist in 1930 to use these cementitious binders, which are called alkaline cements. He studied the setting behavior of alkali cements by adding KOH into the powder mixture of slag. To date, extensive research has been done to find out how much alkalis play a role in preparing this type of cement. Pardon, in 1940, did an extensive laboratory test on clinkerless cements, which is prepared from slag and NaOH [9]. Another breakthrough came in 1967 from Glukhovsky with the development of new binders from the low calcium or calcium-free aluminosilicate (clay) and the hydroxide of alkali metals [10]. He called the new binders "soil cements" and the corresponding concretes, "soil silicates". He divided the binders based on the composition of the precursor materials: alkaline binding systems ($Me_2OAl_2O_3SiO_2H_2O$) and alkali-alkaline earth binding systems ($Me_2O\text{-}MOAl_2O_3SiO_2H_2O$) (where Me=Na, K, and M=Ca, Mg). Alkali-alkaline-earth binding systems were the earlier focus with Scandinavian F-cements [11–13] and alkali activated cements have been examples of products that come out of this research [14–18].

A significant amount of research related to the first group of Glukhovsky work has been done over the last ten years. Another breakthrough came in 1982, when Davidovits produced binders by mixing alkalis into kaolinite, limestone, and dolomite, and he called the binders a "geopolymer". The gradually increased knowledge of alkali activated cements and concretes has an enormous potential impact in terms of low energy consumption, low carbon footprint, and higher mechanical strength and durability [10–12, 14–27]. Extensive research is currently being done on alkaline cements [28].

2.3.1 Classification of Alkali-activated Cements

The two main components are the cementitious component and the alkaline activator. The hydroxide of sodium or potassium is generally used as an alkaline activator. Industry by-products, waste material, and a number of aluminosilicate raw materials have been used

as cementitious binder in alkali activated cements. These materials are fly ash from the coal and the petroleum industry, slag, metakaolin, zeolite, and a non-ferrous slag. Based on the composition of alkali activated cementitious components, alkaline cement has been classified into different categories.

2.4 Alkali-activated Slag-based Cements

The following components are included in this class:

a) Alkali-activated blast furnace slag cement;

b) Alkali-activated phosphorus slag cement;

c) Alkali-activated blast furnace slag-fly ash;

d) Alkali-activated blast furnace slag-steel slag;

e) Alkali-activated blast furnace slag-MGO, and;

f) Alkali-activated blast furnace slag-based multiple component cement.

Alkali-activated blast furnace slag cement was studied in the 1980s and 1990s. The specific findings were:

a) The performance is directly related to the type of slag and the type and amount of the activator solution used. If it is designed based on a specific requirement, it exhibits better strength and enhancement in other properties compared with Portland cement based concrete.

b) The porosity of alkali-activated mortars and paste depends upon the type and the amount of the activator solution used.

c) The alkali activated slag cement and concrete are less permeable to water and chlorides in moist conditions, while it is more resistant to acids, sulfates, and chlorides than traditional Portland cement concretes.

d) The carbonation rate of alkali activated slag concrete for old carbonated concrete blends

is acceptable [29]. However, it shows expansive properties when it is mixed with alkali-reactive aggregate. In terms of workability and setting time, commercial water reducers or superplasticisers have minimal or no effect on alkali-activated slag cement and the concrete.

e) The reaction product of alkali activated slag cement and concrete is C-S-H gel with Al in its structure, and there is no $Ca(OH)_2$. Consequently, fire resistivity is higher in alkali activated slag paste concrete than conventional cement. The ratio of Ca/Si and amount of Al depends on the type of activator solution, as well as the duration and temperature of the curing.

2.5 Alkali-activated Pozzolan Cements

In the early 1960s, Glukhovsky discovered the binders, which he called "soil cements"by mixing an activated solution into aluminosilicate materials, which he later called "geocements" [10]. Later, Davidovits called this binder a "geopolymer" [30]. Other commonly used names include hydroceramics and inorganic polymers. Alkali-activated pozzolan cements are classified into several categories:

a) Alkali-activated fly ash cement,

b) Alkali-activated natural pozzolan ash cement,

c) Alkali-activated metakaolin cement, and

d) Alkali-activated soda lime glass cement.

Many papers were published in the last decade on the alkali-activated aluminosilicate cement, with significant focus on alkali-activated fly ash cement and alkali-activated metakaolin cement.

2.6 Alkali-activated Lime-pozzolan/Slag Cements

Lime-pozzolan is one of the oldest building materials. It was invented in the Neolithic period (7,000 BC), and people came to know it by uncovering concrete slabs in southern Galilee. Lime and lime pozzolan were used to construct aqueducts and arch bridges [31]. In

Iceland, stone buildings were made using mortars. These mortars, prepared from lime and volcanic ash, were strong and durable, and the useful life of these structures was reported to be 90 to 400 years [32]

The invention of Portland cement has drastically reduced the consumption of this cement due to its early high-strength and fast-setting time. However, it is still used in some applications due to low cost and higher durability. The strength and the setting time of lime-pozzolan cements can be improved by mixing with alkali activators or alkali sulfates. These cements include: alkali-activated lime-natural pozzolan cement, alkali-activated lime-fly ash cement, alkali-activated lime-metakaolin cement, and alkali-activated lime-blast furnace slag cement. The main reaction product of alkali-activated lime-pozzolan is C-A-S-H gel. It also forms C-S-H and N-A-S-H gels in high alkaline environments. It has been shown that C-S-H and N-A-S-H gels are well-suited in alkali-activated lime-metakaolin mixtures.

2.7 Alkali-activated Calcium Aluminate Blended Cement

Aluminosilicate materials are activated by alkalis, provided that certain conditions are met:

i) solubility should be high in the media, and

ii) high availability of Al_2O_3 and SiO_2 in the medium. The source of alumina is calcium aluminate cement, which is used in the alkali activation of aluminosilicates. Blends of aluminosilicates with CACs include, Alkali-activated metakaolin/CAC, Alkali-activated pozzolan/CAC, and Alkali-activated fly ash/CAC.

2.8 Alkaline Activation of Aluminosilicates.

The alkaline activation of aluminosilicate materials is basically a mixture of liquid (hydroxide and silicate of sodium or potassium) and a solid (compound of alumina and silica) [33–38]. The liquid-to-solid ratio varies between 0.2 to 1.0, depending on the fineness of the

material. Finer materials need more liquid due to their high-surface area. The resulting mixture sets like Portland cement [35–38]. It can be described in the polymeric model, as with certain zeolites. First, alumina and silica react with the alkali-activator solution to form poly-hydroxy-silicoaluminate complexes [35–38]. Glukhovsky divides the alkaline activation of aluminosilicate material into three stages.

2.8.1 First Stage: "destruction-coagulation"

The hydroxide ion(OH^-) attack and rapture the bond of Si-O-Si, Al-O-Al, Al-O-Si. Glukhovsky believed that the destruction of the solid phase is influenced by the formation of unstable products. Disaggregation lies in the center and is driven by the accumulation of alkaline metals. Due to this, electronic density is redistributed near the silicon atom, by which Si-O-Si bond ruptures more easily. The alkaline metal neutralizes the medium and forms Si-O-Na$^+$, which hinders the backward reaction. These Si-O-Na$^+$ complexes are stable in alkaline media, which help in transporting the structural units and form the coagulated structure. Hydroxyl groups, present on the gel surface, have the same effect on the Al-O-Si bond. Aluminates form a complex structure, Al(OH)$_4$- or Al(OH)$_3$-, based on the pH of the media.

2.8.2 Second Stage: "coagulation-condensation"

The disaggregated products are accumulated and formed a coagulated structure, which led to the formation of a polycondensation reaction. The rate of the polycondensation reaction is dependent on the state of the dissolved ions and the conditions for the presence of alumina and silica required for gel precipitation. Desegregation of the products and condensation of silicic acid depends on the pH. The disaggregation of the Si-O-Si bond produces Si(OH)$_4$ hydroxylated complexes.

2.8.3 Third Stage: "condensation-crystallisation"

The precipitation of particles takes place in the presence of particles from the solid phase, followed by microparticles, which are produced from the condensation reaction. The qualitative and quantitative composition of the crystalline phase is determined by the nature of the alkali metals, the hardening conditions, and the mineralogical condition of the coagulated structure. Fernandez-Jimenez and Palomo offered a model based on MAS-NMR and FTIR findings for the microstructural development of aluminosilicate materials. The model describes the alkaline activation of the aluminosilicate in different stages, which is consistent with Glukhovsky's original model.

2.9 History of Geopolymer Technology

According to Roy [39], ancient binders were produced by a combination of calcined clays with slaked lime. Lime based binder mixtures were used long before the 6th millennium, BC. In ancient times, between 12,000 and 5,000 BC, a terrazzo floor was found in eastern Turkey and, interestingly, the binder was lime mortar. This kind of flooring in a fisherman's huts found in Serbia-Montenegro was dated to 5,600 BC. This type of binder was also found in the Galilei area (Israel) when Malinowsky reported ancient constructions from 7,000 BC and the walls in Britain, to protect the wall from moisture, especially in bathrooms and walls of low lying areas [40, 41].

Lea and Bogue commented that many ancient structures lasted for thousands of years due to the strength of the mortars, like the triumphal arches of the Emperors Claudius and Trajan in Ostia or the bridges of Fabricus and others [42, 43]. The Russian scientist Glukhovsky and his co-workers investigated the binders used in ancient Roman and Egyptian constructions and claimed these are composed of aluminosilicate calcium hydrates [44]. The ancient binder was also used in the valley of the Jodan River [45-47, 47]. Campbell and Folk

suggested that zeolitic compounds produced the mechanical strength and durability of ancient

binders [48]. Ancient Pozzolanic cements are also alkali activated [49,50]. Table 2.5 describes

the history of development of alkali-activated binders.

Table 2.5: Bibliographic history of selected milestones in the development of alkali-activated binders [Adapted from 29].

Author	Year	Significance
Feret	1939	Slags used for cement
Purdon	1940	Alkali-slag combinations
Glukhovsky	1959	Theoretical basis and development of alkaline cements
Glukhovsky	1965	First called "alkaline cements"
Davidovits	1979	"Geopolymer" term
Malinowski	1979	Ancient aqueducts characterized
Forss	1983	F-cement (slag-alkali superplasticizer)
Langton e Roy	1984	Ancient building materials characterized
Davidovits e Sawyer	1985	Patent of "Pyrament" cement
Krivenko	1986	D. Sc Thesis, R_2O-RO-SiO_2-H_2O
Malolepsy e Petri	1986	Activation of synthetic melilite slags
Malek. Et al.	1986	Slag cement-low level radioactive wastes forms
Davidovits	1987	Ancient and modern concretes compared
Deja and Malolepsy	1989	Resistance to chlorides shown
Kaushal et al.	1989	Adiabatic cured nuclear wastes forms from alkaline mixtures
Roy and Langton	1989	Ancient concretes analogs
Majundar et al.	1989	$C_{12}A_7$-slag activation
Talling and Brandstetr	1989	Alkali-activated slag
Wu et al.	1990	Activation of slag cement
Roy et al.	1991	Rapid setting alkali-activated cements
Roy and Silsbee	1992	Alkali-activated cements: an overview
Palomo and Glasser	1992	CBC with metakaolin
Roy and Malek	1993	Slag cement
Glukhovsky	1994	Ancient, modern and future concretes
Krivenko	1994	Alkaline cements
Wang and Scrivener	1995	Slag and alkali-activated microstructure

Purdon described the input of alkali-activated binders in the 1940's, and their potential

applications in the construction industry. He used blast furnace slag activated with sodium

hydroxide and described it as a two-step process. First, silica, aluminum and calcium

hydroxides are liberated. In the next step, formation of silica and alumina molecular structure

takes place with the regeneration of the alkali solution. He concluded that the alkali hydroxide

acted as a catalyst and that the amount of leaching alkali hydroxide is the same as that existing

in the original mixture.

Feret built on the initial work by mixing blast furnace slag with Portland cement rather than alkali-activated binders. Glukhovsky developed new types of binders called "soil cement". He used the word soil because the binder looks like soil obtained from aluminosilicate (raw material) mixed with alkali hydroxide. Initially, he thought the purpose of this soil was to increase the stability and strength when it was added to the Portland cement.

In the 1970s, a French scientist Joseph Davidovits developed and patented binders based on focusing on the alkali activation of metakaolin [51]. He named the new binder Geopolymer. Davidovits argued that pyramids were made by the adjustment of the process used by the Romans and Egyptians. The pyramids were not made by natural stone, but rather by man-made binders. He stated in his research based on chemical and mineralogical studies that blocks of the pyramids were made of a mixture of limestone sand, calcium hydroxide, sodium carbonate, and water. Based on his investigations, blocks of the pyramids are not made of calcium fozzilized layers, which occur in natural stones, but are oriented in a random manner, as found in an artificial binder. He concluded that the major crystalline phase is calcium carbonate as observed by XRD diffraction patterns of specimens collected.

Davidovits defined the empirical formula of the geopolymer. The aluminosilicate binder is mixed with an alkaline solution of sodium or potassium to produce geopolymers. Al-Si minerals present in the binders yield Si-O-Al-O bonds. The composition of the geopolymer depends on the ratio of Si/Al. The fundamental structure is defined by $Mn[-(Si-O_2)_z-Al-O]n.wH_2O$, where n is the degree of polymerization, and z is the ratio of Si/Al, M is either sodium or potassium. Based on this ratio, these bonds are formed: poly(sialate), poly(sialate-siloxo), and poly(sialate-disiloxo) for z = 1, 2, 3, respectively [52].

2.10 Geopolymer Synthesis and Characterization

Calcium Silicate Hydrate (C-S-H) gel is the main hydration product of Portland cement, with all the properties (physical, chemical, and mechanical) ascribed to this gel. A significant research effort has been conducted to investigate the mechanism of C-S-H gel under stable conditions. To date, more than 30 C-S-H crystalline phases have been found [53]. Taylor suggested that C-S-H gel is formed by the hydration of Ca_3SiO_4, which contains two types of local structures, a) tobermorite, and b) jennite [54]. CaO is sandwiched between two rows of silicates (drierketten-type) in jennite like tobermorite. The basic difference between these two structures is that some of the silica tetrahedral is replaced by OH groups in jennite but not in tobermorite [53].

Based on Taylor's assumption, Richardson proposed a model for C-S-H gel with the replacement of silica by aluminium in the tetrahedral. The ^{29}Si NMR disclosed the signal at -882 ppm and referred to $Q^2(1Al)$ units. The charge is balanced by alkali or alkaline earth metal ions in the interlayer region [55]. The composition and structure of C-S-H gel are affected by temperature, relative humidity, pH, and the presence of alkali or alkaline earth metal ions. Many scientists have published papers on the effects of these different parameters on C-S-H gel [55-57]. To synthesize the C-S-H gel at ambient temperature, different methods are described in the literature ranging from hydrothermal treatments of some oxides of silicon and calcium to the reactions of tricalcium silicate or β -dicalcium silicate (C3S or -β C2S) [58,59].

In summary, alkali activated cements are proposed as an alternative to OPC. Alternative binders can be classified as: a) compound of calcium-, silicon-, and aluminium, such as blast furnace slag, b) compounds of silica and alumina, such as metakaolin and type F fly ash. The hydration product of the first group is C-S-H gel, the same as the hydration product of Portland cement. The hydration product of the second group, like metakaolin or fly ash, is substantially different from Portland cement hydration in the composition and

microstructure of the product. The main reaction product is alkaline silicoaluminate after the activation of metakaolin and fly ash.

Alkaline silicoaluminate consists of silicon and aluminium and is arranged in the form of tetrahedra as a three dimensional structure [36, 37, 60–62]. Cavities are formed in the network, which is of Na^+, K^+. An extra cation is accumulated after the replacement of Si(IV) by Al(III), which is balanced by alkali cations. To synthesize the gel, researchers are using natural raw materials or industrial by-products like blast furnace slag, metakaolin, and fly ash [2, 18, 52, 63–65]. Others used laboratory reactants to synthesize the gel [37, 66–68].

N-A-S-H is the reaction product of an alkali activation of fly ash, also called sodium aluminosilicate gel. It is widely acknowledged by the scientific community [69]. It is difficult to characterize the N-A-S-H gel due to its amorphous (or nanocrystalline) nature. However, there are other methods like FTIR or electron microscopy, (SEM, BSEM, and TEM) which provide information about the composition of the gel and how it is synthesized [21, 36, 61, 62, 69–74]. To understand the chemistry and properties of N-A-S-H and C-S-H gel, nuclear magnetic resonance (NMR) is a technique that can provide information the micro and nano levels.

Davidovits first used nuclear magnetic resonance of solids to explain the resulting micro structure, which later he called geopolymers. NMR generates higher resolution spectra of metakaolin [2, 60, 75] and fly ash [36, 37, 61] and synthesizes N-A-S-H gels [68, 76, 77]. It is proven that the main reaction product, hydrated gel of aluminosilicate, is produced by alkali activation of fly ash with a three dimensional structure, consisting of Q4(mAl) (m = 0, 1, 2, 3, 4) units. However, there are differences in a gel structure of both gels, which are due to the degree of ash reaction, curing temperature, and the presence of soluble silica in the activator solution. Different visible silica phases are found at -109.3ppm and -114ppm [signals Q4(OAl)] [78].

Silica plays an important role in the synthesis of gel. Silica comes from the binder as well as from the activator solution. The primary source of silica in the formation of N-A-S-H gel is aluminosilicate binder. Also, silica comes from the activator solution (sodium silicate or potassium silicate), which is highly soluble and incorporated instantly. The degree of silica polymerization in the activator solution plays a vital role in the formation of different structural stages (intermediate, metastable) involved in gel formation. Gel formation also depends on the ratio of oxides of silica to sodium. The alkali activator solution plays a crucial role in the kinetics, microstructure, and composition of the N-A-S-H gel initially produced [78].

Figure 2.1 reveals that the effect of silica on the activating solution is due to a superior degree of polymerization:

a) time is not sufficient for monomer and dimers to induce the formation of gel polymerization,

b) stability of the gel is directly related to the percentage of dimers, with high amount of dimers quickens the formation of gel, but it is less thermodynamically stable, and

c) the gel is more stable in the presence of cyclic silicate trimers; however, it slows the reaction of gel formation. Results suggest that the optimum ratio of Si/Al should be 2 due to the formation of the stable gel.
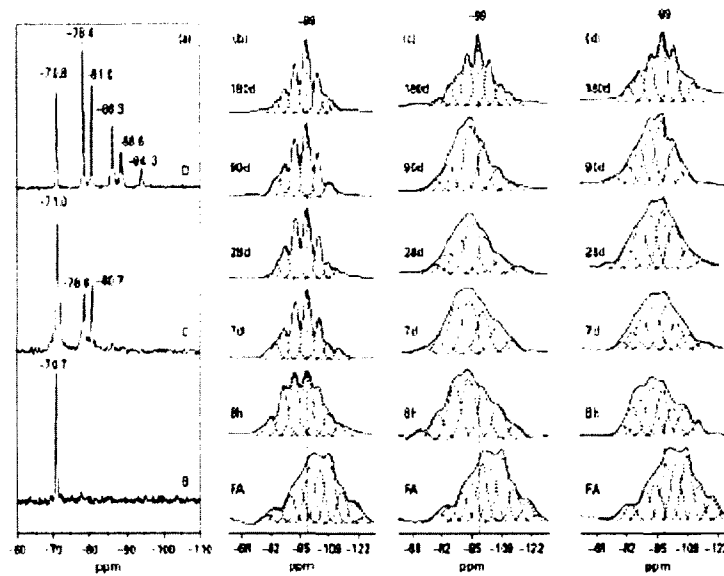
Figure 2.1: Adapted from "Si NMR spectra of the alkaline solutions used; "Si MAS NMR-MAS spectra of AAFA pastes activated with solution (b) B, (c) C or (d) D (Criado *et al.*, 2007b).

Different researchers proposed different structural models based on data, which is obtained by different techniques (XRD, FTIR, NMR) to describe how fly ash is activated based on the amount of silica. The gel formation kinetics are controlled by the amount of a polymerized silica. The polymerized silica decreases the degree of geopolymerization and the rate of a zeolite crystallization. However, thermodynamic stability increases with time [61,70,71]. Silicate and aluminate solutions are mixed together to form aluminosilicate gels followed by zeolites or pre-zeolites [79,80]. Aluminium initiates the condensation reaction, part of the polymerization, though it is unclear how to increase or decrease aluminium availability during the synthesis of aluminosilicate powder. Its release in the reaction is controlled by the activator as well as raw materials.

The amount of aluminium plays a crucial role in determining the formation of the aluminosilicate gel. Some scientists have shown the importance of alumina in gel formation kinetics and mechanical strength by interpreting FTIR and NMR for fly ash with the same

quantity of silica but different quantities of reactive alumina. Reactive alumina, released from the raw material, is directly related to the rate of reaction of the aluminosilicate gel. Opposite to that, the reaction rate is slowed down due to the low amount of alumina, released from fly ash, and most of it is absorbed in the early phase of the reaction. Alumina is beneficial to increase the mechanical strength of the gel if it does not exceed the threshold limit ($\sim$ 20%). However, excess alumina increases the setting time and exhibits more crystalline products [81]. FernBndez-Jimknez explained that alumina rich aluminosilicate gel exhibits increased mechanical strength [37].

2.11 Geopolymer Precursor Design

The three types of raw materials (slags, calcined clays, and coal fly ashes) are used in geopolymer synthesis. All three types of binders are classified as a supplementary cementitious binder in Portland cement-based systems. Performance and properties are mentioned in detail in the literature [55, 82]. Among them, calcined clays (metakaolin) are being used widely but their morphologies, mostly platelike, demand more liquid in geopolymer concrete. Other types of precursors are also used like synthetic powder, but they are not frequent [83].

Blast furnace slag composition, such as gehlenite ($2CaO.Al_2O_3.SiO_2$) and akermanite ($2CaO.MgO.2SiO_2$), is defined as a mixture of crystalline phases and depolymerized calcium silicate glasses. It is also called GGBFS (ground granulated blast furnace slag). It is produced during iron production in the form of liquid at the blast furnace and later quenched. Its composition consists of calcium aluminosilicate framework, in which the extra calcium is used to charge-balance the aluminium and the remaining calcium depolymerizes in the glass network [84]. A geopolymer that is made from slag, Al^{+3} and Si^{+4} serve as network cations, while the divalent Ca^{+2} and Mg^{+2} are the network modifiers.

Slag can be used in either geopolymer synthesis or as a supplementary cementitious binder for ordinary Portland cement. Some researchers explained the reactivity of different slags, either from the blast furnace or other metallurgical processes, in alkali-activated solution. Shimoda *et al.* describes the nature of hydrated slag phases [85]. Still, it is unknown how the structure of the phases of a specific network looks like for a specific slag. Particle size plays an important role in the reactions of slag. Particles smaller than 20 μm diameter reacts slowly while particles greater than 20 μm react with alkali activated solution completely within 24 hours [86, 87]. The particle size of the slag is critical to control the strength of geopolymer concrete [86].

2.11.1 Fly Ash

It is a byproduct of coal combustion and is collected by electrostatic precipitators in the power plant. Due to high temperature, it melts in the furnace but cools quickly in the air upon exiting the boiler, producing spherical glass particles. Heterogeneity is found in both interparticle and intraparticle as well as in crystalline phases [88-90]. Fly ash is a variable material due to not only impurities present in the coal but also during the combustion process and the cooling process. Fly ash stockpiles are classified by ASTM C618 of either Class F, Class C or Class N. Class F fly ash comparison of the composition and data regarding the mechanical properties of the resulting geopolymer are given by Duxson [91]. The strength of geopolymer products tend to increase as a function of chemical composition of the fly ash. It is also observed that as the percentage of low network modifier decreases, the strength of geopolymer products increase as seen in Figure 2.2.
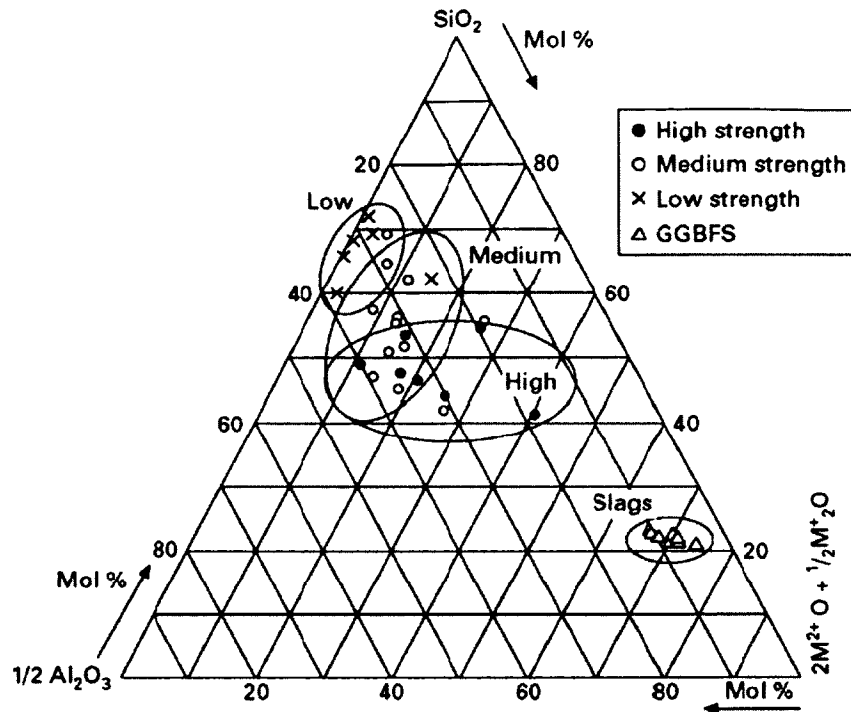
Figure 2.2: Pseudo-ternary composition diagram for fly ashes, showing ashes which give alkali activation products in approximate strength ranges as indicated. Alkali and alkaline earth oxides are summed, and represented as the total number of charges on the respective cations. Composition and strength data are compiled from the literature (Duxson & Provis, 2008). For comparison, composition of a selection of blast furnace slags (data from Shi *et al.*, 2006) is also shown.

There is an overlap between medium and high categories. It shows that there are some other factors: particle size, degree of crystallinity, and other atoms like iron and carbon, which affect the strength of the geopolymer matrix. The diagram concludes that a high strength of geopolymer is derived from high alumina, part of the region, which is shared by other factors. It is also observed that the low strength geopolymer products containing a significant amount of network modifier content lies in the region of lowest Al_2O_3. Class C fly ash network modifier contents, Ca^{2+} and Mg^{2+}, also affect the geopolymerization process. The fast setting time, resulting from rapid nucleation process initiated by the high Ca^{2+} process, resulted in limited research on the geopolymerization of Class C fly ash [92–96]. If the rheology of the mix is controlled, this fly ash can be utilized or preferred in the geopolymer [92,97]. This fly

ash in terms of composition can be seen in between Class F fly ash and GGBFS. Mixtures of Class C fly ash and GGBFS can be used as a potential binder in geopolymer synthesis, and significant technical literature on this method is available [98–100]. It is important to understand the role of chemistry of this fly ash before it is used in geopolymer formulations to ensure the optimum composition of the precursors.

Aluminium plays a significant role in the properties of the geopolymer [2, 37, 101]. The amount of aluminium and the rate of its release during geopolymer synthesis controls the strength, setting characteristics, acid resistance, microstructure and the profile of the strength development. The geopolymerization process is kinetically controlled [102]. It is required to understand the mechanism of the release of aluminium and its availability for the geopolymerization process [103].

Characteristics of the resultant geopolymer can be predicted based on the rate of release of aluminium from the precursors. The alkali concentration and type of alkali used in the activator solution affect the release of aluminium from the precursor, which is generally low [78, 104, 105]. From a thermodynamic point of view [106, 107] and sorption/speciation arguments [107, 108], it is clear that Al(1V)-O-Si bonds are more easily broken than Si-O-Si bonds. Also, the bonds between the network and the network modifier are weakest [109]. The alkaline earth cations change the framework and also form a small concentration of Al-O-Al bonds, provided the amount of Al is sufficiently high [110,111]. The alkaline earth cations, like Ca^{2+} and Mg^{2+} act as network modifiers, and are superb raw materials for alkali activation.

2.12 Activator Solution

An activator solution, either alkali hydroxide and/or silicate, is required to initiate the geopolymerization process. Geopolymer concrete is produced when an aluminosilicate binder is activated by alkali hydroxides and alkali silicates under alkaline conditions (high

pH). Different types of activator solutions, like carbonate and sulfates, are also used but not in a commercial way. Very little research is available other than on hydroxides and silicates. More importantly, the mechanism is still well not understood. To comprehend the synthesis of a geopolymer it is essential to understand the chemistry of the activator solutions.

This section is comprised of three parts. The first part explains the chemistry of alkali hydroxide in geopolymerization reactions. The second part describes the chemical nature of the alkali silicate solution in the process of geopolymerization and its implications. The third part addresses the use of the different activator solutions, especially the use of sodium aluminate.

2.12.1 Alkali Hydroxide Solution

The most commonly used activator solution is sodium and/or potassium hydroxide. Few publications are available for mixing of both sodium and potassium. It is highly alkaline and hence highly corrosive for the preparation of these hydroxide solutions, but the main significant consideration is given to viscosity and heat of dissolution.

The temperature increases when heat is released while preparing a concentrated hydroxide solution. Dissolution of NaOH contributes 10% of the enthalpy when it dilutes from ~10 M to infinite dilution, while 90% comes from the dissolution of the crystalline solid. It is observed that when 10 moles of NaOH are dissolved in one liter of water, 90% of the heat is released in moving to infinite dissolution, which is equivalent to 400 KJ. This heat is sufficient to raise the temperature of water by 90° C [112]. Some of the heat is lost in the surroundings and some is lost during vaporization of the solution.

During the mixing of the geopolymer concrete, special care must be given to address the rise in temperature associated with the mixing of the hydroxide solution. The wide usage of sodium hydroxide (NaOH) activator solution in geopolymer synthesis is due to its general availability, low viscosity, and low cost compared with other hydroxides. It is used in both

types of precursors: fly ash and metakaolin. Specialized processing equipment is required to use sodium hydroxide in geopolymer synthesis due to the caustic nature of concentrated NaOH. Apart from structural and performance issues, silicate solution is favored. Solubility is dependent on the temperature of the environment, and it is concentrated in cooler regions [113,114]. NaOH is widely used in geopolymer synthesis and leads to the formation of zeolite [34], even in aggressive environments with elevated temperature and moist conditions.

Research is still on going concerning whether there is any effect on material performance. While there is a correlation between the salt formation and loss of strength, it is still unknown whether loss of strength is due to the formation of salt or if it is the result of a combination of other factors which causes the zeolite formation and loss of strength. Potassium hydroxide (KOH) solubility does not decrease considerably with a decrease of temperature, as it is the case with NaOH. Its solubility is 21 M at 25° C [113]. Hydrate phases are not found, and the phase diagram is also not complicated as with NaOH-H_2O.

During geopolymer synthesis, it is believed that precipitation after using potassium hydroxide as an activating solution is not a problem. Salt is also formed by using potassium hydroxide as an activator solution as with NaOH for geopolymer synthesis. However, formation of crystallization takes place in KOH/metakaolin not as quickly as with NaOH/metakaolin [75], but it is less suppressed in KOH/fly ash systems as compared to NaOH/fly ash [72]. Carbonation is not well understood in geopolymers using the KOH activator solution.

2.12.2 Alkali Silicate Solutions

Different regions are marked in Figure 2.3. Low-silica activating solutions with metastable compositions are occupied in region A ('partially crystalline mixtures'). Region B is covered by commercial silicate solutions. Activated solutions in region C are susceptible to crystallization and region D shows high viscosities. Potassium silicate phases are not common

as with sodium silicate phases in terms of precipitation. However; the stability range of

hydrated potassium silicate phases is extensive. Figure 2.3 shows the different regions and its

importance in geopolymer synthesis.
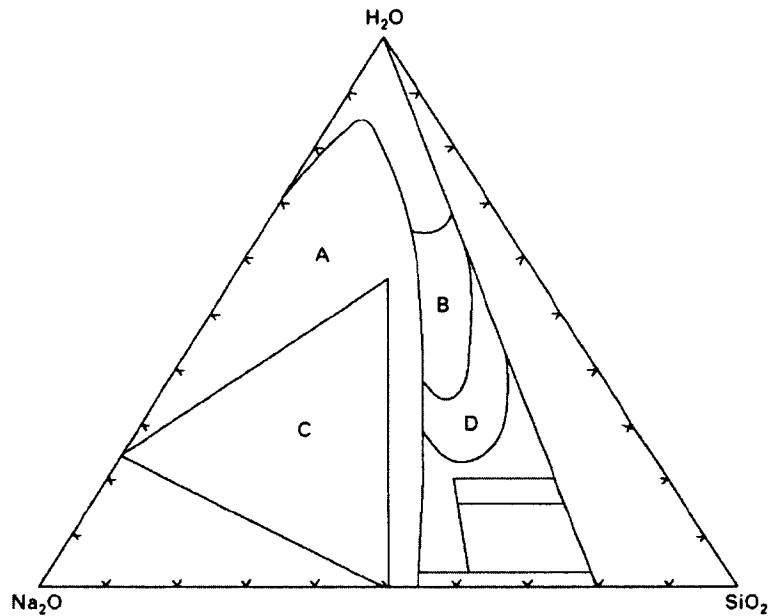
Figure 2.3: Compositional regions leading to different types of products in the Na_2O-SiO_2-H_2O system, after Vail (1952). Regions of importance in geopolymer synthesis are discussed in the text.

Vail [115] and Iler [116] discussed lithium silicate solutions. The low solubility of

hydrated lithium metasilicate phases hinders the preparation of lithium silicate at elevated

temperatures. Vail [115] developed techniques and explained how to produce these solutions

commercially. With the right composition, silicate of sodium and potassium is prepared

by dissolving in a waterglass when amorphous silica is dissipated into aqueous LiOH [116].

Rubidium and caesium silicate solutions are like potassium, except for solubility of phases,

which is high.

2.13 Calcium Silicate Hydrate (C-S-H) gel

Calcium Silicate Hydrated (C-S-H) gel is the main hydration product of Portland cement. Interestingly, all the properties (physical, chemical, and mechanical) are ascribed to this gel. Much research is being conducted to investigate the mechanism of C-S-H gel at surrounding temperature and stability conditions. More than 30 C-S-H crystalline phases have been identified [117]. Taylor suggested that C-S-H gel is formed by the hydration of Ca_3SiO_4, which contains two types of local structures, tobermorite, and jennite [54]. The CaO is sandwiched between two rows of silicates (drierketten-type) in jennite and tobermorite. Calcium atoms and water molecules lie in the interplay. The basic difference between these two structures is that some of the silica tetrahedral is replaced by OH groups in jennite but not in tobermorite. Also, it causes a wave like motion in the CaO layer [118]. With Taylor's assumption, Richardson *et al.* [119] proposed a model for C-S-H gel with the replacement of silica by aluminium in the tetrahedral. The ^{29}Si NMR disclosed the signal at -882 ppm and referred to $Q^2(1Al)$ units. The charge is balanced by alkali or alkaline earth metal ions in the interlayer region. Composition and structure of C-S-H gel are affected by temperature, relative humidity, pH and presence of alkali or alkaline earth metal ions.

Many scientists have published papers on the effects of these different parameters on C-S-H gel [56, 120, 121]. To synthesize the C-S-H gel at ambient temperature, different methods are described in the literature ranging from hydrothermal treatments of some oxides of silicon and calcium to the reactions of tricalcium silicate or β-dicalcium silicate (C_3S or β- C_2S) [122, 123]. Scientists started searching for new cementitious binders less harmful to the environment and more long-lasting than traditional Portland cement. Also, they found that an alkali activated cement is a reliable alternative to Portland cement. Two types of materials are found under this category: a) compound of calcium-, silicon-, and aluminium, such as blast furnace slag, b) compounds of silica and alumina, such as metakaolin and type F

fly ash. The hydration product of the first group is C-S-H gel, the same as a hydration product of Portland cement. The hydration product of the second group, like metakaolin or fly ash, is substantially different from Portland cement hydration in the composition and microstructure of the product. The main reaction product is alkaline silicoaluminate after activation of metakaolin and fly ash. The alkaline silicoaluminate consists of silicon and aluminium and is arranged in the form of tetrahedra in the three dimensional structure [61, 67, 124–126]. Cavities are formed in the network containing Na^+ and K^+. An extra cation is accumulated after replacement of Si(IV) by Al(III) which is balanced by alkali cations [18,33,52,63,66–68, 75,78,127].

2.14 Chemical Durability of Geopolymer Concrete

The durability of the concrete structure is the ability of a concrete to resist extreme physical conditions (abrasion, erosion, and cavitation), chemical attack, and the corrosion of reinforced steel bars while preserving its engineering properties. Durability is dependent on the selection of the material, design, and weather conditions. Durability is directly related to the service life of the structure. Regular inspection and maintenance are required to optimize the service life.

2.14.1 Sulfate Attack - Overview

Sulfate, occurring in natural or industrial environments, reacts with cement paste to form gypsum and ettringite. Sulfate attack is classified as either external or internal. Sulfate (for example calcium/sodium/magnesium sulfate) present in soil or/and groundwater ingresses into the pore solution of the concrete and forms gypsum and ettringite (external attack). Sulfate that comes from the aggregate or mixer at the time of cement preparation is considered to present an internal sulfate attack. A sulfate attack changes the composition and microstructure of the cement, resulting in the following effects [128–130]: Volume expansion,

formation of microcracks; disruption of the bond between the cement paste and aggregate; changes in the composition of the paste, leading to the formation of ettringite and gypsum.

2.14.2 Mechanism of Sulfate Attack

Calcium, magnesium or sodium sulfates attack the calcium hydroxide and hydrated compounds, forming gypsum and ettringite. Magnesium sulfate forms brucite (Magnesium hydroxide), lowers the pH of the pore solution, and decomposes the calcium silicate hydrate. Magnesium sulfate attack is the most aggressive among all sulfates. Mortars prepared with alkali-activated metakaolin display good strength after dipping in aggressive solutions: deionized water, sodium sulfate solution (4.4% wt.), and sulfuric acid (0.001 M) [131]. Interestingly, the aggressive solution did not have a negative effect on the development of microstructure and strength of the materials. Only slight changes were perceived in flexural strength due to dissolution-phenomenon between 7 days and 90 days of immersion, irrespective of the type of aggressive agent. However, it created a negative impact on the development of mechanical strength. This change from amorphous aluminosilicate network into a crystalline structure partly is due to the length of the immersion.

Stability of alkali-activated fly ash in aggressive environments (5% solution of sodium sulfate, 5% solution of magnesium sulfate, and mixture of both) depends on how the basic atoms are arranged in aluminosilicate gel [132]. It was observed that geopolymer materials prepared with sodium hydroxide solution have shown a more crystalline structure than sodium silicate activators. Stability is higher for higher degree of crystallinity in intense environments. It is due to the formation of cross-linked aluminosilicate polymer structure when the activator is sodium hydroxide.

Different authors claimed that alkali-activated fly ash pastes and mortars perform better in aggressive environments such as sulfates and seawater compared with their OPC counterparts [132, 133]. Interestingly, they did not find any changes in composition and

microstructure of the fly ash after immersion in saline conditions. Sodium sulfate was detected in the gaps or pores in the matrix due to a large amount of sodium ion in the system. Magnesium ion was also observed in the cement matrix. Due to the exchange of Mg and Na ion in the pore solution, it causes change in composition and morphology. Silicon-rich gel was found with a magnesium ion intermittently in specimens, engrossed in seawater. The durability of geopolymer pastes and mortars is related to Si/Al in the system. It is also a function of the amount of crystalline phases (zeolite) in the matrix. Basically, soluble silicate in the activating solution hinders the crystallization of alkaline silicoaluminate as well as zeolite [134,135]. Furthermore, silicate ions encourage the formation of compact structures of Si rich gel [21,37,61,69].

This explains the reason why the mechanical strength of geopolymeric mortars prepared with sodium silicate is higher than those prepared with sodium hydroxide. Li [136] reported little expansion in mortars prepared with geopolymer (prepared from metakaolin) and immersed in 0.31 M sodium silicate solution. Mortars, prepared with Portland cement, have shown larger expansion. Geopolymer does not contain $Ca(OH)_2$ and monosulfoaluminate as they are formed using source materials that contain calcium. So, when geopolymer materials react with sodium sulfate solution, there is little to no formation of gypsum and ettringite, which causes expansion in the matrix.

2.15 Alkali Silica Reaction

The alkali-aggregate reactivity (AAR) is a barrier in concrete production because it causes substantial expansion [137, 138]. Two common types are alkali-silica reaction (ASR) and alkali-carbonate reaction (ACR). The alkali-silica reaction is more destructive, due to the presence of reactive silica minerals in aggregates, which causes expansion of the concrete structure. ASR is a reaction between the hydroxyl ion in the cement's pore solution and

reactive forms of amorphous silica in the aggregates (quartzite, strained quartz crystals). This forms a swelling gel of alkali silicate called calcium silicate hydrate (CSH). This gel increases in volume and exerts a force, which causes spalling and cracking of concrete. This expansion and cracking cause structural failure of the concrete structure. The mechanism of ASR tends to include the following steps:

The hydroxyl ion of the solution converts silica present in the aggregate into an alkali silicate gel. Alkali is consumed in the reaction and produces Ca^{2+} ions, which react with the gel and forms calcium silicate hydrate (CSH). Siliceous minerals are converted into a bulky alkali silicate gel in the presence of an alkaline solution. This produces extra stress, which is stored in the aggregate. The extra pressure cracks the concrete structure when it exceeds the tolerance level of the structure.

2.15.1 Factors Affecting ASR

These conditions need to be fulfilled before ASR can take place:

a) The silica of the aggregate should be in reactive form,

b) Pore solution of the cement should be highly alkaline (Na_2O, K_2O),

c) Calcium dominant phases, and

d) Optimum moisture.

2.15.2 Alkali-Carbonate Reaction (ACR).

The hydroxyl ion of the alkaline solution reacts with the dolomite, which is present in the aggregate, and forms brucite and calcite. Dolomite is a calcium-magnesium carbonate, and calcite is calcium carbonate. Dolomite is susceptible to ACR and also has low strength potential. The reaction mechanism can be written as follows:

$$CaMg(CO_3)_2 + 2NaOH(Dolomite) \longrightarrow CaCO_3 + Na_2CO_3 + Mg(OH)_2 \text{ (Calcite).}$$
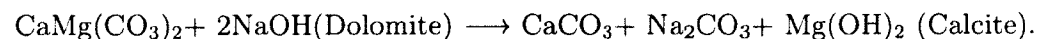
Dedolomitization and absorption of the moisture are responsible for volumetric expansion of the concrete structure. Alkali-activated fly ash contains a high amount of alkali but a low amount of calcium. Thus, expansive sodium-calcium silicate gels are not formed. During early stages of the dissolution and condensation polymerization process [139], alkali-silica reaction is formed in geopolymer mortars when the material is in gel form. It is beneficial due to the formation of paste-aggregate chemical bonding, which increases the tensile strength of the geopolymer concrete. At later stages, it is not possible due to the formation of the dense bond zone near each aggregate particle during curing. Also, the pH of the solution is low, about 10 to 11, and cement matrix contains unreacted fly ash [25,140]. Mortars prepared with alkali-activated fly ash, with sodium hydroxide or sodium silicate solutions, have shown only 0.1 % expansions in a standard test after 160 days. It was revealed by SEM/EDX that the specimen was healthy without any cracking or ASR products. However, aluminosilicate gel (N-A-S-H) and crystalline zeolite present during the investigation.

Alkali reacts with fly ash in two successive steps. First, alkali is used to activate the vitreous component of the fly ash and change it into cementitious material, but at the same time it undergoes to a second reaction and attacks the aggregate. Alkali activation in the first phase forms an inorganic polymer and zeolite crystal, but at the same time, alkali aggregate reaction also takes place. However, AAR product is not expansive due to the absence of calcium in fly ash. Therefore, fly ash system is less expanded compared to Portland cement.

The durability of concrete structures is directly associated with their mineralogical composition and the microstructure of the material. Alkaline aluminosilicate gel is present in the inorganic polymer cement (IPC), which is responsible for the durability and strength of the material. Aluminosilicate gel with three dimensional structures is different from C-S-H gel, which is found in ordinary Portland cement (OPC). Zeolite is also formed as a secondary product in this reaction [18,124,141]. The durability of inorganic polymer cement

is discussed in the context of commonly acknowledge deterioration mechanism such as alkali-aggregate reaction (alkali-silica reaction and alkali-carbonate reaction), elevated temperature, inferno resistance and freeze-thaw attack. Parameters like compressive strength, expansion in volume, weight loss, and structural changes at the micro level and the protection provided to the steel reinforcement are deciding factors in determining the performance of the cementitious matrices.

2.16 Chemical Corrosion of Geopolymer Concrete

Iron is found in nature in the form of ores, natural oxides, and their different products. Energy must be exerted to extract the metals from the ore using a process called smelting. Because the metallic form is unstable, it tries to return to its natural state. The process of returning to its original form is called oxidation, or corrosion [142]. The corrosion rate of steel depends on moisture, oxygen, presence of aggressive elements (such as chloride or carbon dioxide), pH of the solution, and temperature [142]. Formation of a protective oxide layer takes place on the surface of the steel reinforcement at high pH (about 13). This oxide layer protects the steel from corrosion. Once the protective layer breaks down, oxygen will react with the steel, and corrosion begins. Oxygen and water are required to initiate corrosion. If the concrete cover inhibits the ingress of oxygen and water, the embedded reinforcement is protected against corrosion.

Corrosion in reinforcement is the main cause of failure in reinforced concrete structures (RCS). Repairs or sometimes demolitions are needed due to corrosion and service life is reduced to only 10–20 years. Among several reasons, aggressive environment is one of the main reasons. Large sums of money are spent, with 40–60% of resources exhausted on maintenance and repair. It has an economic and social impact in the construction sector and it becomes a principal challenge in developed countries. Keeping this in mind, it is required to study the

ability of alternate binders to passivate the steel reinforcement and strengthen the durability of reinforced concrete structure. To date, little research was completed on the durability and logivity of reinforcement in geopolymer matrices. Researchers have reported regarding the passivity of steel reinforcement of mortars and concrete structure prepared from fly ash based geopolymer. Though the stability of the passive layer was related to the type of activation solution used in changing the environmental condition, they made the following observations [143, 144].

Passivation of steel reinforcement in activated fly ash mortars is similar to Portland cement mortars in terms of speed and efficiency. The extent of passivity depends mainly on the compounds that activate the fly ash. Geopolymer mortars using waterglass and caustic soda as an activator solution have low permeability, which decreases carbonation significantly, and increases the duration of passivity in reinforcement provided there is an absence of chloride ions. It has been shown that the presence of chloride ion above the certain threshold level multiplies the corrosion rate by roughly 100 times,similarly to Portland cement mortars. They analyzed the effect of electrodes entrenched in mortars of Portland cement and alkali activated fly ash with different activator solution: NaOH, and sodium silicate solution by measuring corrosion potential (Ecorr) and polarization resistance (Rp) over a period of 2.5 years.

Mortars prepared from both types of binder are shifted for several months from high relative humidity (RH $\approx$ 95%) to the dry atmosphere (RH $\approx$ 30%). The changes in Icorr was measured for: (a) Portland cement mortars, (b) alkali activated fly ash with an activator solution of NaOH, (c) alkali activated fly ash with a chloride content of 0 and 2%. It was shown that the corrosion rate multiplied by a factor of nearly 100 in humid conditions with the addition of chlorides. Mortars prepared from activated fly ash rapidly passivates the steel reinforcement compared to Portland cement, but depassivation of steel reinforcement is the same in both types of binders [145, 146]. It is noticed that depassivation of steel is higher in

fly ash activated with 8 M NaOH compared with fly ash activated with NaOH and waterglass in a chloride-free environment. It is due to the formation of sodium carbonate when fly ash is activated with only 8 M NaOH. This causes a decline in pH which is confirmed by phenolphthalein test. The intense carbonation was found due to the presence of pores bigger in size. This matches with previous references which identified the permeability of the material to be key parameters [147, 148]. The number and size of the pores facilitate the penetration of atmospheric CO_2 through the network.

Chemical reactions used to initiate the geopolymerization process do not depend only on types of alkali activator solution but also on the curing method. The current research has shown that the curing method for fresh pastes makes matrices less porous and more resistant to carbonation [147, 148]. Another group of researchers used electrical currents to study the intensity of corrosion in alkali activated fly ash concretes in accelerated condition. They found that geopolymer concrete has better corrosion resistance for materials of similar compressive strength compared with Portland cement. Additionally, it was reported that those materials which has higher compressive strength showed better resistance to steel bar corrosion [149].

2.16.1 Carbonation Effect

Carbonation is accelerated near industrialized areas due to high concentration of CO_2 in the atmosphere. Gaseous form of Carbon dioxide (CO_2) dissolves into the pore solution of the concrete and form carbonic acid as shown in Figure 2.4.
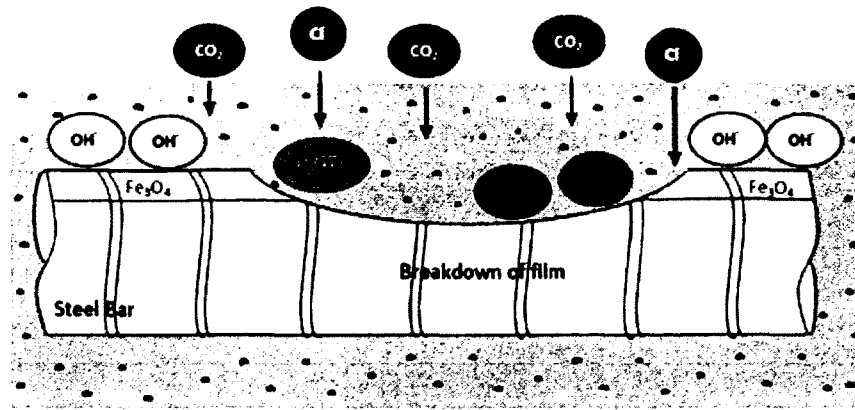
Figure 2.4: Concept of carbonation in concrete.

Carbonic acid neutralizes alkalis in the pore solution by reacting with calcium hydroxide. Eventually, all of the calcium hydroxide is consumed and the pH value of the concrete matrix drops from 14.0 to about 8.0. At this low pH condition, the protective oxide layer (Fe_2O_3 or Fe_3O_4), which protects the steel reinforced bar from corrosion break down, and starts to corrode. From a thermodynamic point of view, free energy of calcium carbonate is lower than calcium hydroxide which favors the carbonation reaction if carbon dioxide is present [19]. The principal reactions of hydrated cement with carbon dioxide are:

$$CO_2 + H_2O \longrightarrow H_2CO_3 (Carbonic acid) \tag{2.3}$$

$$H_2CO_3 = H^+ + HCO_3^- (decrease in pH) \tag{2.4}$$

$$H_2CO_3 + Ca(OH)_2 \longrightarrow CaCO_3 \cdot 2H_2O. \tag{2.5}$$
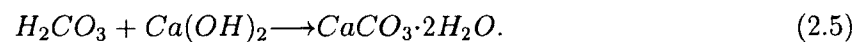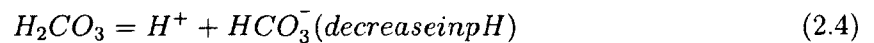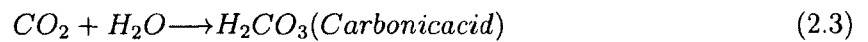
2.16.2 Examination of Geopolymer at Elevated Temperature

There are many applications where the resistance of concrete structures to fire and heat is an important design criteria. Fire resistant concrete structures are required in tunnels, basement buildings, underground railways, and skyscrapers. Traditional concrete structures, made by OPC, are not fire resistant due to damaged to the cement gel at elevated temperatures

or bonded and unbonded water in the matrix convert to steam. This could hinder in rescue operations in case of an emergency.

2.17 Microbial Induced Corrosion (MIC)

Corrosion of concrete is a typical form of deterioration and it is commonly associated with an economic impact in the order of billions of dollars per year in repair or replacement of existing concrete structures. According to a report published by the U.S. Federal Highway Administration [150], the industrial cost of corrosion in the U.S. is about $138 billion/year, of which 25% is attributed to corrosion in water pipelines and sewer systems. One of the main reasons for corrosion of concrete in buried utilities is the presence of hydrogen sulfide, which later leads to microbial induced corrosion via the formation of sulfuric acid. Microbial induced corrosion (MIC) of concrete sewer pipes was first reported by Olmstead and Hamlin in 1900, who stated that hydrogen sulfide, the byproduct of an anaerobic reduction of sulfate in sewage/wastewater was the causing agent of severe corrosion of sewer pipes.

Two types of bacteria lead to MIC in concrete structures in wastewater collection systems, namely, sulfate reducing bacteria (*Desulfovibrio desulfuricans*) and sulfate oxidizing bacteria (*Thiobacillus spp*). The submerged part of concrete sewer pipes where anaerobic conditions exist, SRB resides between the anaerobic and anoxic zones, and converts sulfates present in the wastewater stream to hydrogen sulfide [151]. The hydrogen sulfide produced in the sewer pipes reacts with oxygen to form elemental sulfur on the concrete surface. This elemental sulfur is metabolized by the sulfate oxidizing bacteria (Thiobacillus spp) to produce sulfuric acid, which reacts with the cement hydration products, deteriorating the concrete and eventually leading to failure of the structure. Structures built out of ordinary Portland cement are not highly resistant to MIC and/or sulfuric acid corrosion [152].

An alternative to OPC binders are geopolymers, and a different combination of geopolymers appears to perform very well in acidic environments [153]. Previously, acid resistivity tests on cementitious binders were performed by exposing them to commercially available sulfuric acid. Munn [154] reported that geopolymer cement was able to maintain its compressive strength even after exposing it to 10% and 1% sulfuric acid solution over a period of 8 weeks and 18 months, respectively. Thokchom et al. studied the resistivity of geopolymer cement by exposing it to 10% sulfuric acid solution over a period of 18 weeks. Resistivity was evaluated in terms of visual appearance, residual alkalinity, changes in weight, compressive strength, and microstructural analysis at regular intervals. From the results obtained, no significant changes in strength and color of the specimens were observed. It was concluded that geopolymer cement offers high resistance to sulfuric acid corrosion.

CHAPTER 3

EXPERIMENTAL PROCEDURE, RESULTS AND DISCUSSION: CARBONATION

3.1 Introduction

The durability of concrete is a key concern in civil infrastructure, as it could lead to a reduction in service life and progressive deterioration of the structures, ultimately resulting in the catastrophic failure of the structure [175]. Alternative cementitious materials are being developed to provide a resilient infrastructure while reducing the carbon footprint of construction projects by utilizing waste materials such as fly ash to make green concretes [176]. CO_2 induced corrosion is one of the major durability issues faced by civil infrastructure components made using cementitious materials. The carbonation mechanism of Ordinary Portland Cements (OPC) is well understood and has been documented in several research studies [177–181]. However, limited studies have been undertaken to explore the effect of carbonation on green cementitious binders, such as geopolymer concretes [182–185].

Geopolymers are a group of inorganic binders that form zeolites (sodium aluminio-silicate hydrates) upon alkali activation [186]. This polymerization process involves a rapid reaction of a reactive aluminosilicate powder, such as fly ash, with an alkaline solution [187]. Alkaline liquids commonly used include sodium hydroxide (NaOH) or Potassium Hydroxide (KOH) in combination with sodium silicate. This reaction results in the formation of zeolitic phase, commonly known as geoploymeric gel. The zeolitic phase consists of Si content which can be derived from fly ash, slag or rice husk. In addition to Si, Al rich materials such as kaolin,

43

bentonite and clays can also serve as precursors for the geopolymerization process [177,178]. Low and high calcium based fly ash stockpiles can be used for the production of geopolymer concretes. Factors such as location of glass diffraction maximum, degree of vitrification, particle size distribution, the nature and percentage of impurities, and loss of ignition (LOI) can affect the mechanical properties of the resulting GPC such as compressive strength and elastic modulus [179].

Little research has been conducted to date regarding corrosion resistance of steel reinforcement embedded in GPC matrices when subjected to accelerated carbonation treatment. Previous durability related studies suggested that fly ash based geopolymers are able to passivate the steel reinforcement, and the stability of the passive layer depends on the concentration of the activator solution [3]. Other studies have shown that geopolymer cements have superior carbonation resistance due to the presence of a protective layer of calcium or sodium alumino silicate hydrate (C-A-S-H and N-A-S-H). Decalcification of this protective layer of C-A-S-H due to carbonation could lead to the deterioration and degradation of the cementitious matrix as shown in Figure 3.1, and is documented in studies conducted by Bernal *et al.* [182–185].
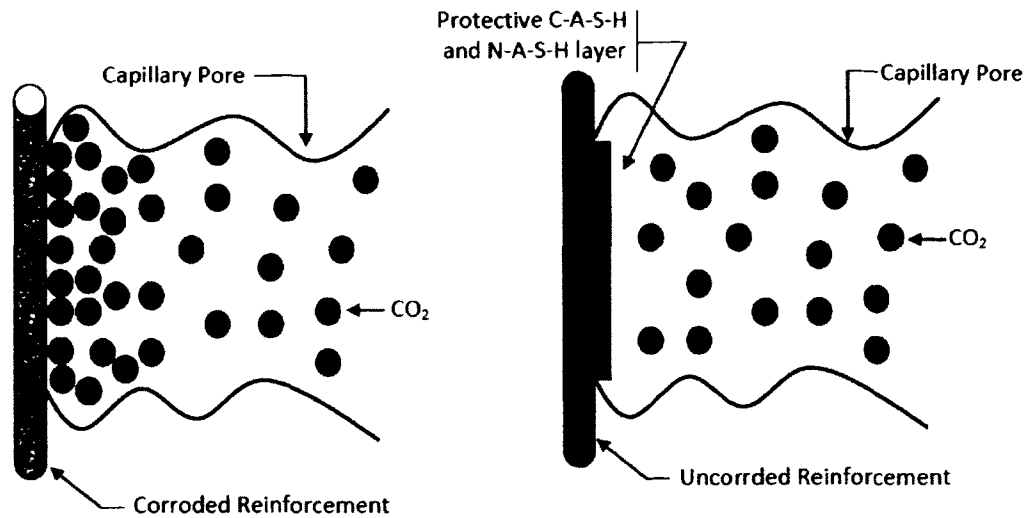
Figure 3.1: Concept of reinforcement corrosion due to CO_2 ingress and prevention of corrosion via the formation of a N-A-S-H zone.

With, previous studies conducted on geopolymer concretes without steel reinforcement, the current study examines the effect of carbonation using steel reinforced geopolymer concretes. The deterioration of the C-A-S-H protective layer could be attributed to the formation of carbonation product phases such as natron, trona, calcite and vaterite [184,185]. A hypothesis concerning the mechanism of carbonation in geopolymer concretes where the effect of carbonation depends on the concentration of CO_2 was reported by Bernal et al. [184,185]. A computational study of the carbonation of highly alkaline pore solutions indicates that activation occurs in multiple stages.

The primary process involves carbonation of the pore solution by adsorption of CO_2 from the atmosphere, leading to reduction in pH and the formation of Na-rich carbonates. The second step involves reaction of carbonates with the cement matrix, forming calcium bicarbonates. If geopolymer is prepared from fly ash with high calcium content, it could lead to higher initiation of calcium bicarbonates, which leads to reduction in the amorphous content, resulting in deterioration of the C-A-S-H/N-A-S-H gels. These geopolymeric gels

play a crucial role in controlling the durability resistance of geopolymer concretes. A separate computational study was conducted by the author to examine the effect of N-A-S-H gels when subjected to extreme conditions [188]. The Si/Al ratio plays a crucial role in providing guidelines for durability and strength initiation of N-A-S-H gels. The significance of the current work is to examine the effect of carbonation on reinforced geopolymer concretes when subjected to accelerated carbonation conditions. Detailed electrochemical, microstructure and pore structure characterizations were conducted to examine the effect of carbonation at the rebar/concrete interface.

3.2 Experimental Procedure

3.2.1 Raw Materials

This study examines the effect of carbonation on reinforced geopolymer concretes prepared from Class C and F fly ash stockpiles. The chemical composition of the fly ash stockpiles obtained from X-ray fluorescence (XRF) spectroscopy is shown in Table 3.1.

Table 3.1: Chemical composition of fly ash stockpiles.

Raw Material (%)	SiO_2	Al_2O_3	SiO_2/Al_2O_3	CaO	Fe_2O_3	MgO	SO_3	Na_2O	K_2O	Mc	LOI
Class F Fly Ash (DH)	58.52	20.61	2.84	5.00	9.43	1.86	0.49	0.52	-	0.14	0.05
Class F Fly Ash (OH)	55.07	28.61	1.92	1.97	6.22	1.08	0.19	0.38	2.63	0.12	1.82
Class C Fly Ash (MN)	55.61	19.87	2.80	12.93	4.52	2.49	0.49	0.67	0.86	0.02	0.22

Mc: Moisture content
LOI: Loss of ignition

Two different types of Class F fly ash were obtained from Dolet Hills power generation station (PGS) located in Mansfield, LA and Avon Lake PGS, OH. Class C fly ash was obtained from Monticello PGS located in Mount Pleasant, TX. Particle size distribution (PSD) of the fly ashes obtained using PSD analyzer (Microtrac S3500, Microtrac solutions) with a mean

particle size of 20.8 μm to 27.5 μm. The results of the PSD analysis are summarized in Table 3.2.

Table 3.2: Particle size distribution (PSD) analysis of fly ashes.

Fly Ash Type		%Passing										Particle less than 45 μm	Calculated Surface (m²/m³)	Mean Particle Size micron s	Specific Gravity
		10	20	30	40	45	50	60	70	80	90				
MN	C	32.6	48.9	59.7	66.0	68.7	71.4	76.5	81.1	84.7	87.3	68.7	1.33	20.87	2.38
DH	F	16.9	39.8	52.3	59.9	63.5	67.0	73.1	77.6	80.8	83.2	63.5	0.57	27.52	2.32
OH	F	26.4	46.1	59.2	67.5	71.2	74.9	81.5	86.4	89.7	91.9	71.2	1.08	22.30	2.17

3.2.2 Specimen Preparation

Cylindrical reinforced concrete specimens 6 in (0.15 mm) tall by 3 in (0.07 mm) in diameter were casted using GPC. GPC specimens were prepared using an alkali activator solution which was mixed with the designated fly ash, fine and coarse aggregates. The activator solution consisted of sodium silicate and 14 M sodium hydroxide. The sodium silicate was manufactured by PQ Corporation with a 45% by weight and SiO_2/Na_2O of 2:1. The activator solution was comprised of a 1:1 blend of sodium silicate and sodium hydroxide solution. Fine aggregate had a bulk density of 1,680 kg/m3 and specific gravity of 2.63. P-gravel was used as a coarse aggregate with (3/8 in) in diameter and the bulk density of 1,960 kg/m3. The geopolymer specimens were prepared with an activator to binder ratio of 0.5 and cured at 80° C for a period of 72 hours. A single carbon steel deformed rebar 0.25 in diameter was sand blasted and placed at the center of each cylinder mold prior to casting the concrete. Elemental composition of the 1.018 carbon steel rods was C = (0.14-0.2)%, Mn = (0.6-0.9)%,

S = 0.05% max, P = 0.04%, and Fe = (98.81-99.26)%. Each reinforcement was 30 mm (12 in) in length and 6 mm (0.25 in) in the outer diameter.

3.2.3 Carbonation Exposure

The carbonation process was conducted in an environmental chamber in which both the temperature ($24\pm5°$ C) and relative humidity ($65\pm5\%$) were controlled. A CO_2 gas tank was used to pass the gas inside the chamber and was tightly sealed to prevent leakage as shown in Figure 3.2.
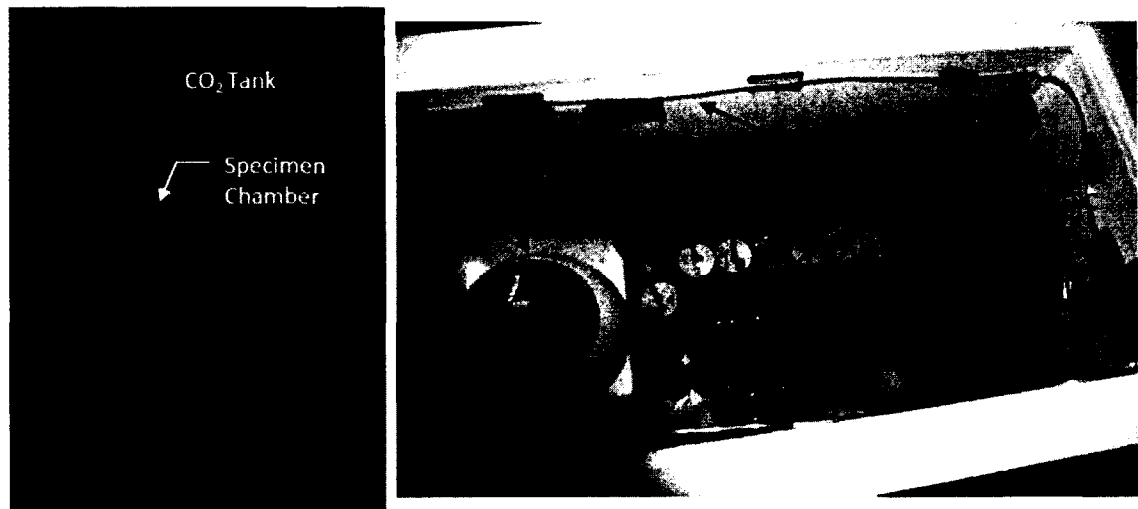
Figure 3.2: Experimental setup for carbonation for reinforced geopolymer concretes.

The process of carbonation was performed by injecting 100 cm3/min of CO_2 into the climatic chamber. The carbonation test was conducted at CO_2 concentration of $5.0\pm0.3\%$. To expedite the carbonation process, a 14 day period of wet and dry cycle of exposure was followed. We maintained the carbonation exposure for 450 days.

3.2.4 Electrochemical Evaluation

Corrosion potential was measured as per ASTM C 876. A $Cu/CuSO_4$ reference electrode was used to measure the half cell potential. The corrosion rates were measured using linear polarization resistance (LPR) technique with a Solsrtron potentiostat (Model No.

1287) manufactured by Roxboro Company, UK. The scans taken ranged from -25 mV to + 25 mV at a rate of 0.2 mV/s. The Stern-Geary equation was used to relate the corrosion current density (I_{corr}) and the polarization resistance (R_p)

$$I_{corr} = \frac{B}{R_p}.$$ (3.1)

We used the resulting value of Icorr to calculate the corrosion rate (CR) which was derived from the Faraday's law as per ASTM G102 (ASTM 2010):

$$CR = \frac{(K_1 X I_{corr} X EW)}{\rho},$$ (3.2)

where CR is the corrosion rate (mpy $=$ mils per year), I_{corr} $=$ Corrosion Current density, K_1 is Faraday's constant, EW is the Equivalent Weight, and ρ is density (8.02 g/cm^3). The internal resistance (IR) drop was corrected by using a feedback compensation technique. The guidelines for relating corrosion rate with the severity of corrosion are shown in Table 3.3.

Table 3.3: Guidelines for interpretation of corrosion rates [150].

Corrosion Rate (mpy)	Damage (Years)
< 0.10	No Corrosion Damage
0.10 < CR < 0.5	10-15
0.5 < CR < 5.0	2-10
> 5.0	< 2

3.2.5 Mechanical and Chemical Analysis

The indirect tensile test was conducted as per ASTM C 496-96. This procedure consists of application of uniform diametrical force, which is distributed along the length of the specimen at a rate of 150 psi/min until failure. Following the indirect tensile test, the specimens were subjected to chemical analysis for pH indication using phenolphthalein and alizarin yellow indicators. In case of phenolphthalein, the color changes to pink if the pH is greater than 9.5, or else it remains colorless for a pH range of 8.0-9.5, while for Alizarin

Yellow R a color change from yellow to red for pH greater than 12.0 or else it remains yellow for a pH range of 10-12.

3.2.6 Microstructure and Pore Structure Characterization

The reinforcement and the reinforcement/concrete interface were studied using an emission field scanning electron microscope (model: Hitachi S-4800), and quantitative elemental analysis was performed using Genesis Microanalysis software manufacture by Ametek, Inc. Attenuation total reflectance (ATR)-Fourier Transform Infrared Spectroscopy (FTIR) was conducted using Nicolet IR-100 spectrometer and X-ray diffraction (XRD) using a Bruker D8 AXS, Inc. with Cu K radiation using nickel filter, step size of 0.020° with a 2θ range of 3-90°. Quantitate XRD analysis for GPC was conducted on a solid specimen using a commercial software (Diffrac Plus, Bruker Topas 4.2, Bruker AXS GmbH, Karlsurhe, Germany). Pore structure characterization was conducted using mercury intrusion porosimetery (MIP) with solid sample. MIP was conducted using an Autopore IV 9500 and high pressure was applied, delivering a peak of 230 MPa. The porosity utilizing MIP was calculated using

$$Porosity(\%) = \frac{100xV_T}{V_B},$$ (3.3)

where, V_T = Total intrusion volume, and V_B = Bulk volume. The Bulk volume was defined as,

$$V_B = V_P - V_m,$$ (3.4)

where, V_p = user entrained volume for the penetrometer, V_m = volume of mercury in the penetrometer.

3.3 Results and Discussion

3.3.1 Corrosion Potential and Rates

The corrosion potential measurements of the reinforcement during the carbonation exposure period are shown in Figure 3.3.
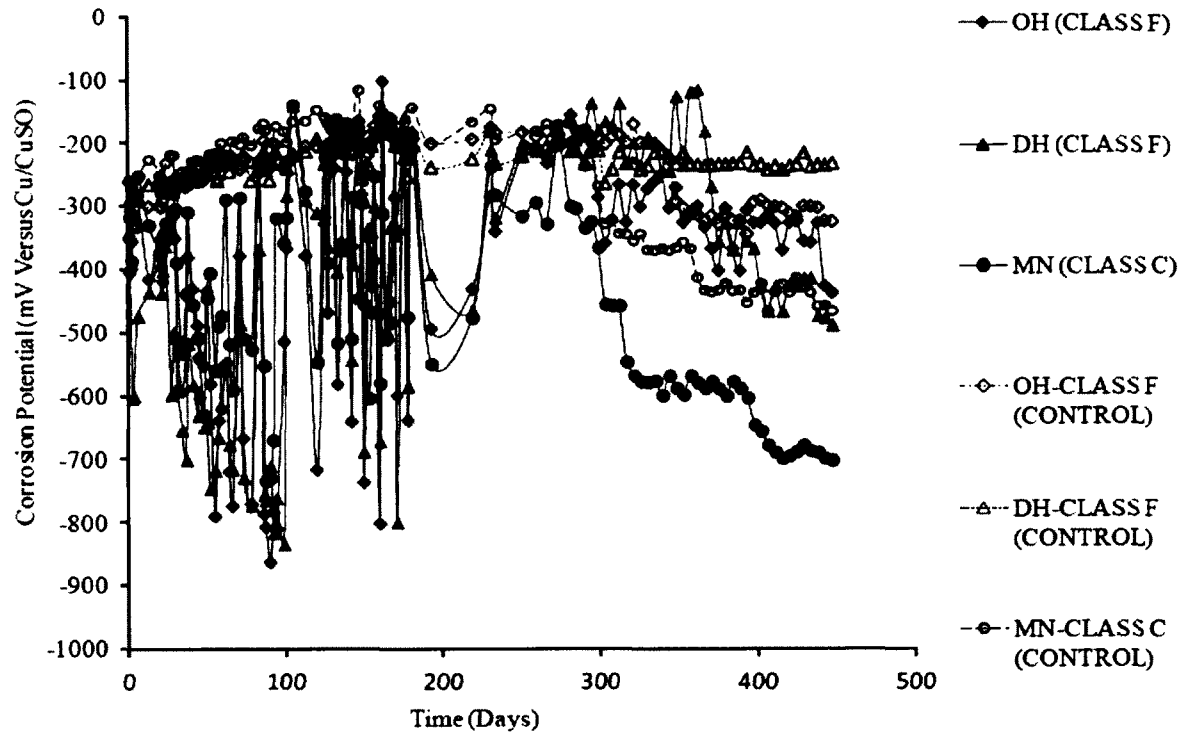
Figure 3.3: Corrosion potential analysis of reinforcement.

The time lines in these figures start one week following batching. The values shown represent the average of three specimens. During the initial period (up to 200 days) of carbonation exposure, the corrosion potential dropped to -850 mV versus CSE for OH-GPC, -820 mV versus CSE for GPC-DH and -620 mV versus CSE for MN-GPC. The sudden drop in corrosion potential could be related to the lack of oxygen, which was also observed by other carbonation studies [156,157]. After 280 days of exposure, the GPC prepared with Class C fly ash showed a constant decrease in corrosion potential from -350 mV to -720 mV versus CSE, while GPC prepared with Class F exhibited a decrease in corrosion potential up to

-520 mV versus CSE for DH-GPC and -498 mV for OH-GPC. The GPC control prepared

from Class F GPC exhibited corrosion potential values up to -280 mV versus CSE (GPC-

OH), -310 mV versus CSE (GPC-DH), while GPC-MN showed an increase in negativity of

corrosion potential to - 480 mV. These observations suggest that the GPC prepared from Class

C fly ash is more susceptible to atmospheric carbonation when compared to GPC prepared

from Class F fly ashes [158–160]. GPC-MN, which was subjected to accelerated carbonation

exposure, showed indication of initiation of severe corrosion when compared with geopolymer

concrete specimens made using Class F fly ash. Corrosion rates were measured using the

linear polarization resistance method as shown in Figure 3.4.
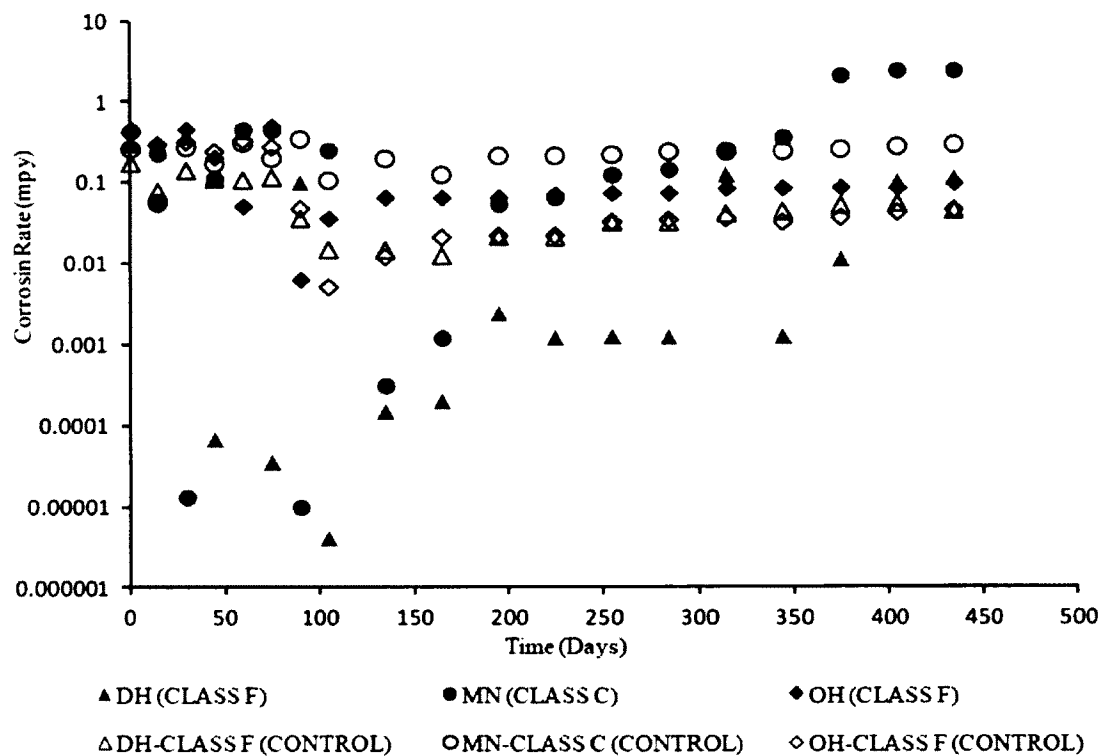
Figure 3.4: Corrosion rates of GPC prepared with Class C and F fly ash.

Corrosion rates were monitored regularly until the end of the carbonation exposure

period (450 days). The corrosion rates for GPC-MN increased from 0.0012 mpy after 165

days to 2.455 mpy at the 450th day when exposed to accelerated carbonation, while GPC-OH

and GPC-DH exhibited 0.098 mpy and 0.114 mpy, respectively (refer to Table 3.4).

Table 3.4: Corrosion potential and corrosion rates for GPC prepared with Class F and C fly ash.

Time (Days)			105		225		325		450	
Binder Type	Fly ash Type	Exposure Type	Ecorr (mV)	CR (mpy)	Ecorr(mV)	CR (mpy)	Ecorr (mV)	CR (mpy)	Ecorr(mV)	CR (mpy)
GPC MN	Class C	Carbonated	-138	0.2525	-475	0.0652	-567	0.254	-701	2.455
GPC DH	Class F	Carbonated	-139	0.000147	-463	0.0012	-198	0.1242	-487	0.114
GPC OH	Class F	Carbonated	-224	0.03626	-430	0.07125	-265	0.0854	-436	0.0985
GPC MN	Class C	Control	-165	0.10673	-165	0.221	-354	0.221	-465	0.2948
GPC DH	Class F	Control	-216	0.01480	-223	0.032	-231	0.041	-234	0.045
GPC OH	Class F	Control	-219	0.005120	-192	0.0325	-169	0.035836	-323	0.0458

Ecorr: Corrosion Potential, CR: Corrosion rate

GPC-MN exhibited a higher corrosion rate by a factor of 21 and 24 when compared

with GPC-DH and GPC-OH after 450 days of carbonation treatment. The controls prepared

with Class C fly ash (GPC-MN) showed an increase in the corrosion rate by a factor of 6 when

compared to GPC control specimens prepared with Class F fly ashes. The electrochemical

analysis indicated that the reinforcement inside GPC prepared with Class F fly ash showed

superior corrosion resistance as compared with GPC prepared with Class C fly ash by

maintaining the passivation film when exposed to accelerated carbonation treatment. The

deteriorated performance by GPC's prepared with Class C fly ash could be attributed to the

formation of calcium carbonate. The high calcium oxide (12.93%) content of the fly ash could

have led to the formation of calcium carbonates, which in return led to the reduction of the pH,

causing degradation at the rebar/matrix interface due to accelerated carobnation treatment.

Upon completion of 450 days of carbonation exposure, the specimens were subjected to an

indirect tensile test as per ASTM C 496.

3.3.2 Mechanical Testing

Results of the indirect tensile test for the control and carbonation treated specimens are shown in Figure 3.5.
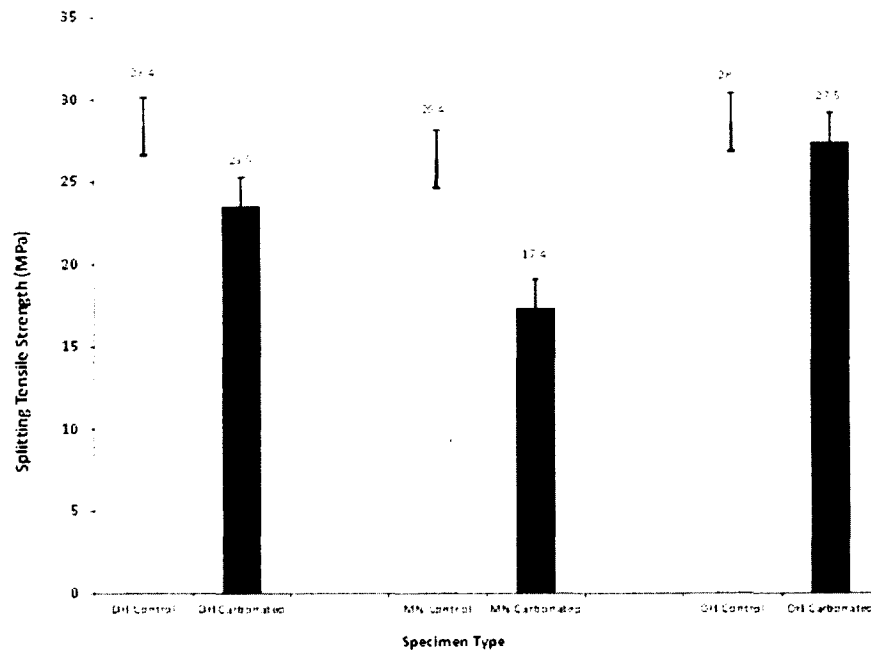
Figure 3.5: Splitting tensile test of GPC specimens of control and carbonated specimens after 450 days of carbonation exposure.

The GPC MN, DH and OH exhibited a splitting tensile strength of 17.4 MPa, 23.5 and 28.6 MPa, respectively, after 450 days of accelerated carbonation exposure. Both the carbonation treated and controls for the GPC-MN showed the least strength as compared to their counterparts prepared from Class F fly ash (GPC DH, OH). GPC-MN exhibited a 34% strength loss when compared to the controls. For GPC-DH and GPC-OH, the strength loss when compared with the controls were 17% and 3%, respectively. The rebar concrete/interface of GPC DH, OH and MN are shown in Figures 3.6 and Figure 3.7, respectively.
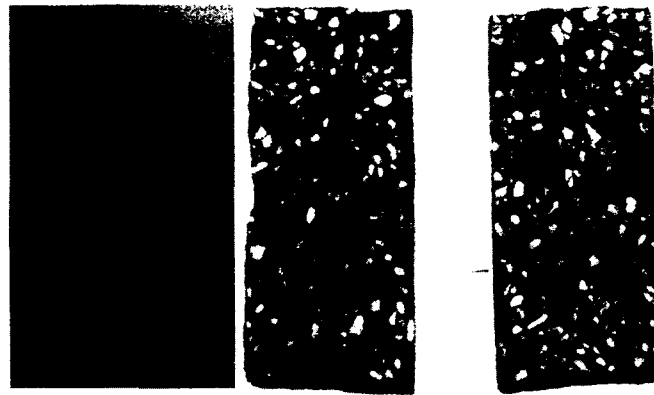
Figure 3.6: Reinforcement/concrete interface A) OH and B) DH prepared with Class F GPC.
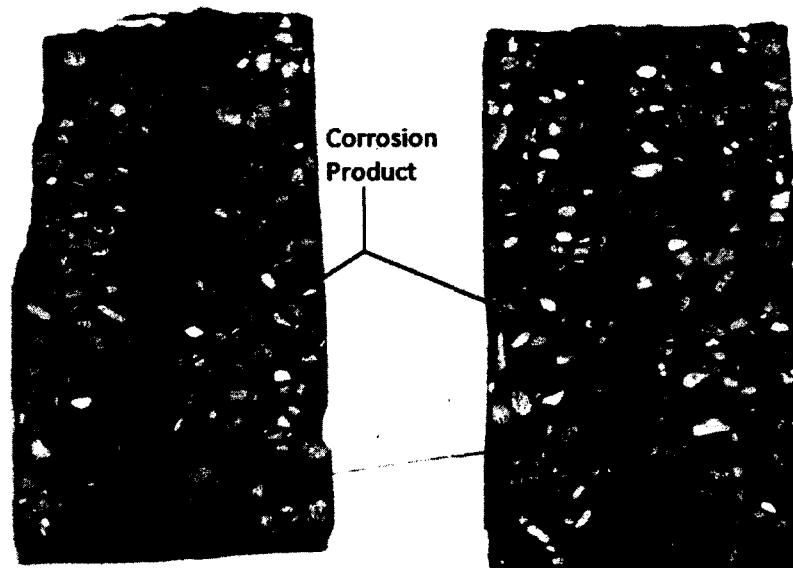
Figure 3.7: Reinforcement/concrete interface of MN-GPC prepared with Class C fly ash.

GPC prepared with Class F fly ash did not show any signs of corrosion products after 450 days of carbonation exposure, while GPC-MN exhibited signs of corrosion products at the rebar/concrete interface as shown in Figure 3.7.

The visual observations support the results of the electrochemical analysis and it indicates that the corrosion of the steel reinforcement at the GPC-MN specimen led to the formation of corrosion products, which in return led to the expansion of these products, thus

weakening the cement/matrix at the rebar/concrete interface. GPC's prepared with Class F fly ashes exhibited superior corrosion resistance while maintaining their passivity and strength, as compared with geopolymer concrete prepared using Class C fly ash.

3.3.3 Chemical Analysis

The results of the chemical analysis that were conducted using phenolphthalein and Alizarin Yellow indicators are shown in Figures 3.8 and 3.9, respectively.
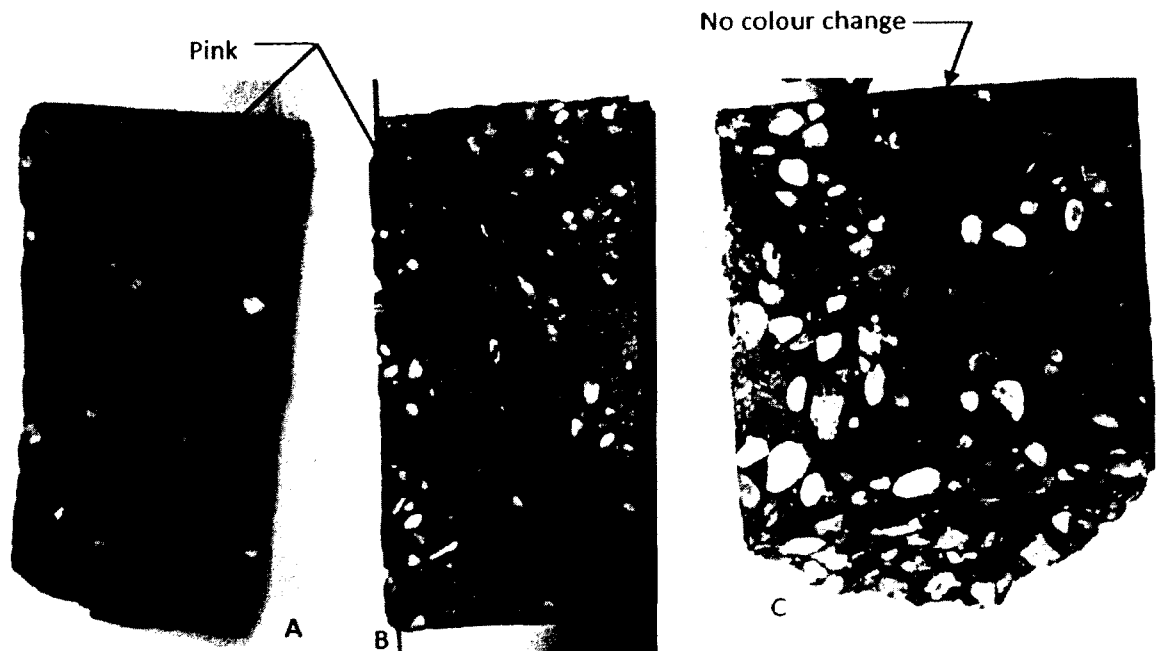
Figure 3.8: Geopolymer concrete subject to phenolphthalein test A: GPC-OH, B: GPC-DH, C: GPC-MN.
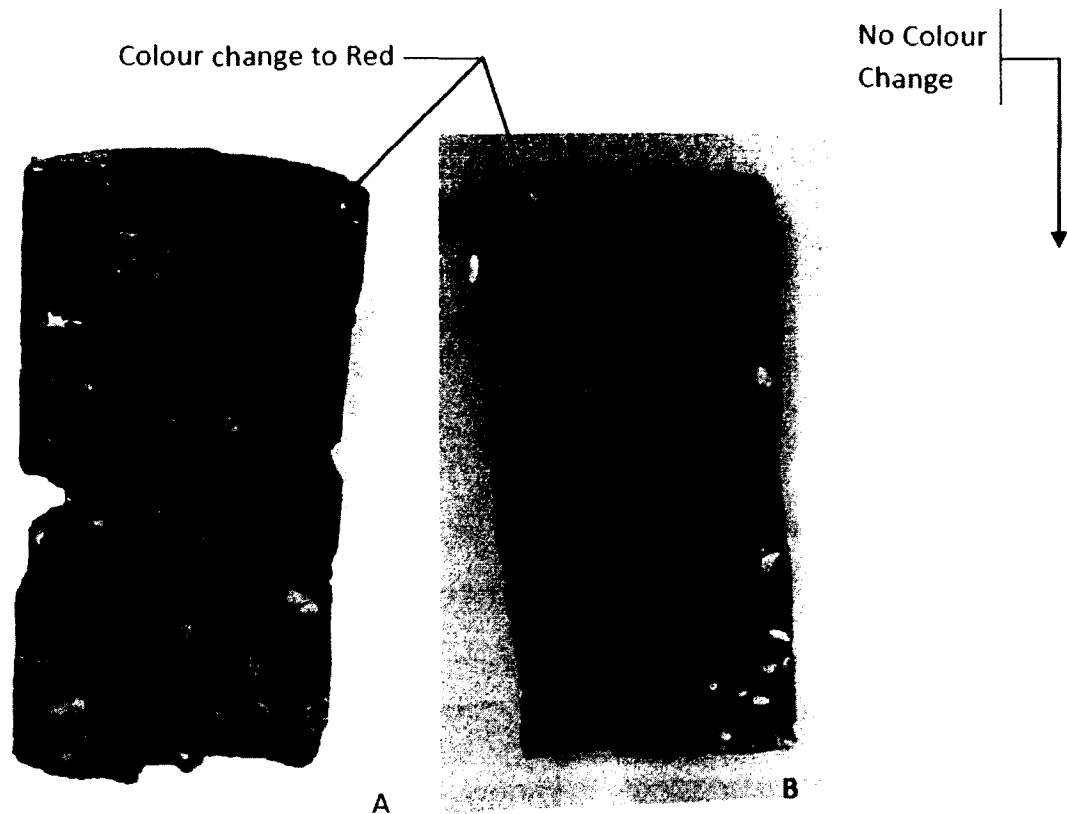
Figure 3.9: Geopolymer concrete subject to alizarin yellow test A: GPC-OH , B: GPC-DH, C: GPC-MN.

GPC-OH and DH prepared from Class F fly ash showed a color change from colorless to pink at the reinforcement/concrete interface, while GPC-MN remained colorless at the interface. This indicates that the pH range was between 8.0-9.5 for GPC-MN while the pH was greater than 9.5 for GPC-DH and OH (Refer to Figure 3.8). GPC-OH and DH showed a color change from yellow to red when subjected to alizarin yellow indicator, indicating the pH was greater than 12.0. The matrix retained its alkaline nature, which means it maintained the passivation protection around the steel reinforcement (Refer to Figure 3.9).

GPC-MN did not exhibit a color change for either phenolphthalein or Alizarin Yellow R indicators. Steel corrodes at a pH range below 10-11 due to the breakdown of the passive layer, leading to corrosion of the reinforcement [155]. GPC DH and OH did exhibit a color

change to red when exposed to the alizarin yellow R indicator, indicating a pH greater than 12. Thus, it is of little surprise that no signs of corrosion were observed after 450 days of carbonation treatment. The results of the study demonstrated that GPC prepared from Class F fly ashes are less vulnerable to carbonation when compared to GPC prepared from Class C fly ashes. XRF analysis of grounded GPC samples taken at the reinforcement/concrete interface is shown in Figure 3.10.
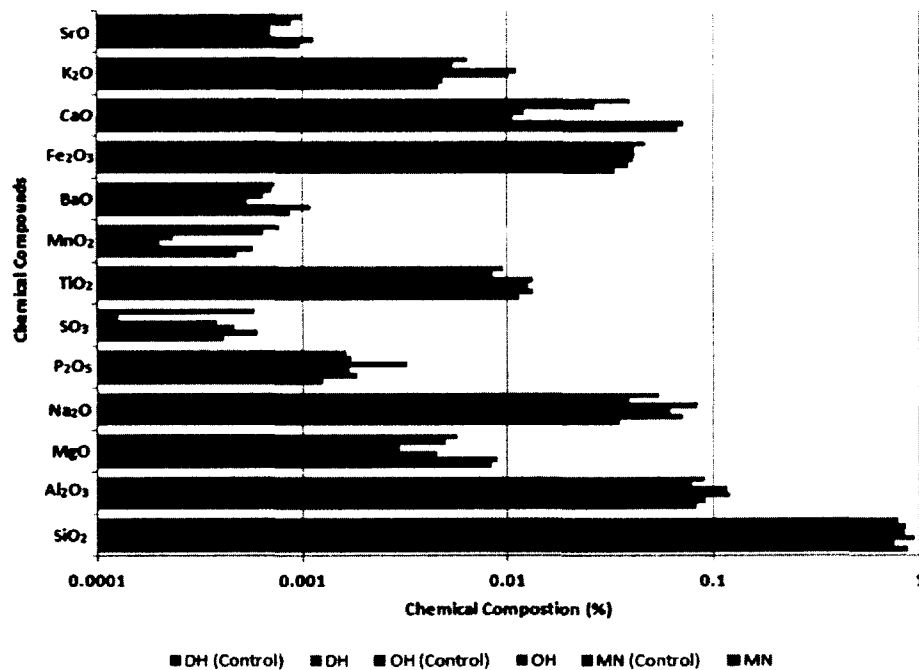
Figure 3.10: X-ray fluorescence (XRF) spectroscopy of GPC prepared with Class C and F fly ash.

The carbonated and control specimen of GPC-MN exhibited CaO content of 6.74% and 7.17%, respectively, while GPC's prepared with Class F fly ash showed 1.08% (GPC-OH carbonated), 1.20% (GPC-OH Control), 2.60% (DH-Carbonated), and 3.99% (DH-Controls). In addition, GPC-MN showed higher concentrations of MgO for both controls and carbonation treated specimens when compared with GPC specimens made from Class F fly ash.

GPC-OH and GPC-DH showed higher content of Al_2O_3 and SiO_2 when compared to GPC-MN at the rebar/concrete interface. The formation of calcium alumino silicate hydrate (C-A-S-H) may have contributed to the formation of a dense zone which may have prevented the ingress of CO_2. This may indicate that GPC's prepared with Class F fly ash led to sufficient formation of the amorphous C-A-S-H zone (strength initiation phase) and thus led to a strong bond at the rebar/matrix interface. Additional microstructure and pore structure characterization conducted using SEM/EDS and MIP are reported in the following sections.

3.3.4 SEM and EDS Analysis

Results for SEM analyses of the rebars after 450 days of carbonation exposure, which were embedded in geopolymer concrete specimens, are shown in Figures 3.11, 3.12 and 3.13.
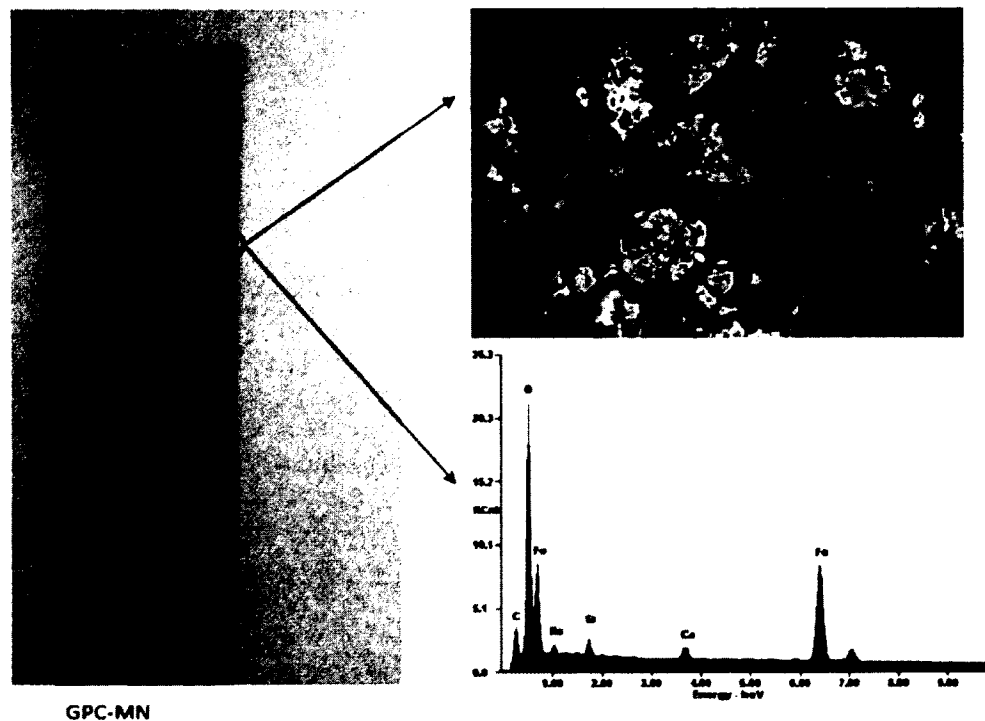
GPC-MN

Figure 3.11: SEM image of the reinforcement embedded in the GPC-MN geopolymer specimen (Class C fly ash) after 450 days of carbonation exposure.
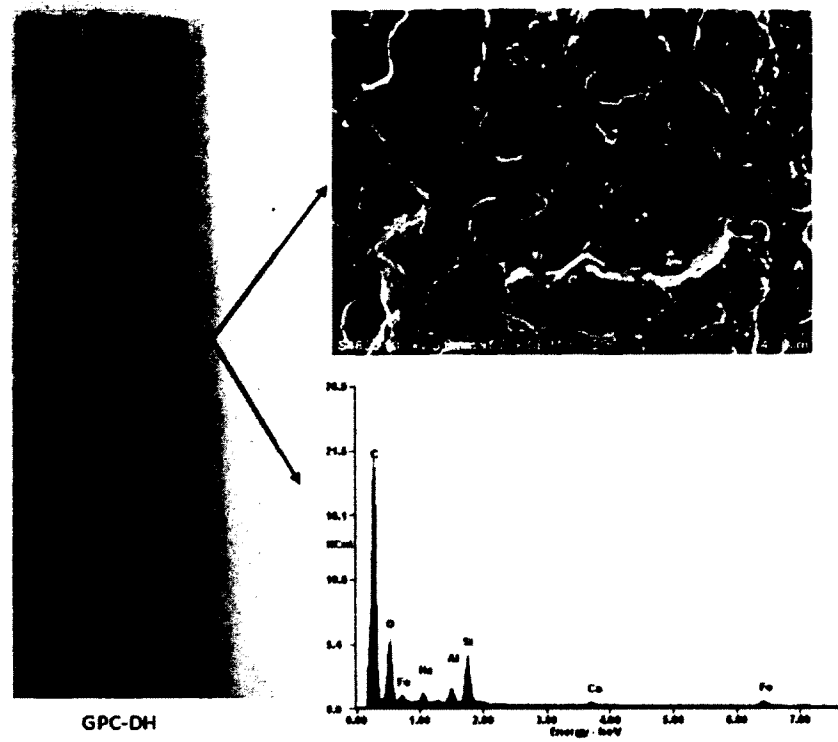
Figure 3.12: SEM image of the Reinforcement embedded in the GPC-DH specimen after 450 days of accelerated carbonation exposure.
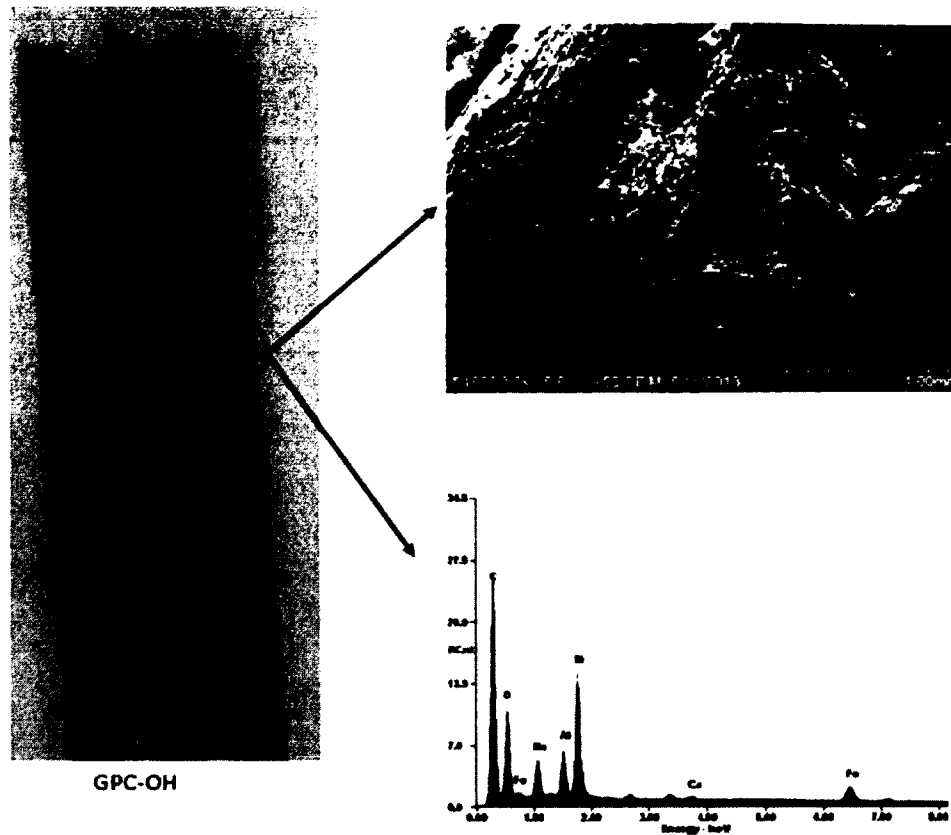
Figure 3.13: SEM image of the reinforcment embedded in the GPC-OH specimen after 450 days of accelerated carbonation exposure.

The rebar which was embedded in the GPC MN specimen was completely corroded after 450 days of accelerated carbonation treatment as shown in Figure 3.11. The corrosion analysis indicates that the rebar inside MN was completely corroded ($\sim$100%), while DH and OH rebars showed 9% and 4 % surface corrosion, respectively. The elemental composition of EDS analysis on the rebar showed the presence of Fe (24.09%) and O (2.08%), indicating the possible formation of ferrous oxide. The GPCs prepared from Class F fly ashes were found to have minimal presence of Fe (2.08%), and higher traces of Al (0.7% for DH Rebar, 1.62% for OH Rebar) and Si (2.21% for DH, 4.57% OH) on the rebars as shown in Table 3.5.

Table 3.5: Elemental composition of Reinforcement and Reinforcement/concrete interface after carbonation exposure.

Binder Type	Location	Elemental Compositon (%)						
		C	O	Na	Al	Si	Ca	Fe
GPC MN	Rebar	28.8	43.4	1.40	0.12	1.19	1.12	24.09
GPC DH	Rebar	79.61	15.73	0.58	0.7	2.21	0.21	0.95
GPC OH	Rebar	73.75	15.93	1.89	1.62	4.57	0.16	2.08
GPC MN	R/C Interface	30.85	36.14	0.05	0.36	1.78	0.73	30.08
GPC DH	R/C Interface	-	54.40	4.65	9.1	25.26	2.22	2.71
GPC OH	R/C Interface	-	55.93	3.83	7.17	13.27	1.15	15.96

R/I: Rebar/Concrete Interface

Data obtained from electrochemical, SEM and EDS analyses indicate that the reinforced GPC prepared from Class F fly ashes are more resistant to carbonation, as compared with GPC prepared from Class C fly ashes. Higher traces of alumina and silica suggest that a protective layer of N-A-S-H might provide a chemical bond at the rebar/concrete interface, which, combined with a dense cementitious matrix, resulted in elevated resistance to carbonation. Pore structure, XRD and IR analyses were conducted to examine the effect of the C-A-S-H gels on the densification of geopolymer concretes [161–163]. SEM and EDS analyses at the rebar/concrete interface for GPC DH, OH and MN are shown in Figure 3.14, 3.15 and 3.16, respectively.
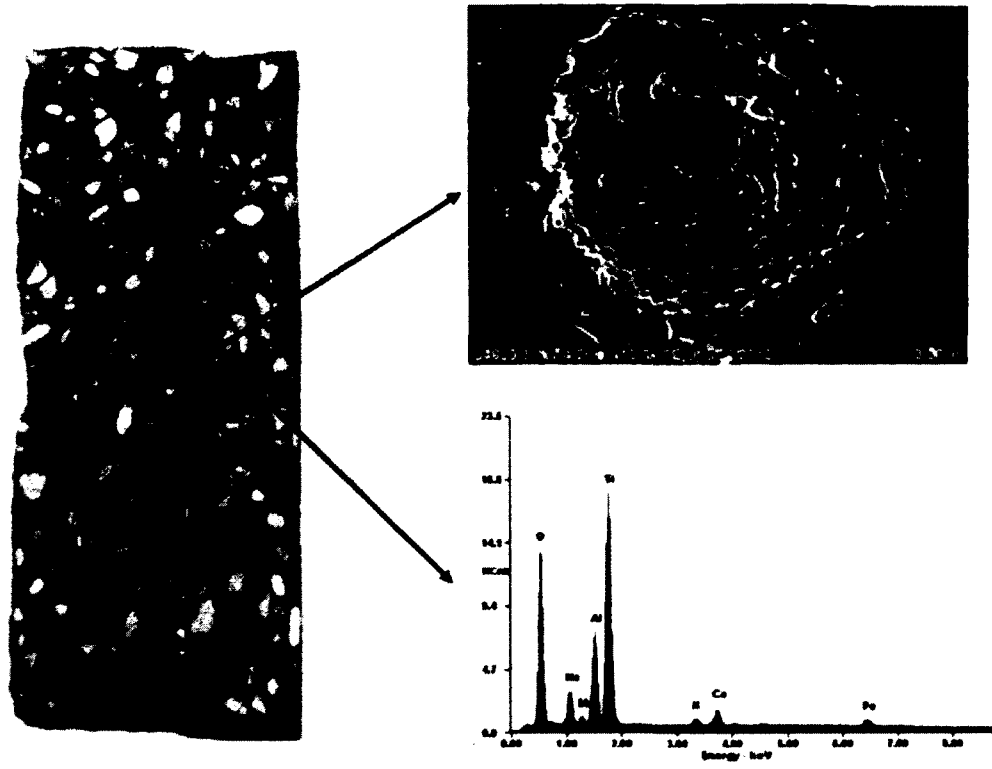
Figure 3.14: Reinforcement/Concrete interface of GPC-DH after 450 days of exposure.
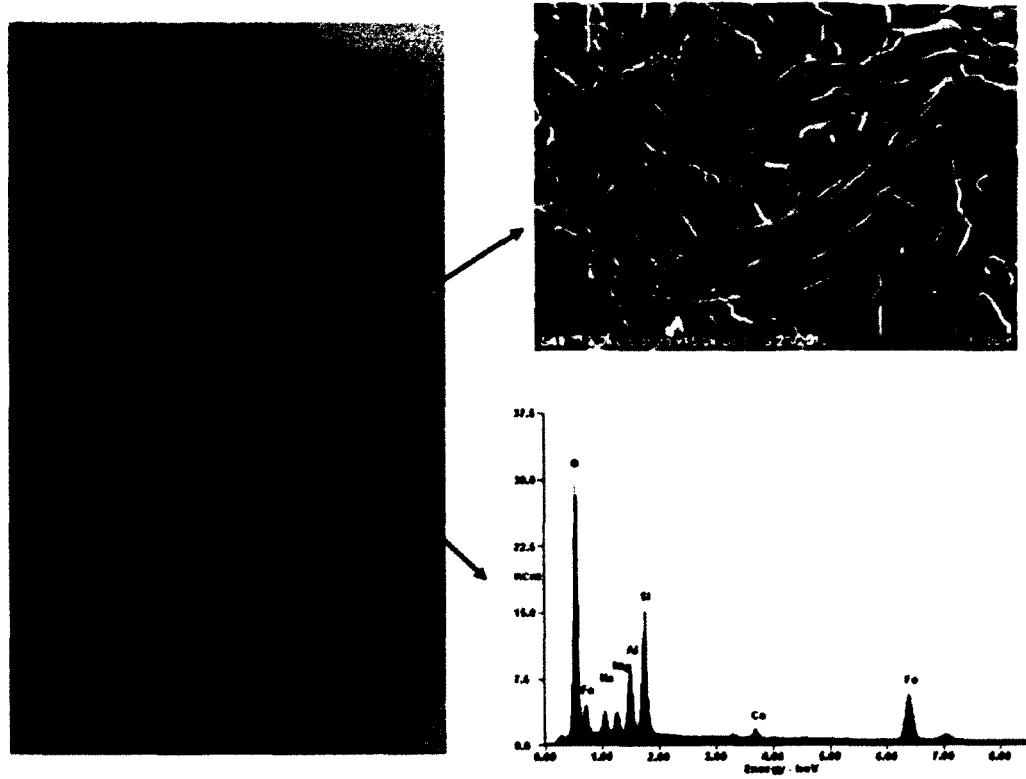
Figure 3.15: Reinforcement/Concrete interface of GPC-OH after two years of exposure.
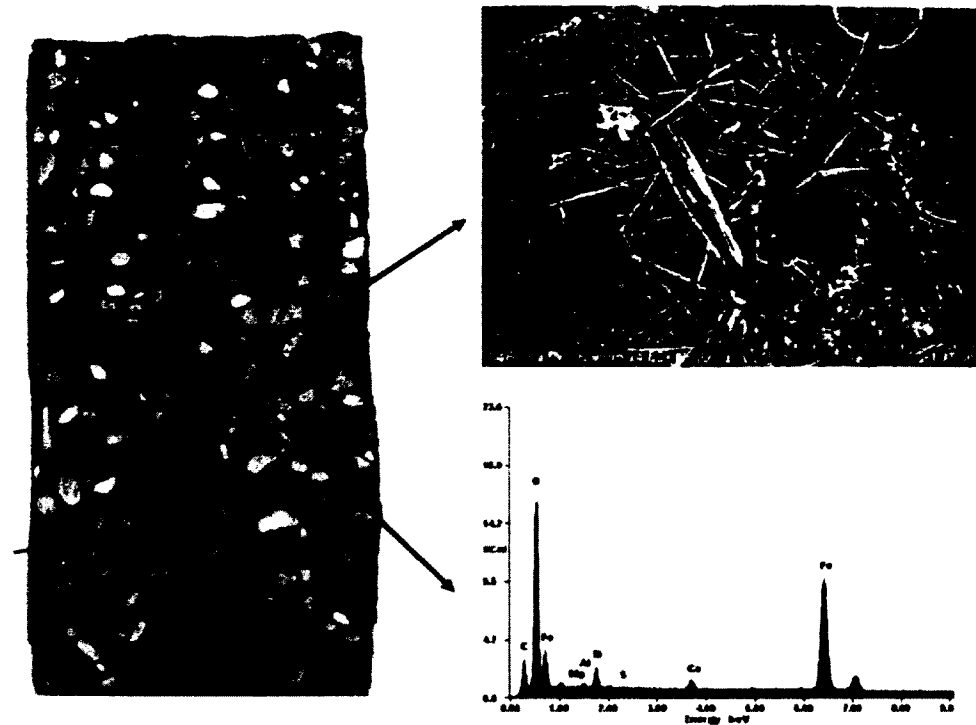
Figure 3.16: Reinforcement/Concrete interface of GPC-MN (GPC-Class C fly ash) after 450 days of carbonation exposure.

The Fe content at the rebar/concrete obtained via EDS were 30.08%, 15.96% and 2.71% for GPC-MN, OH and DH, respectively (Refer to Table 3.5). Higher traces of Si (25.26% = DH, 13.27 % = OH), Na (4.65% = DH, 3.83 % = OH) and Al (9.1 % = DH, 7.17 % = OH) were detected for GPC's prepared with Class F fly ashes. GPC-MN exhibited Al = 0.36%, Na= 0.05%, and Si = 1.78%. Additionally, the SEM analysis indicated an amorphous zone in the case of GPC-DH, as shown in Figure 3.15. Figure 3.16 presents the SEM/EDS results for the GPC-MN specimen, revealing needle like corrosion products at the re-bar matrix interface.

GPCs prepared with Class F fly ash had higher traces of Al and Si by factors of 22 and 11, respectively, at the rebar/concrete matrix as compared with GPC prepared with Class C fly ashes. This might be attributed to the formation of an additional N-A-S-H zone, which led

to densification in the immediate vicinity of the rebar and provided an enhanced mechanical interlock at the rebar/concrete interface [163, 164].

3.3.5 Pore Structure Characterization

Pore structure characterization of geopolymer concrete at the reinforcement/concrete interface was performed using mercury intrusion porosimetry (MIP) as shown in Figure 3.17.
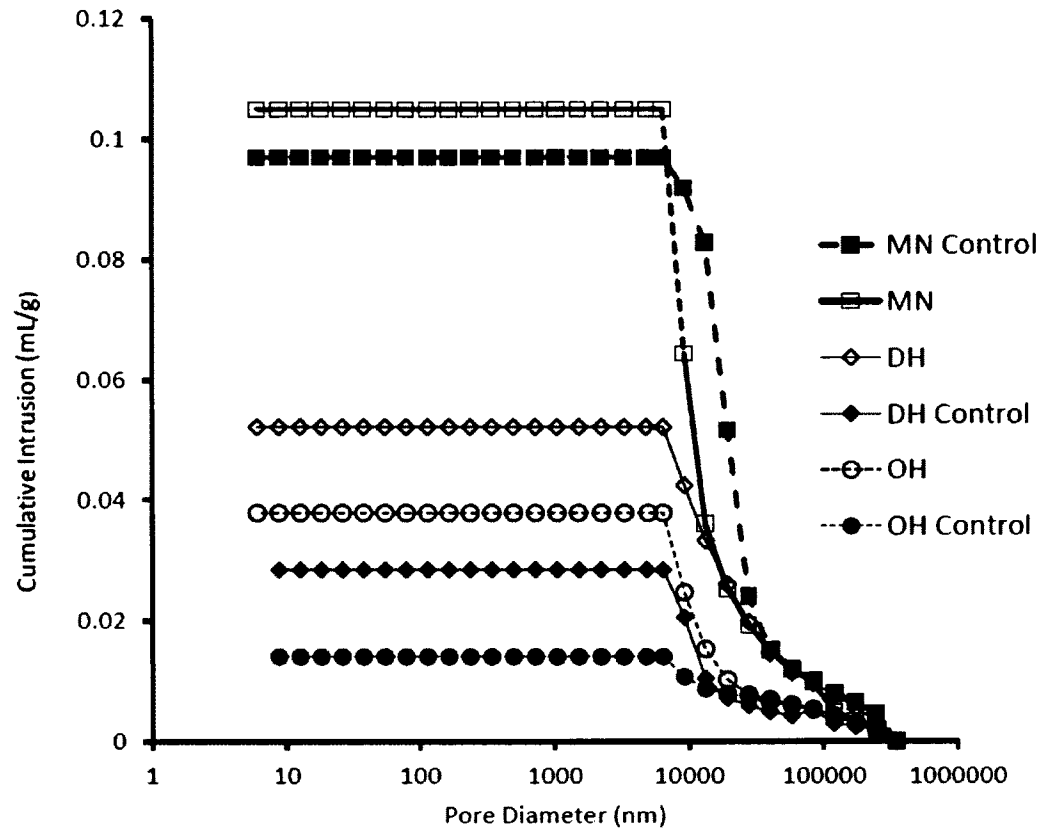
Figure 3.17: Mercury intrusion porosimetry analysis of control and carbonation exposed GPC specimens.

GPC-MN exposed to 450 days of carbonation exhibited the highest porosity (28%) while the control exhibited 15% porosity. Threshold pore diameters were calculated using the second inflection point method which indicates the minimum diameter of the pores that lead to the formation of a continuous pore network throughout the cement matrix along with the inception of percolation [165].

GPCs prepared with Class F fly ash exhibited lower porosity values (GPC-OH=10%, GPC-DH = 12%) as compared with GPC-MN (28%) when subjected to accelerated carbonation. The average of GPC OH and DH exhibited a reduction in threshold pore diameter by a factor of 10 as compared with GPC-MN. The porosity data indicates that the GPCs prepared with Class F fly ash (GPC-DH and OH) exhibited a dense structure at the rebar/concrete interface. This dense microstructure prevented the ingress of CO_2, which helped in mitigating the adverse effects of carbonation. In addition, the dense microstructure exhibited by GPC-DH and OH led to the mobilization of a higher mechanical strength when subjected to an indirect tensile test as shown in Table 3.6.

Table 3.6: Pore structure and mechanical strength analysis.

Specimen Type	Fly Ash Type	Porosity (%)	Threshold Pore Diameter (nm)	Splitting tensile strength (MPa)
DH Control	Class F	9	13245	28.41
OH Control	Class F	7	10354	23.54
MN Control	Class C	15	35684	26.44
DH	Class F	12	17411	23.54
OH	Class F	10	16254	24.47
MN	Class C	28	175468	17.35

3.3.6 XRD and ATR-FTIR Analysis

XRD analysis of carbonated and control specimens is shown in Figure 3.18.

V
C
Q

Q : Quartz, N: Natron, C: Calcite, V: Vaterite,

M: Mullite, He: Hematite, Ak: Akaganeite

M

Q
V
N
Ak
He
Ak C V Ak
Q
C
He
M
MN

M
N C V Ak
He
DH

M
N N V Ak
He
OH

M
Q
N
N N N V Ak
He
OH Control

Q
N N V Ak
He
MN Control

N N V Ak
He
DH Control

0   10   20   30   40   50   60   70   80   90   100

Angle (2θ)
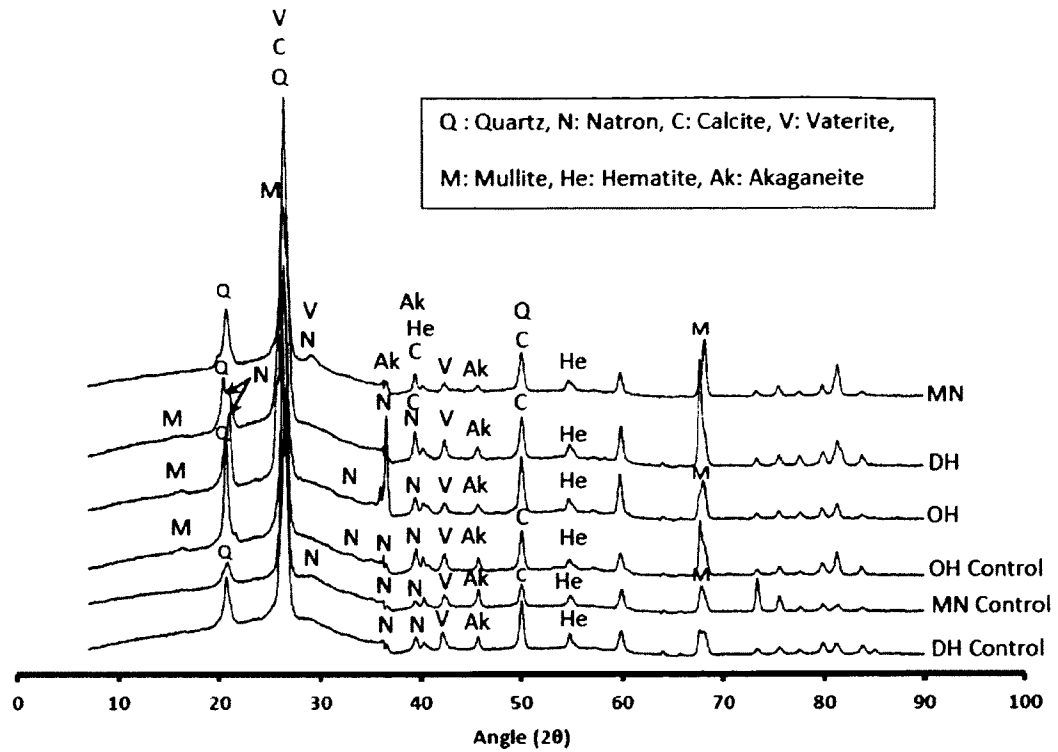
Figure 3.18: X-Ray diffraction (XRD) analysis of control and carbonation exposed geopolymer concretes.

Phases detected include Mullite, Quartz and Hematite, Natron, Calcite, Vaterite, Mullite and Hematite. Natron phase was detected, which can be related to sodium rich carbonation, since 14 M NaOH solution was used in the alkali activation [163]. Calcite, along with natron and vaterite, was the main carbonation product in GPC-MN.

The formation of carbonation products could lead to the destabilization of the N-A-S-H gel, which was related to the loss of mechanical strength in GPCs prepared with Class F fly ash, as shown in Figure 3.4. The results of the quantitative phase analysis for carbonated and uncarbonated specimens are shown in Figure 3.19.
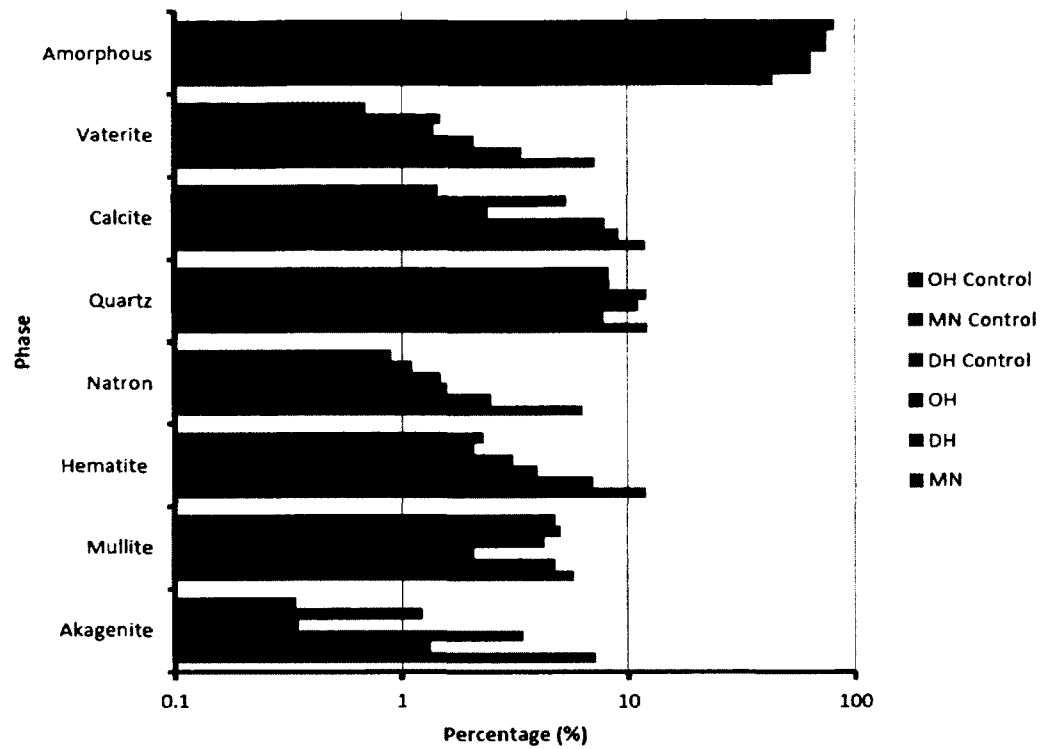
Figure 3.19: Quantitative phase analysis of control and carbonation treated specimens.

The carbonated specimens prepared with Class C fly ash exhibited higher contents of carbonation phases such as Natron (6.3%), Calcite (12%) and Vaterite (7.2%). In addition, a severe form of corrosion product known as akaganeite was detected at the rebar/concrete interface [158]. GPC specimens prepared from Class F fly ashes exhibited lower percentages of carbonation and corrosion product phases. Calcite and vaterite are exposed to higher CO_2 concentrations. Vaterite is considered to be least stable, and it indicates that overall carbonation capacity is higher as compared to calcite. Vaterite and calcite are transformed phases of calcium carbonate. Carbonated concrete transforms to vaterite and in later stages it transforms to aragonite [166]. In addition, the amorphous content of GPC (MN) decreased to 44% due to the effect of carbonation while GPC DH and OH had higher amorphous contents of 75.17% and 63.95%, respectively. This reduction in amorphous content was attributed to

the more extensive carbonation of GPC-MN specimen when compared with their GPC-DH and OH counterparts. The higher amorphous content could also be attributed to the greater dense pore structure. The dense cement matrix inhibits the ingress of CO_2, which along with the protecting C-A-S-H layer mitigated the carbonation process [162]. This indicates that the C-A-S-H gel may have been depleted under accelerated carbonation conditions (i.e, decrease in amorphous content) leading to the breakdown of the protective layer in the case of the GPC-MN specimens, causing the rebar inside the GPC-MN specimens to corrode (refer to Figure 3.11), and subsequently leading to the loss of strength at the rebar/concrete interface.

3.4 Conclusions

The results of this study suggest that the resistance of geopolymer concrete binders to carbonation depends on several key parameters such as the formation of a protective coating of C-A-S-H and N-A-S-H gels as well as the nature of the pore structure of the resulting matrix [163, 164, 167].

CHAPTER 4

EXPERIMENTAL PROCEDURE, RESULTS AND DISCUSSION : ELEVATED TEMPERATURE

4.1 Introduction

Ordinary Portland Cement is the most widely used construction material, but it has a severe limitation when subjected to elevated temperature. Traditional OPC based structures, when subjected to elevated temperature, suffer from loss of mechanical strength leading to a catastrophic failure [189]. The primary reason for OPC-based materials to fail during or after a fire is the destruction of the calcium silicate hydrate (C-S-H) gel along with various crystalline hydrates [190–192].

A conventional approach to enhance the thermal properties of OPC is to use pozzolanic additives for binding calcium hydroxide to C-S-H gel, although this method could extend the temperature of application up to 700° C. It is associated with the initial loss of mechanical strength and tends to lose strength further after exposure to fire. The pore structure of OPC concrete indicates that gel porosity increases significantly with an increase in temperature. The gel and capillary water evaporate at 100-150° C while accompanied by cracking and shrinkage between the temperature range of $\sim$ 150-250° C. At 250-300° C, the compressive strength of the concrete decreases, due to the evaporation of chemically bound water from aluminum and ferrous constituents. An additional strength decrease was observed with the increase in temperature from 300-400° C, as the calcium hydroxide dehydrates to calcium

oxide, while decomposition of C-S-H is completed at (400-650° C), exhibiting a significant strength reduction.

Alternative cements used for high temperature applications are costly and have disadvantages such as variations in mechanical strength, high viscosity, and short setting time [193]. Studies have shown that alkali activated slag cements have exhibited higher resistance when subjected to elevated temperatures. The reasons for this superior behavior could be attributed to the formation of crystalline phases called anhydrous alumino silicates such as sodalite, analcime, and chabazite. These phases improve the crystallinity during heating up to 200-400° C, maintaining the structure up to approximately 800°C, and then recrystallize to new zeolite phases such as nepheline or albite. These contribute to enhancement of the mechanical strength [194,195]. Variables such as the type of fly ash (Class C or F), activation mechanism, silica to alumina ratio of the sodium alumino silicate hydrate (N-A-S-H) on the resistance of geopolymer concretes to elevated temperature were investigated in the study reported herein.

A comparison of advantages and disadvantages associated with alternative cementitious binders is shown in Table 4.1 [189].

Table 4.1: Comparison of alternative binders to Portland cement [187].

	Portland cement	Calcium Aluminate Cement	Calcium Sulfoaluminate Cement	Alkali-activated binder	Super sulfated cement
Primary phases/materials	C_3S	CA	$C_4A_3\bar{S}$, C_4AF	Aluminosilicate alkali	Slag, CS/CSH_2
Hydrates	C-S-H, CH, Aft	CAH_{10}, C_2AH_8, C-S-H	Aft, AFh, AFm, C_2ASH_8	Gel (N-A-S-(H) and C-(A)-S-H, zeolytes	Aft, C-S-H, AFm
Advantages	• Long History • Standard Composition	• Rapid Strength • Sulfate Resistant • Abrasion Resistant	• Low energy • Rapid Strength	• Low heat of reaction • Heat and acid resistant	• Low heat of hydration • Durable in aggressive environment
Disadvantages	• High Energy • High CO_2 • Limited early strength • Poor in aggressive environment	• Strength loss on conversion of metastable to stable hydrates	• Costly	• Durability unproven • Challenging rheology • Durability unproven	• Slow strength gain

Research in recent years has shown dramatic improvements in the performance of alternative cementitious binders, although a more in depth understanding is required of their chemistry, reaction mechanisms and property development. Geopolymer concrete is the next generation binder technology which is green in nature, sustainable, has a low carbon foot print, environmentally friendly, and possesses high durability when compared to Ordinary Portland Cement [190, 191]. Although the material shows superior durability in terms of

high temperature, acid resistance and corrosion, a comprehensive study is needed to provide quality guidelines for the utilization of this product for public construction. The proposed study relates the result of durability testing to the changes at the microstructural level when subjected to elevated environment, so to gain understanding of behavior of GPC at elevated temperatures.

Geopolymer concrete has the potential to be at the leading edge of a shift in the construction industry towards sustainable, durable, and minimum energy consuming cementitious binders with greatly reduced carbon footprint. Geopolymer cements offer an intriguing combination of characteristics such as higher mechanical strength, excellent chemical durability, a variety of environmental benefits, and strong potential for commercial applications [198–200]. The field of geopolymer cements also provides significant scientific challenges associated with the need for better understanding of polymerization reactions, kinetics and the precursors involved in this reaction, the relationships between mix design and the mechanical properties of the resulting cementitious matrix, and durability mechanisms when subjected to extreme environments [189,201].

4.2 Experimental Procedure

Geopolymer concrete (GPC) was prepared by using eleven types of fly ashes obtained from three different countries (USA, Israel and China). The specimens were 50 mm cubes. White fused alumina with a nominal size of 5 mm was used as coarse aggregate. Silica sand and commercially available fine alumina aggregate (tabular alumina of nominal size of 2.36 mm) was used as fine aggregate in the preparation of the GPC specimens as shown in Table 4.2.

Table 4.2: Sample designation, fly ash and aggregate type used in preparation of geopolymer concrete.

Sample Name	Fly Ash type used to prepare GPC	Country of origin of fly ash	Fine Aggregate	Test of exposure	Sample Name	Fly Ash type used to prepare GPC	Country of origin of fly ash	Fine Aggregate	Test of exposure
TS-W-1	Class F	USA	'P' Gravel	TS	TS-W-7	Class C	USA	'P' Gravel	TS
C-W-1	Class F	USA	'P' Gravel	Control	C-W-7	Class C	USA	'P' Gravel	Control
TS-WO-1	Class F	USA	Alumina	TS	TS-WO-7	Class C	USA	Alumina	TS
C-WO-1	Class F	USA	Alumina	Control	C-WO-7	Class C	USA	Alumina	Control
TS-W-2	Class F	USA	'P' Gravel	TS	TS-W-8	Class F	Israel	'P' Gravel	TS
C-W-2	Class F	USA	'P' Gravel	Control	C-W-8	Class F	Israel	'P' Gravel	Control
TS-WO-2	Class F	USA	Alumina	TS	TS-WO-8	Class F	Israel	Alumina	TS
C-WO-2	Class F	USA	Alumina	Control	C-WO-8	Class F	Israel	Alumina	Control
TS-W-3	Class F	China	'P' Gravel	TS	TS-W-9	Class F	Israel	'P' Gravel	TS
C-W-3	Class F	China	'P' Gravel	Control	C-W-9	Class F	Israel	'P' Gravel	Control
TS-WO-3	Class F	China	Alumina	TS	TS-WO-9	Class F	Israel	Alumina	TS
C-WO-3	Class F	China	Alumina	Control	C-WO-9	Class F	Israel	Alumina	Control
TS-W-4	Class F	China	'P' Gravel	TS	TS-W-10	Class F	China	'P' Gravel	TS
C-W-4	Class F	China	'P' Gravel	Control	C-W-10	Class F	China	'P' Gravel	Control
TS-WO-4	Class F	China	Alumina	TS	TS-WO-10	Class F	China	Alumina	TS
C-WO-4	Class F	China	Alumina	Control	C-WO-10	Class F	China	Alumina	Control
TS-W-5	Class F	China	'P' Gravel	TS	TS-W-11	Class C	USA	'P' Gravel	TS
C-W-5	Class F	China	'P' Gravel	Control	C-W-11	Class C	USA	'P' Gravel	Control
TS-WO-5	Class F	China	Alumina	TS	TS-WO-11	Class C	USA	Alumina	TS
C-WO-5	Class F	China	Alumina	Control	C-WO-11	Class C	USA	Alumina	Control
TS-W-6	Class F	China	'P' Gravel	TS					
C-W-6	Class F	China	'P' Gravel	Control					
TS-WO-6	Class F	China	Alumina	TS					
C-WO-6	Class F	China	Alumina	Control					

TS: Thermal Shock

The chemical composition of the fly ashes is shown in Table 4.3.

Table 4.3: Chemical composition of fly ash stockpiles.

SI. NO	Fly Ash Type	Country of Origin	SiO_2	Al_2O_3	SiO_2/Al_2O_3	CaO	Fe_2O_3	MgO	SO_3	Na_2O	K_2O	LOI
1	Class F	USA	55.07	28.61	1.92	1.97	6.22	1.08	0.19	0.38	2.63	1.82
2	Class F	USA	58.52	20.61	2.84	5.00	9.43	1.86	0.49	0.52	-	0.05
3	Class F	CHINA	47.98	31.17	1.54	8.14	6.50	1.06	0.44	0.25	0.89	1.11
4	Class F	CHINA	48.14	27.12	1.78	8.51	9.14	2.07	1.22	0.28	1.19	0.54
5	Class F	CHINA	55.65	20.93	2.66	7.25	5.55	2.93	0.16	3.39	1.35	0.45
6	Class F	CHINA	56.41	21.47	2.54	11.2	7.3	0.73	0.24	0.87	1.28	0.24
7	Class C	USA	55.61	19.87	2.80	12.93	4.52	2.49	0.49	0.67	0.86	0.22
8	Class F	ISREAL	52.48	25.63	2.05	3.30	9.36	1.69	0.20	0.70	2.20	2.10
9	Class F	ISREAL	55.05	24.58	2.24	3.46	8.52	0.95	0.18	0.73	1.27	2.36
10	Class F	CHINA	45.96	37.00	1.24	2.74	8.49	0.79	0.25	0.33	0.99	0.82
11	Class C	USA	37.77	19.33	1.97	22.45	7.33	4.81	1.56	1.80	0.41	0.17

LOI: Loss of ignition

This study examines geopolymer concrete when subjected to elevated temperature prepared from both Class C and F fly ash stockpiles. Sodium hydroxide (14 M NaOH) and sodium silicate obtained from PQ Corporation (Valley Forge, PA, USA) was used as an activator in the preparation of fly ash based geopolymer concrete. Sodium silicate composed of 45% by weight and SiO_2 to Na_2O ratio of 2:1 was used in preparation of the GPC. Sodium silicate to sodium hydroxide ratio was 1:1 and the activator (sodium hydroxide + sodium silicate) to binder ratio was 0.45. Twenty-four hours after batching, the geopolymer concrete specimens were demolded and cured at a temperature of 80° C for 72 hours.

The specimens were subjected to thermal shock testing by keeping them in the oven at 1093° C and quenching them in water after one hour. Specimens prepared from silica sand and commercially available fine alumina aggregate were then subjected to 5 cycles of thermal shock as shown in Figure 4.1.

Sample No.	Cycle 1	Cycle 2	Cycle 3	Cycle 4	Cycle 5
TS-WO-5					
TS-WO-7					Sample Failed
TS-WO-3					
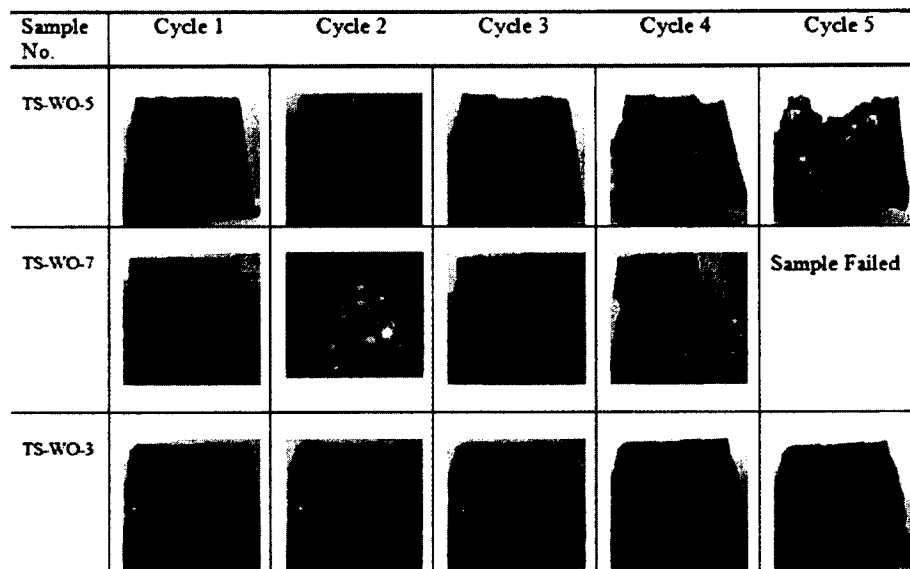
Figure 4.1: Geopolymer concrete cubes with alumina aggregate subject to 5 cycles of thermal shock.

Each thermo-stock cycle for each specimen was evaluated for cracks (classified as minor or major), expansion and total failure. Visual analysis was conducted after each

cycle and digital micrographs of each specimen were taken. Chemical composition of the GPC specimens (controls and thermal shock) was conducted via Energy Dispersive-X-Ray fluorescence (XRF) spectroscopy (ARL QUANT'X EDXRF Spectrometer). In addition, microstructure characterization was conducted using scanning electron microscopy (SEM) and X-Ray diffraction analysis was performed using D8 Advanced Bruker AXS spectrometer. In addition, X-ray micro tomography was conducted to analyze the pore structure of the geopolymer concrete when subjected to thermal shock treatment.

Measurements were carried out using X-ray synchrotron radiation (25 keV) in a parallel beam configuration, with 0.25^o rotation per step with 2 second exposure time per step. X-ray detection was achieved with (Ce) YAG X-ray scintillation and CCD camera, capturing 2,048 X 512 pixels with voxel resolution of 2.5 μm.

4.3 Result and Discussion

Performance evaluation of GPC specimens prepared with silica sand and alumina as a fine aggregate was subjected to five thermal shock cycles as shown in Table 4.4.

78

Table 4.4: Performance evaluation of geopolymer concrete subjected to 5 thermal shock cycles.

Sample No	Fly Ash Origin	Fly Ash Type	Fine Aggregate	1	2	3	4	5
TS-W-1	USA	Class F	Silica sand	●	▲	▲	▲	X
TS-WO-1	USA	Class F	Alumina	●	●	●	●	●
TS-W-2	USA	Class F	Silica sand	▲	▲	◆	◆,X	◆X
TS-WO-2	USA	Class F	Alumina	●	▼	▲	X	X
TS-W-3	China	Class F	Silica sand	◆▼	◆▼	◆▼	◆,▼	◆▼
TS-WO-3	China	Class F	Alumina	●	●	●	▲	▲
TS-W-4	China	Class F	Silica sand	X				
TS-WO-4	China	Class F	Alumina	●	▲	▲	▲	▲
TS-W-5	China	Class F	Silica sand	●	●	●	●	▼
TS-WO-5	China	Class F	Alumina	●	●	●	●	X
TS-W-6	China	Class F	Silica sand	▼,◆,X				
TS-WO-6	China	Class F	Alumina	▲	▲	▲	▲X	X
TS-W-7	USA	Class C	Silica sand	X				
TS-WO-7	USA	Class C	Alumina	▲	▲	◆	X	X
TS-W-8	Israel	Class F	Silica sand	X				
TS-WO-8	Israel	Class F	Alumina	X	▼X			
TS-W-9	Israel	Class F	Silica sand	▼	◆,▼	◆,▼	◆,▼	◆,▼
TS-WO-9	Israel	Class F	Alumina	▼	▼	X		
TS-W-10	China	Class F	Silica sand	●	▲	X		
TS-WO-10	China	Class F	Alumina	▲	▲	X		
TS-W-11	USA	Class C	Silica sand	X				
TS-WO-11	USA	Class C	Alumina	●	●	●	●	●

No Cracking: ● Minor Crack: ▲ Major Cracking: ◆Expansion: ▼ Total Failure: X

GPC specimens [TS-WO-1 (Class F) and TS-WO-11 (Class C)] prepared with fine alumina aggregate did not suffer any physical damage nor showed signs of cracking or expansion as compared to other samples. GPC specimen [TS-W-5 (class F)] prepared with silica sand did not suffer any mechanical damage for the initiall four cycles, when signs of major cracking and ultimately failure were observed at the end of the fifth cycle. In contrast, certain GPC specimens [TS-W-4, TS-W-6 and TS-W-8 (Class F), TS-W-7 (Class C)] suffered severe damage after only one cycle of thermal shock, while the rest of the samples suffered moderate deterioration in the form of cracking and expansion.

Digital micrographs after each cycle for GPC specimens (TS-WO-3, 5,7) prepared with fine alumina aggregate and with silica sand (TS-W-3,5,7) are shown in Figures 4.1 and 4.2, respectively.

Sample No	Cycle 1	Cycle 2	Cycle 3	Cycle 4	Cycle 5
TS-W-5					
TS-W-3					
TS-W-8		Failed			

Figure 4.2: GPC with silica sand subjected to 5 thermal shock cycles.

The GPC's prepared with fine alumina aggregate from Class F Fly ash (TS-WO-5) and (TS-WO-3) did not exhibit major signs of deterioration until the last cycle, while GPC prepared with Class C fly ash showed signs of cracking and deterioration after only one cycle of thermal shock followed by complete failure at the end of cycle five. Digital micrographs of the GPC specimens (TS-W-3, 5 and 8) prepared with silica sand and Class F fly ash are shown in Figure 4.2. Specimen (TS-W-5) did not suffer any signs of deterioration after 5 thermal shock cycles while GPC specimen (TS-W-3, TS-W-8) prepared with Class F fly ash exhibited major cracking and complete failure after one thermal shock cycle as shown in Figure 4.2. The GPC specimens were studied for chemical analysis via XRF and microstructure characterization using XRD and SEM.

XRF analysis of all the specimens prepared with alumina aggregate and silica sand as a fine aggregate is shown in Figures 4.3 and 4.4, respectively.
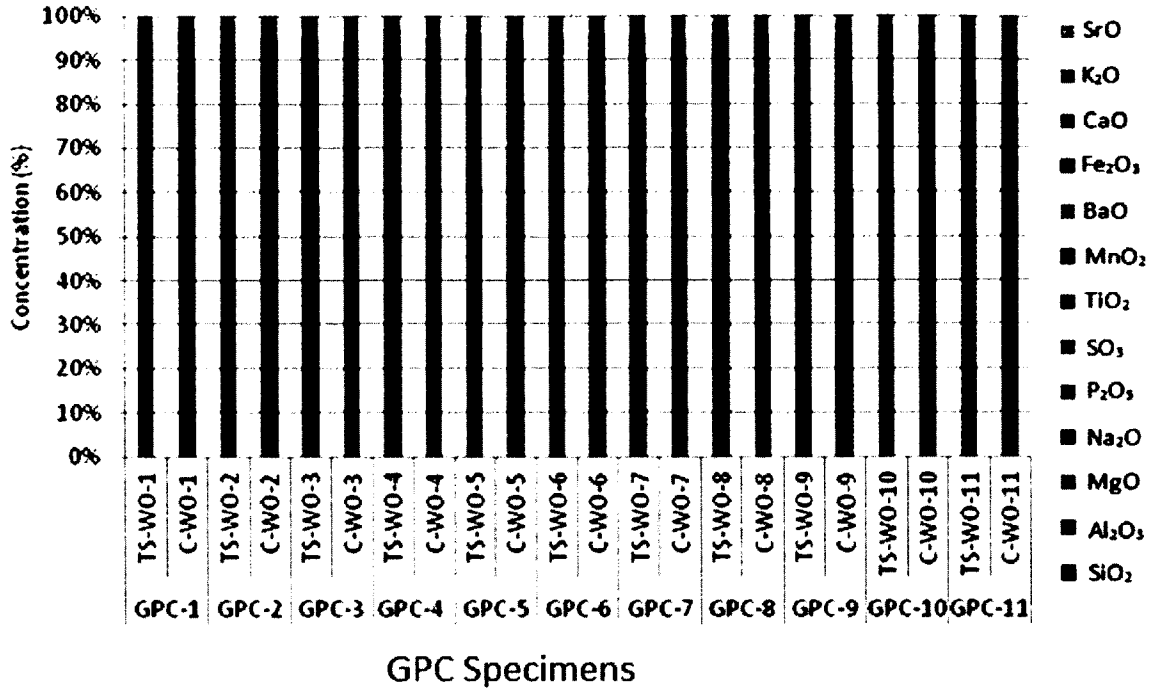
Figure 4.3: XRF analysis of GPC prepared with fine alumina aggregate.
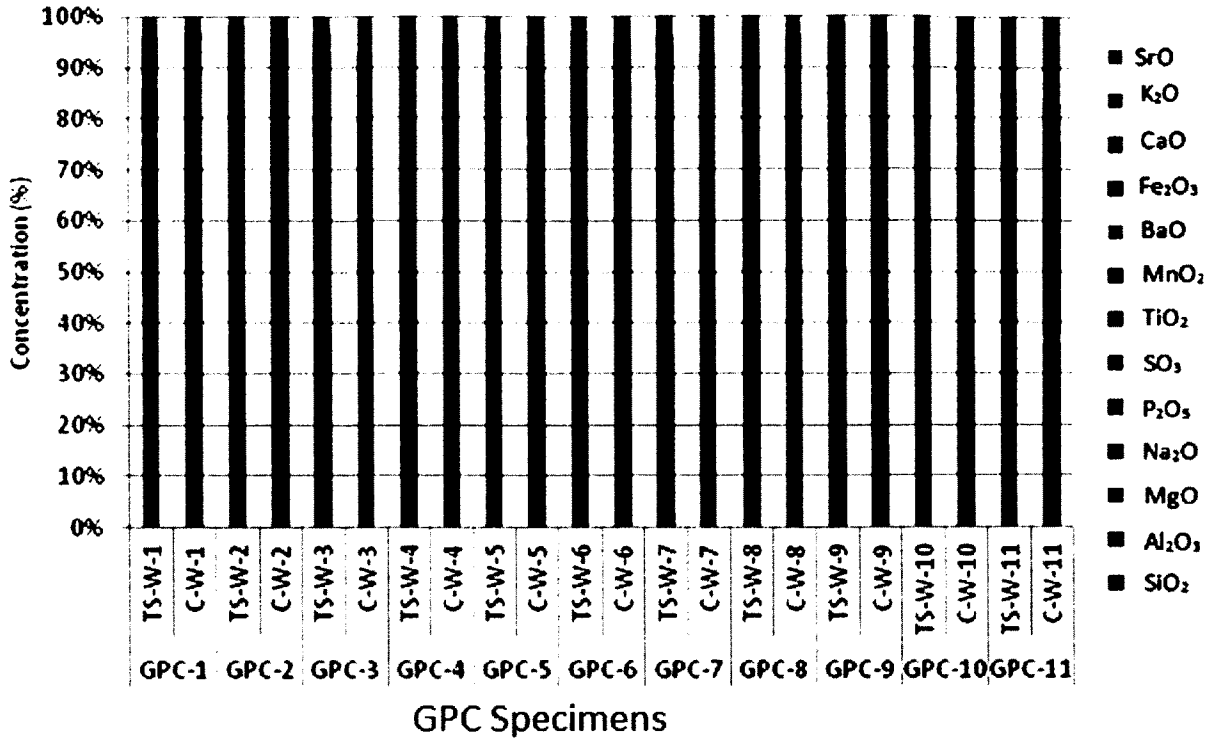
Figure 4.4: XRF analysis on Geopolymer concrete with silica sand.

Figure 4.3 exhibits the control and thermal shock specimens batched with alumina aggregate. The Al_2O_3 increased for most of the specimens after thermal shock treatment as compared to the controls, except for certain specimens (TS-WO-1, TS-WO-2 and TS-W-4) as shown in Figure 4.3. The alumina from the fine aggregate contributed in the formation of additional Al_2O_3 when subjected to elevated temperature. In contrast, for specimens TS-WO-1, TS-WO-2 and TS-W-4, the Al_2O_3 decreased by ~50% when subjected to 5 cycles of thermal shock treatment, causing the SiO_2/Al_2O_3 ratio to increase for these samples by 8-9%. These samples (TS-WO-1, TS-WO-2 and TS-WO-4) exhibited an average or above average performance when subjected to thermal shock treatment (See Table 4.4). This may indicate that aluminum oxide might be involved in the formation of an amorphous zone of geopolymer.

Further studies using Nuclear Magnetic Resonance (NMR) technique are required to quantify this process [3, 169].

The XRF analysis for GPC specimens prepared with silica sand is shown in Figure 4.4. GPC specimens prepared with silica sand suffered more extensive mechanical damage as compared to specimens prepared with alumina aggregate. The SiO_2/Al_2O_3 ratio was much higher in specimens prepared with silica sand as compared to alumina aggregate (See Figure 4.5).
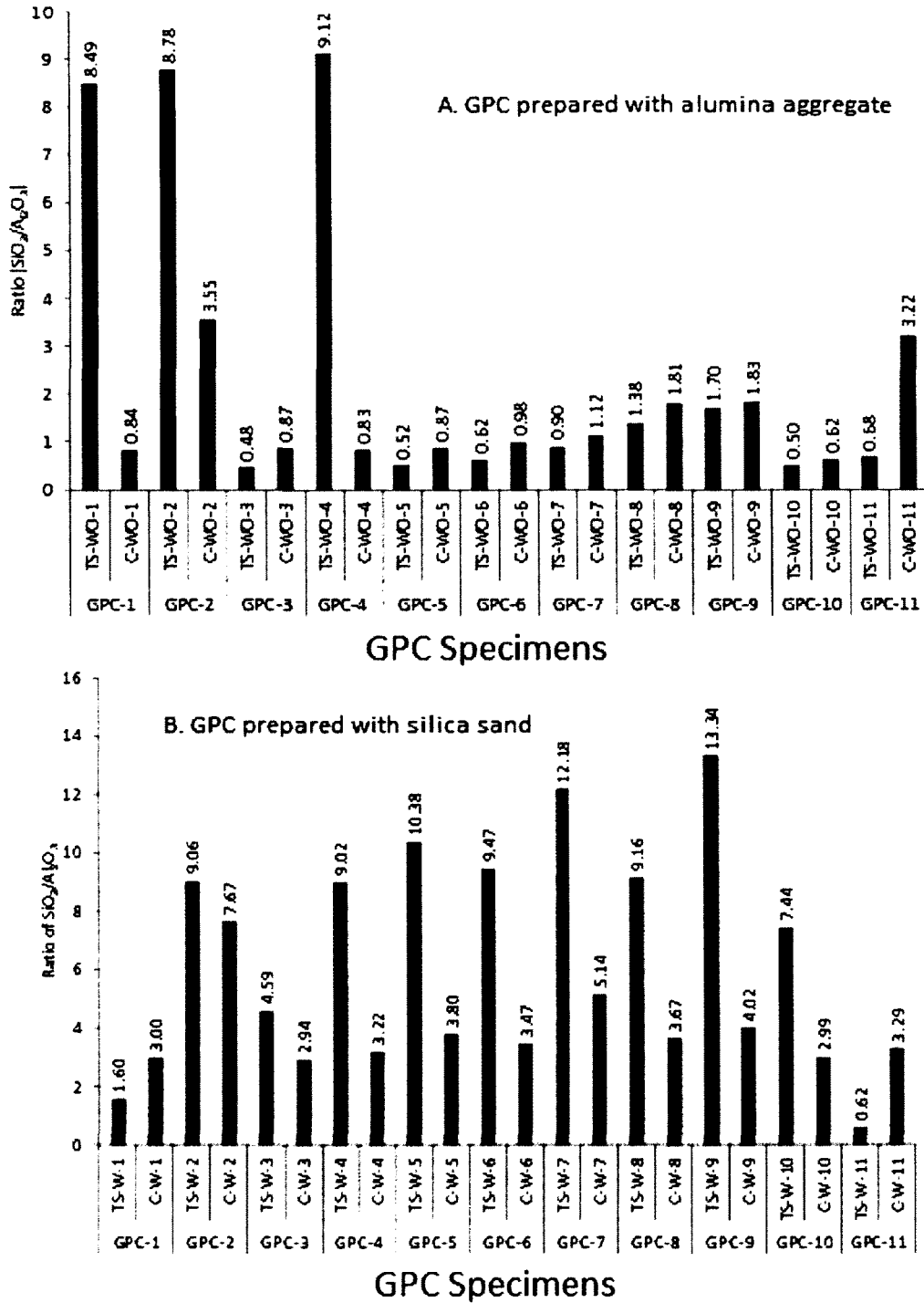
Figure 4.5: Ratio of SiO_2/Al_2O_3 for GPC with alumina aggregate and silica sand.

GPC prepared with silica sand did not have additional alumina and had greater content of un-reacted silica; therefore, sufficient formation of an amorphous zone in the form of sodium

aluminosilicate hydrate (N-A-S-H) was not formed [170]. This shows that additional alumina is required to form an amorphous zone of N-A-S-H, which plays a vital role in the durability and mechanical performance of the binder at elevated temperatures [19,164]. XRD analysis of three specimens (two class F and one class C) GPC's are shown in Figure 4.6.

S: Sodalite Q: Quartz M: Mullite N: Nepheline A: Albite F: Fayalite G: Gehlenite An: Analcime
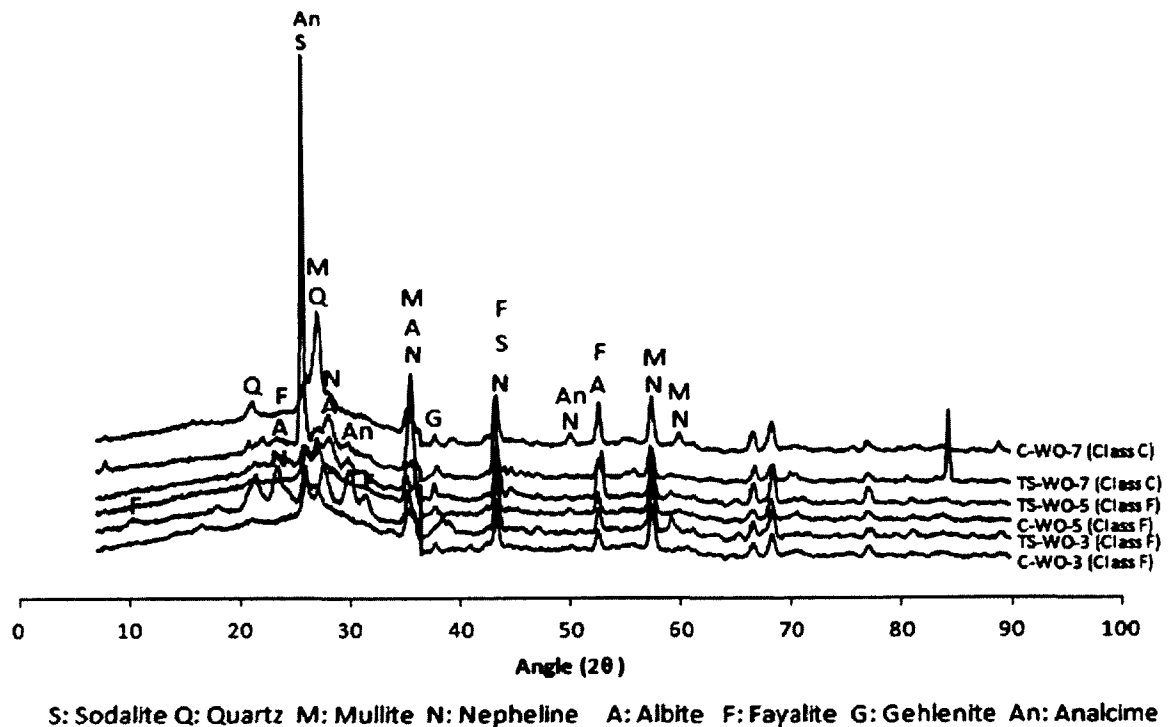
Figure 4.6: XRD analysis of Geopolymer Concrete (control and thermal shocked specimens) with Class C and F fly ashes prepared with fine alumina aggregate.

XRD studies of GPC control (C-WO-07) prepared with Class C fly ash shows phases such as quartz, albite, nepheline and gehlenite. The thermal shock treated specimens showed strong peaks of analcime and sodalite in addition to nepheline. XRD analysis of GPC with Class F fly ash (TS-WO-3) exhibited similar crystalline zeolitic phases as GPC with Class C fly ash in addition to fayalite and mullite. The control specimens exhibited mullite and after thermal shock treatment the mullite phase disappeared, suggesting that it was involved in the regeopolymerization reaction. Later it may have formed an amorphous geopolymer.

Thermally stable phases such as sodalite and analcime were detected after the thermal shock treatment. These phases possess similar structures as does N-A-S-H gel and they recovered their crystallinity during 204-426° C, then retained their structure up to approximately 815° C [171, 172]. The precursor plays a crucial role in the formation of crystallization of stable phases, which leads to amorphization of geopolymeric gels [3, 91].

Studies have shown that at temperatures below 500° C, the primary reaction products of amorphous aluminosilicate semicrystalline gels such as N-A-S-H are formed, along with zeolite crystals such as mullite. The formation of zeolite crystals depends on the composition of the fly ash and the chemical activator used for alkali activation of the fly ash. Zeolite products such as analcime and chabazite are formed up to 572° C. Upon increasing the temperature to 752° C promotes recrystallization and the formation of silica stable structures (crystalline feldspathoid) such as nepheline, leucite and labradorite. Thermally stable phases such as sodalite detected via XRD in the GPC exposed to thermal shock cycles, indicates reduced contraction after exposure to thermal shock cycles. This phase (sodalite) then re-crystallizes to nepheline and albite without destruction of the alumino silicate framework, which is responsible for the formation of the N-A-S-H geopolymer gel. SEM analyses for GPC specimens (C-WO-3, TS-WO-3) prepared with Class F fly ash are shown in Figure 4.7.
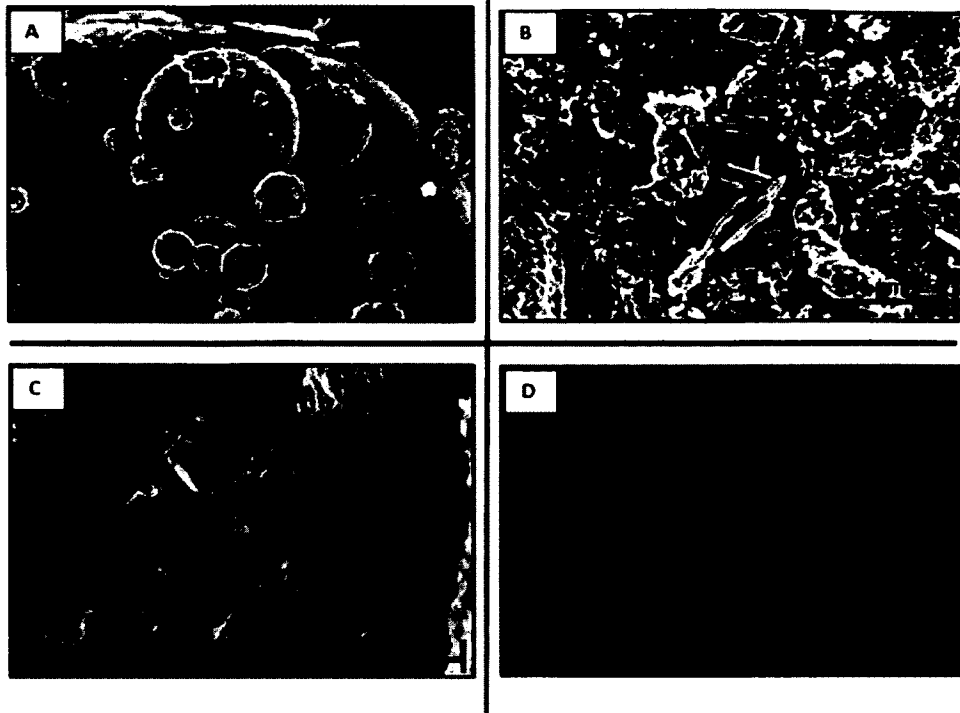
Figure 4.7: SEM micrographs of control sample (C-WO-3) exhibiting unreacted fly ash crystals and zeolite crystals (A and B), C and D show amorphous zone with nepheline crystals on the specimens subjected to thermal shock.

The control specimens (C-WO-3) showed un-reacted fly ash crystals along with crystals of mullite. The specimen subjected to thermal shock treatment exhibited crystals of nepheline along with the amorphous zone, which could suggest that the thermal shock treatment led to the crystallization of unreacted fly ash, which was not involved in the original geopolymerization. In addition, microcracks were observed in this specimen after the thermal shock treatment. The performance evaluation after 5 cycles also indicated minor cracking for three cycles along with major cracking in the fourth and the fifth cycles.

SEM analysis of GPC (TS-WO-5) prepared with a Class F fly ash procured from China is shown in Figure 4.8.
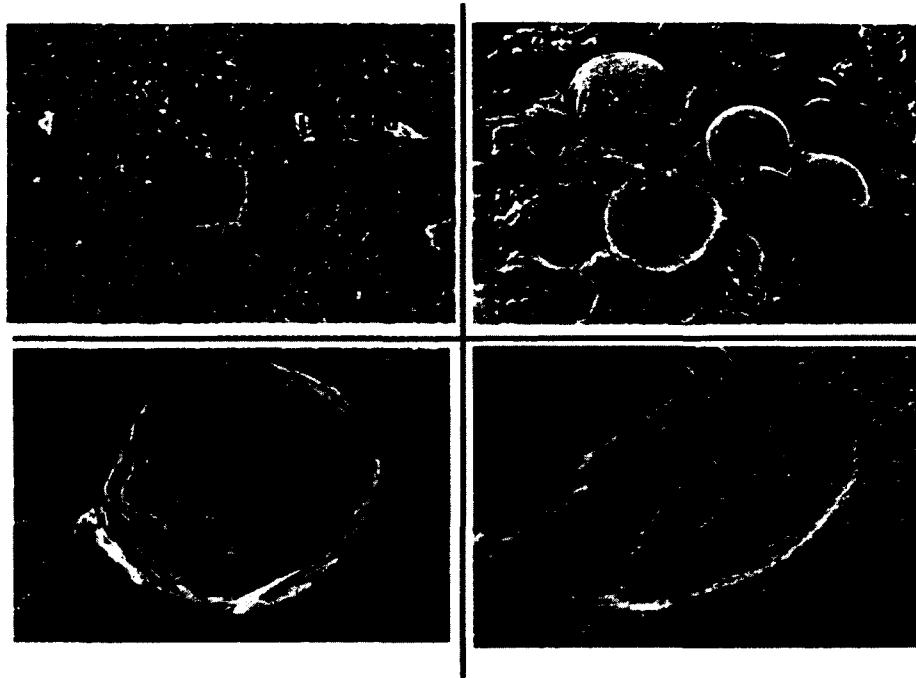
Figure 4.8: SEM micrographs of control sample (C-WO-5) showing of unreacted crystals, and intact fly ash spheres; images C and D show amorphous zone in specimen TS-WO-5.

The control specimen (C-WO-5) exhibited un-reacted fly ash particles along with some zeolite crystallization (Figures 4.8A and B). Upon thermal shock treatment, the unreacted fly ash underwent geopolymerization, forming an amorphous zone. The specimen (TS-WO-5) exhibited superior performance when subjected to 5 cycles of thermal shock treatment as shown in Table 4.4 and Figure 4.2.

The superior performance of this specimen could be attributed to the formation of an amorphous zone and almost a full geopolymerization of the fly ash particles which were not involved in the initial geopolymerization [3, 173, 174]. Related research has shown that geopolymer concrete, when subjected to elevated temperatures retain its amorphous nature while exhibiting some changes in the crystalline phase composition. Sodium-based geopolymer concretes showed crystalline phases such as nepheline, albite and tridymite. These phases have

been reported to be responsible for the improvement of thermal resistance of geopolymer concretes [173]. SEM analysis of Class C fly ash is shown in Figure 4.9.
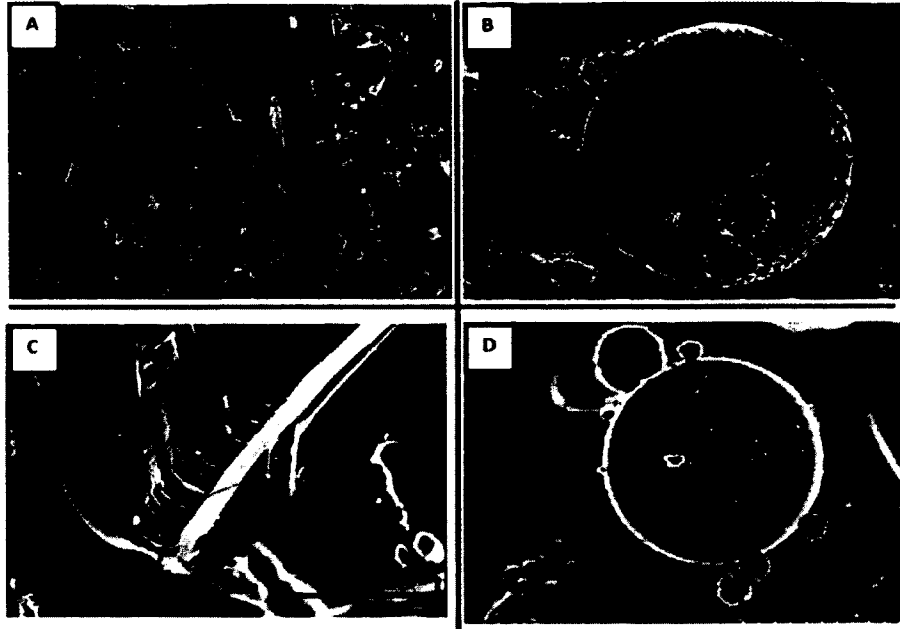
Figure 4.9: SEM micrographes of zeolite-T crystals (A) and unreacted reacted fly ash particles (B), while image (C) reveals in the thermally shock specimen along with unreacted crystals (D).

Figure 4.9A exhibits crystallization in the form of zeolite T crystals; in addition, un-reacted fly ash particles were observed as shown in Figure 4.9B. Amorphization was observed in the un-reacted fly ash spheres, suggesting that the size of the fly ash particles plays an important role in the geopolymerization process. Further study is required to examine the effect of particle size on geopolymerization, which will lead to the successful formation of the amorphous phase. The thermal shock led to the crystallization of geopolymeric gel, resulting in the formation of analcime crystals in the form of plates, as shown in Figure 4.9. The presence of the analcime phase indicates that thermally stable zeolite structures were developed under elevated temperature, contributing to the durability of the geopolymer matrix. X-ray micro tomographs, exhibiting a slice through the image of GPC prepared with

Class F (TS-WO-2) and Class C fly ash (TS-WO-7) after thermal shock treatment are shown in Figure 4.10.
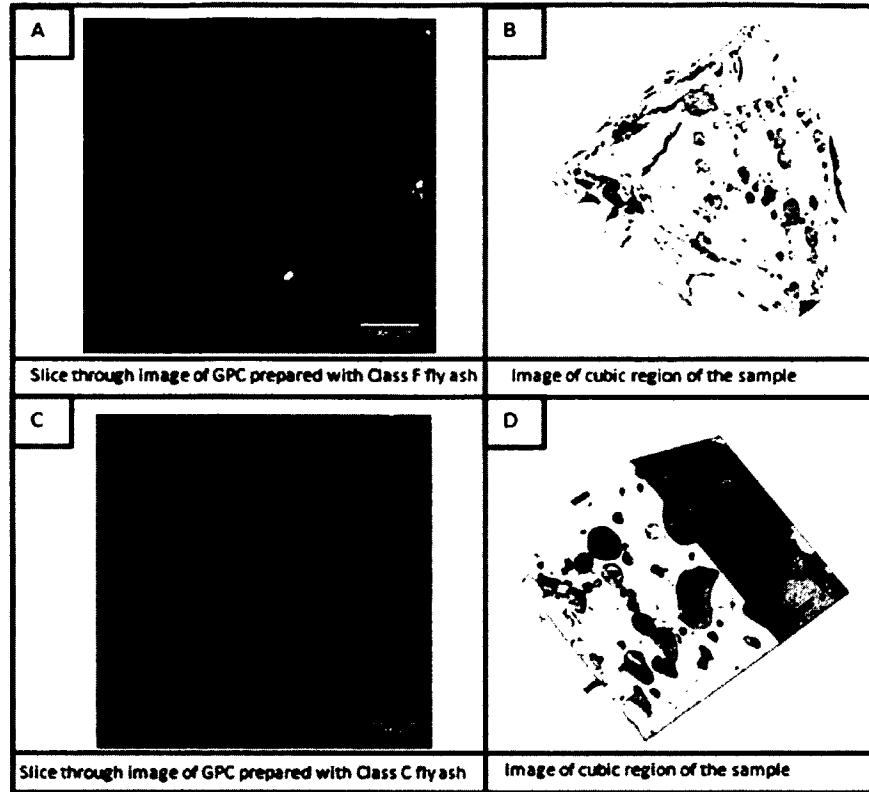
Figure 4.10: X-ray μC tomography of Class F fly ash (TS-WO-2) and Class C fly ash (TS-WO-07).

Both GPC's prepared from Class F and C fly ash showed micro-cracks after 5 cycles of thermal shock testing. The corresponding cubic images of GPC specimens are shown in Figures 4.10B and D, respectively. These images exhibited a 3D porous view of the specimens when exposed to elevated temperature.

The maximum pore diameter determined via X-ray micro tomography for class F GPC (TS-WO-02) and Class C GPC (TS-WO-07) was 2000 μm and 2500 μm, respectively. GPC prepared with Class C fly ash exhibited an increase in pore diameter by a factor of 1.5. The pore connectivity network of the GPC's was examined using the ortho-slice view as shown in Figures 4.11A and B.
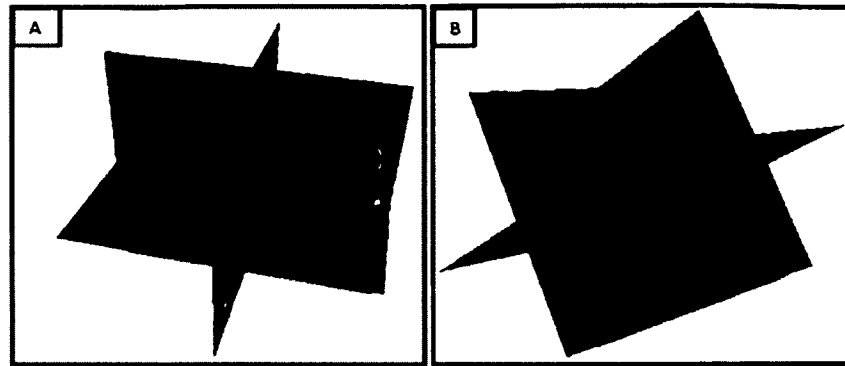
Figure 4.11: Ortho-slice view of Class F and Class C geopolymer concrete showing the pore connectivity network.

Class F specimens showed pore connectivity after the thermal shock treatment while GPC prepared with Class C fly ash did not exhibit signs of pore connectivity. This shows that due to elevated temperature exposure, the pores were expanding and connecting to form a pore connectivity network. Further studies are required to quantify the pore connectivity network and to examine the tortuosity of the pore network, which plays a critical role in controlling the thermoshock treatment. Due to elevated temperature, the pores expand to form a pore connectivity network. Further studies are required to quantify the pore connectivity network and to examine the tortuosity of the pore network, which plays a critical role in controlling the strength and preventing the ingress of deleterious species such as chlorides and sulfates, which lead to the degradation of concrete structures.

4.4 Conclusion

Geopolymer concrete specimens prepared using eleven different types of fly ashes obtained from three countries were subjected to thermal shock treatment. The specimens prepared with alumina filler as fine aggregate exhibited superior performance as compared to the specimens made with silica sand. This indicates that thermal shock treatment leads to additional formation of N-A-S-H phase, which is responsible for higher strength and

durability of geopolymer concrete. Thermally stable phases such as sodalite and analcime were detected after the thermal shock treatment. The formation of the amorphous phase of geopolymerization plays a crucial role in the formation of stable phases, which leads to the amorphization of geopolymeric gels. This shows that additional alumina is required to form the amorphous zone of N-A-S-H, which plays a vital role in durability, resistance and mechanical performance of the binder at elevated temperatures.

CHAPTER 5

EXPERIMENTAL PROCEDURE, RESULTS AND DISCUSSION: MICROBIAL INDUCED CORROSION

5.1 Microorganisms

Anaerobic bacteria, Desulfovibrio desulfuricans, were cultured in the biology lab. The source of the bacteria is American Type Culture Collection, 10801 University Boulevard, Manasas, Virginia, 20110-2209, USA. Further details of the bacteria are Item number - 13541, LOT - 58052392, Shipment - SOE83596, Biosafety level - 1, and product format is freeze dried. One liter of concentrated medium of Desulfovibrio was prepared. Nitrogen gas was used to remove the oxygen from the bacterial media to create anaerobic conditions. To sterilize the medium solution, it was autoclaved at 120° C for 15 minutes. One gram of bacteria, in the form of a pellet, was mixed with concentrated media and kept in the incubator for four to five days at a temperature of 25° C. Tables 5.1 and 5.2 show the composition of the medium solution and nutrient solution, respectively.

Table 5.1: Composition of Desulfovibrio medium solution.

Compound	Quantity
Peptone	5.0 g
Beef extract	3.0 g
Yeast extract	0.2 g
$MgSO_4$	1.5 g
Na_2SO_4	1.5 g
$Fe(NH_4)_2(SO_4)_2$	0.1 g
Glucose	5.0 g
Tap water	1.0 L

Table 5.2: Compositions of the nutrient solution.

Chemicals	Stock solution concentration	Amount taken to dilute to 20 L
Glycerol	48 ml/L	1.92 ml
NaHCO₃	58 g/L	0.23 g
Ammonium Sulfate	401 g/L	2.6 g
MgSO₄.7H₂O	209 g/L	6.8 g
CaCl₂.2H₂O	68 g/L	0.45 g
KH₂PO₄	71 g/L	0.47 g
FeCl₃	3 g/L	445 µl
CuSO₄.5H₂O	50 mg/L	0.001 g
Na₂MoO₄.2H₂O	390 mg/L	0.0066 g
ZnCl₂	690 mg/L	0.0046 g
CoCl₂.6H₂O	1 g/L	0.0067 g

5.2 Nutrient Solution

Two thirds of the pipe was filled with nutrient solution. For the three pipes, one hundred and ten liters of nutrient solution were prepared in a Nalgene plastic container and thoroughly mixed. Nitrogen gas was used for five hours to decrease the oxygen concentration of the nutrient solution by bubbling the solution with the nitrogen gas.

5.2.1 Mechanism

There are four stages of microbial induced corrosion in sewer pipes.

Stage 1: Normally, concrete pipe has a pH of 12-13 in which sulfate reducing bacteria (SRB) does not survive. However, SRB is active in the biofilm layer, which lines the submerged part of the sewer pipe, reduces sulfates into hydrogen sulfide, and at the same time oxidizes organic carbon into carbon dioxide

$$Organicmatter + SO_4^2 \xrightarrow{SRB} H_2S + CO_2. \qquad (5.1)$$
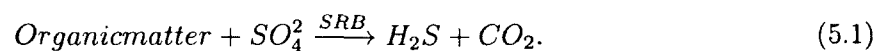
The hydrogen sulfide is transported into the wastewater, where it is present in the form of dissociated ions, H^+ and HS^-. Another product, carbon dioxide, of which some amount is

dissolved in carbonate and bicarbonate ions, also goes into the wastewater. H_2S and CO_2 are volatilized and reach all the way to the sewer's headspace. The carbonic acid, which forms in the headspace, reacts with calcium hydroxide of the cement and lowers the pH of the concrete surface (pH = $\sim$9). Figure 5.1 shows the corrosion process within a sewer pipe.
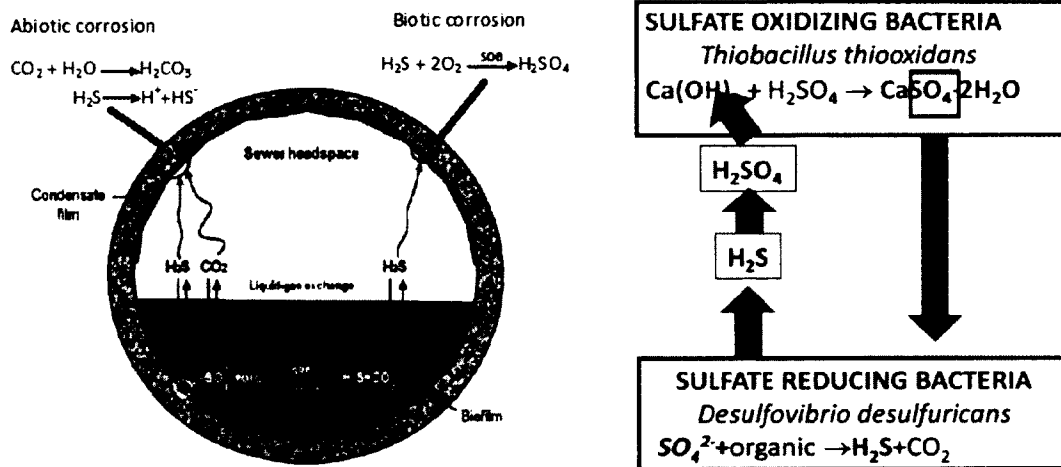
Figure 5.1: Schematic of the corrosion process within a sewer (Wells *et al.*, 2009).

Stage 2: Over a period of time, the pH goes down further. At this low pH and in the presence of oxygen, nutrients, and moisture, neutrophilic sulfur oxidizing bacteria, such as the Thiobacillus, colonize and produce H_2SO_4. This acid further reduces the pH of the concrete surface.

Stage 3: Due to successive growth of bacteria, the pH goes down to $\sim$4. At this pH, acidophilic sulfur oxidizing bacteria (ASOM) start colonizing at the concrete surface. It oxidizes the H_2S into H_2SO_4 and also oxidizes thiosulfate and elemental sulfur, which are deposited on the sewer walls. It further lowers the pH around $\sim$1-2.

Stage 4: At this low pH, ASOM produces sulfuric acid, which reacts with silicate and carbonate of the concrete surface and forms gypsum. This leads to an increase in volume of more than 127% [151] and weakens the structure. The volume is increased more than

700% [190] when gypsum reacts with tricalcium silicate and forms ettringite. This leads to internal cracking and pitting of the concrete surface. It increases the surface area of the concrete surface, which allows easy penetration of moisture and microorganisms.

Over a long period of time, a white layer on the concrete surface, gypsum, forms, which gradually thickens. Furthermore, ettringite is formed, which causes cracks in the concrete's surface [191].

$$H_2SO_4 + CaO.SiO_2.2H_2O \rightarrow CaSO_4 + Si(OH)_4 + H_2O \tag{5.2}$$

$$H_2SO_4 + CaCO_3 \rightarrow CaSO_4 + Si(OH)_4 + H_2O \tag{5.3}$$

$$H_2SO_4 + Ca(OH)_2 \rightarrow CaSO_4 + H_2O \tag{5.4}$$

$$CaSO_4 + 3CaO.Al_2O_3.6H_2O + 25H_2O \rightarrow 3CaO.SO_4Al_2O_3.3CaSO_4.31H_2O. \tag{5.5}$$
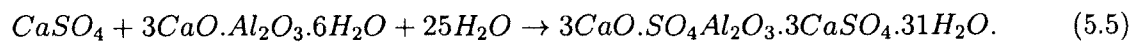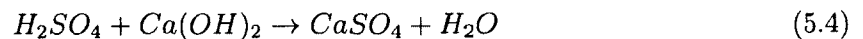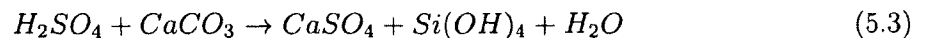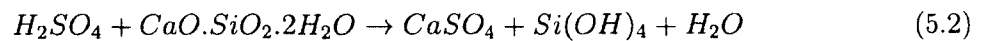
5.3 Experimental Setup

The experimental setup consisted of three 12"diameter and 30"long concrete pipe specimens made and coated with different formulations of GPC. Both ends of the pipe specimen were sealed to prevent hydrogen sulfide gas from escaping. One pipe was coated with GPC that had a biocide agent entrained in it, the 2nd pipe was coated with regular geopolymer without biocide agent, while the third pipe specimen was not coated and served as a control. Figure 5.2 displays the three pipe specimen inside the closed chamber.
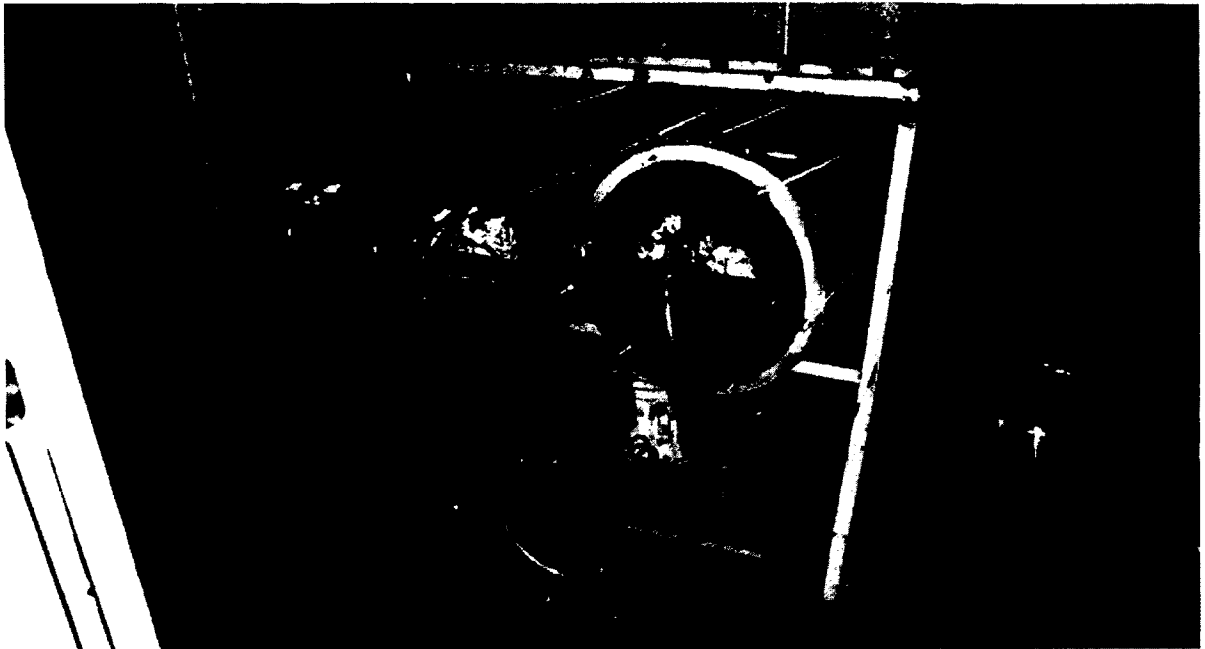
Figure 5.2: Experimental setup.

5.4 Analytical Methods

After filling up the three concrete pipes, pumps were run for 10 minutes to provide a uniform distribution of the nutrient solution inside the concrete pipes. Various parameters were measured to assess the effect of the two coatings on the growth of Desulfovibrio Desulfuricans bacteria and the generation of sulfide. All parameters measured in the current study were performed according to Standard Methods (American Public Health Association, 1998). The various parameters were divided into three groups:

1. General environmental parameters such as pH and temperature: pH was measured at regular intervals. Temperature (65-70^0 F) and humidity are maintained throughout the experiment.

2. Substrates and products that include COD and sulfide concentrations: COD was measured using the Hach Method (APHA, 5220D). Sulfide concentration was measured

by the methylene blue method (APHA, 4500-S-2D). Bacterial count was measured by the spectrophotometry method (APHA, 9215B).

5.5 Results and Discussion

5.5.1 pH

After the test began in all three pipe specimens, the pH dropped gradually. However, pipe specimens 2 (control) and 3 (Geospray AMS^{TM}) started decreasing more quickly after Week 5 until the pH reached 6.65. This indicates that the activity of bacteria, or organic compound, is greater in specimens 2 and 3. The Chemical Oxygen Demand (COD) of pipe specimens 2 and 3 also confirms that bacterial activity or total organic compound is more in these two pipes. The pH of all three pipe specimens increases from Week 14 to 16. This may be due to a scarcity of nutrient solution. SRB reduce the amount of sulfates, which are present in the nutrient solution. This process produces H_2S and CO_2. CO_2 forms carbonic acid in the presence of moisture, which lowers the pH of the nutrient solution. Figure 5.3 shows the pH level of pipe specimens.
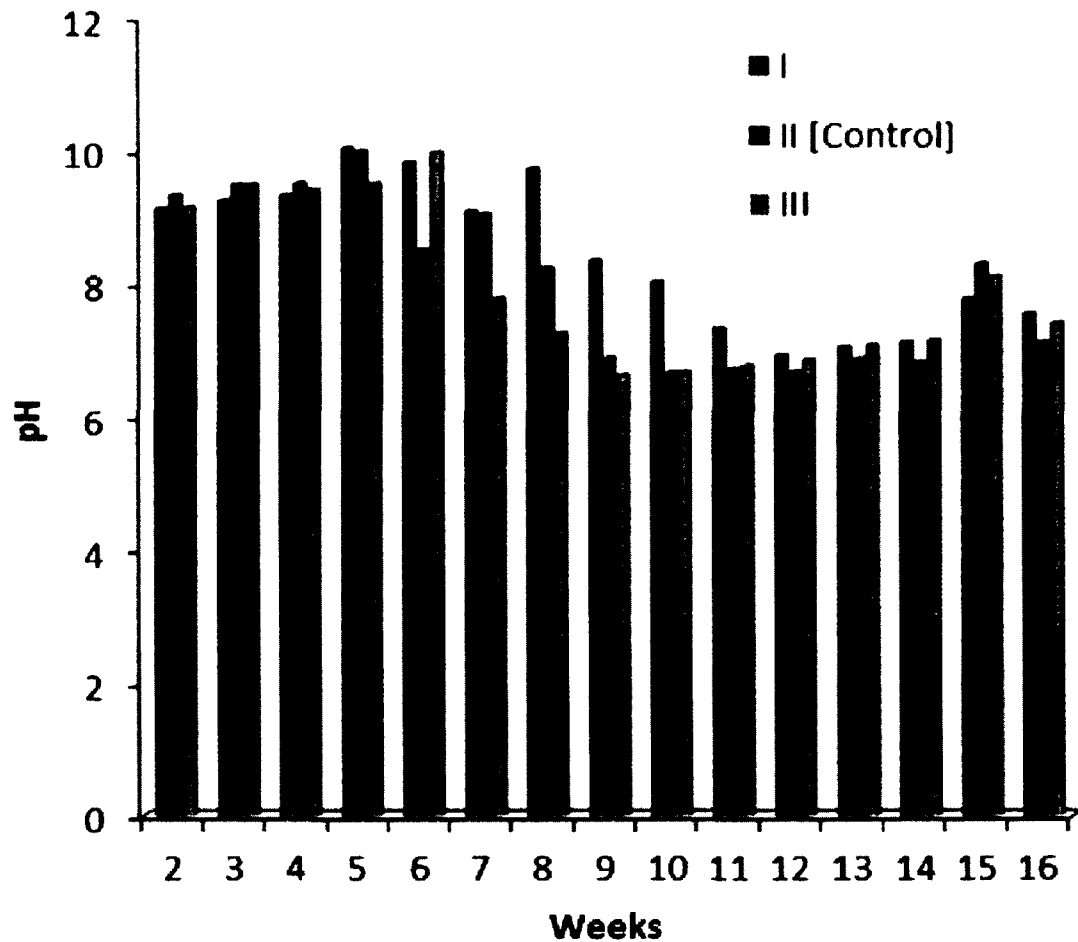
Figure 5.3: pH Levels of Pipe Specimens.

5.5.2 Bacterial Concentration

The bacterial concentration is increased until Week 5 in all three pipe specimens. The bacterial concentration gradually increases from Weeks 8 to 13 for pipe 2 (control) and the same trend occurs for pipe 3 from Weeks 8 to 11. Initially, the concentration of bacteria is greater in pipe 2 compared to the other two pipes. Bacterial concentration is greater in pipe 2 and pipe 3 from Week 8 to 13 and Week 8 to 11, respectively. The pH values also validate the bacterial concentration of these two pipes. Figure 5.4 shows the bacterial concentration of Pipe Specimens.
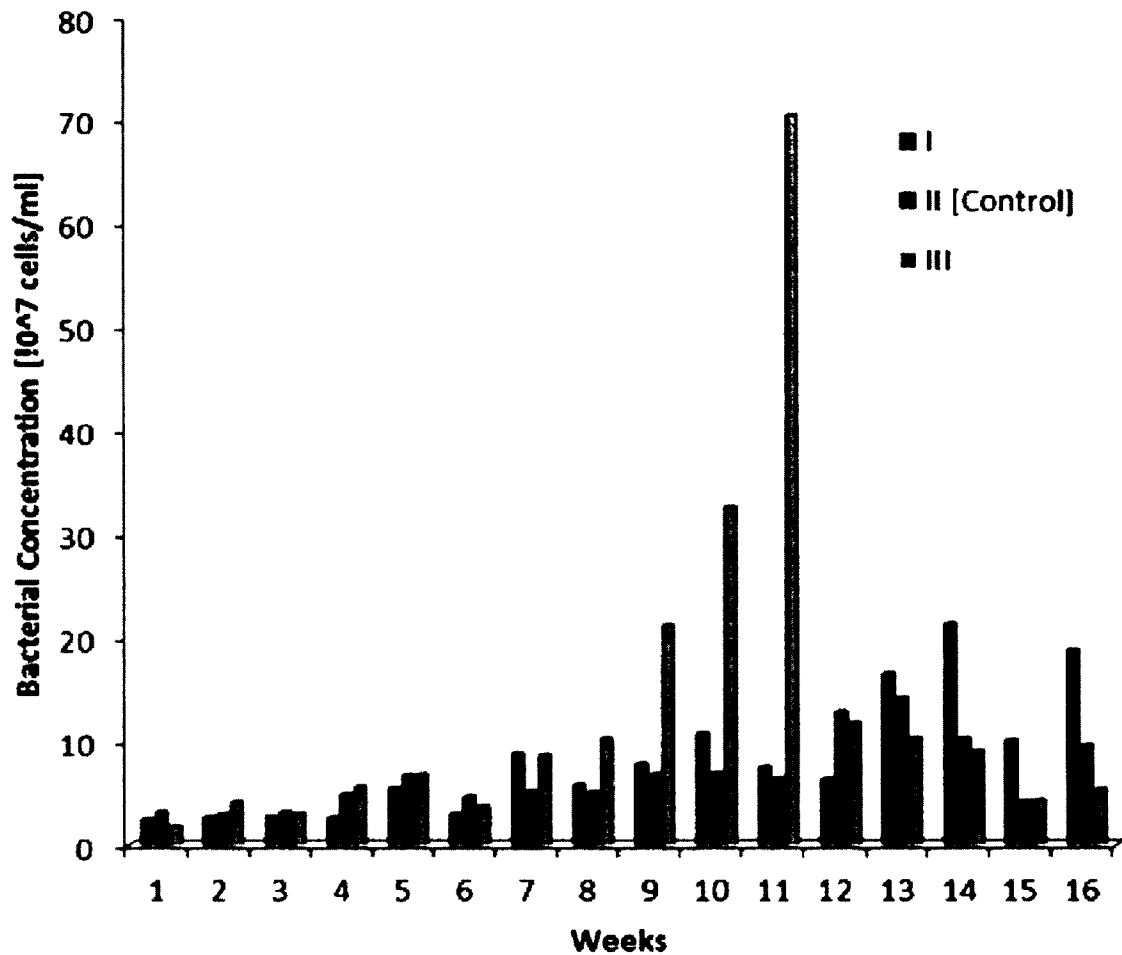
Figure 5.4: Bacterial Concentration of Pipe Specimens 10^7 cells/ml.

5.5.3 Chemical Oxygen Demand (COD)

The Chemical Oxygen Demand (COD) shows the amount of bacterial concentration or organic compound in the solution. COD levels are greater in pipe specimen 2 from Weeks 1 to 8 compared to specimens 1 and 3. This shows that pipe 2 has more bacterial concentration or organic compound compared to the other two pipes. Figure 5.5 displays the COD of Pipe Specimens.
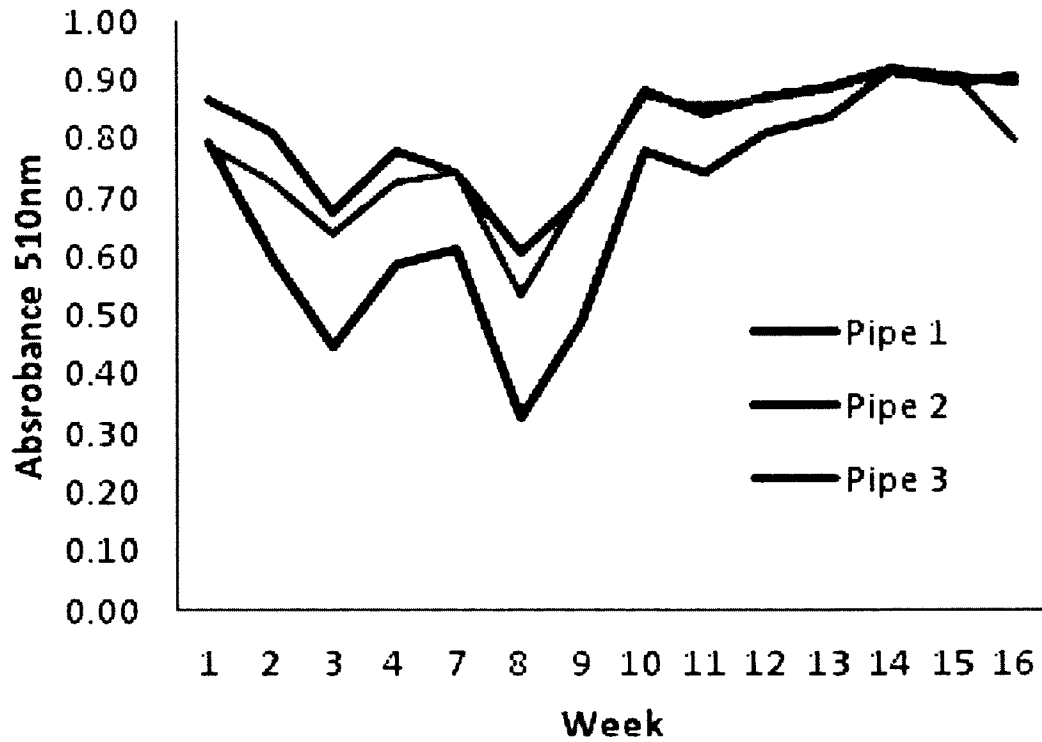
Figure 5.5: Chemical Oxygen Demand of three pipes.

5.5.4 Slime Layer

The slime layer of each pipe specimen was measured at three different positions. The average depth of the slime layer in pipe 1 (Geospray^{TM}) and pipe 3 (Geospray AMS^{TM}) are around one millimeter. However, the average depth of the slime layer in pipe 2 (control) is around 4 mm. Figure 5.6 shows the depth of the slime layer of Pipe Specimens.
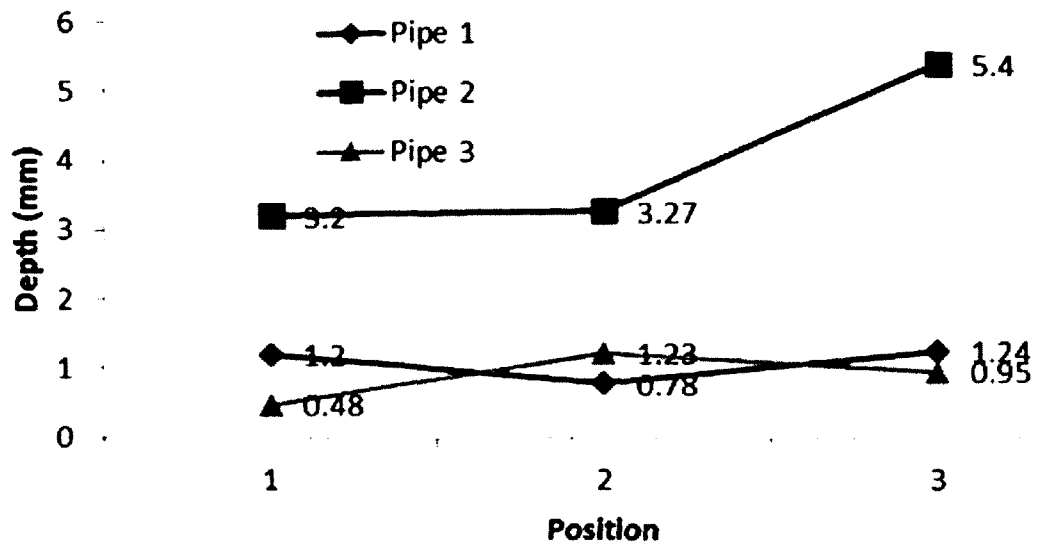
Figure 5.6: Depth of slime layer in pipe specimens (mm).

CHAPTER 6

CONCLUSION

6.1 Carbonation

Reinforced geopolymer concretes prepared with three different fly ashes (two Class F and one Class C) were examined for accelerated carbonation for a period of 450 days. The electrochemical test data indicated that GPC made using Class C fly ash exhibited a corrosion rate 20 times greater than fly ash F based geopolymer specimens, after 450 days of accelerated carbonation treatment. Steel reinforcement in the GPC prepared with Class F fly ash maintained its passivity and showed a superior corrosion resistance when compared with GPC made with Class C fly ash. The corrosion in GPC-MN (Class C precursor fly ash) affected the mechanical strength by exhibiting a loss in splitting tensile strength by a factor ~ 1.5 when compared with the average of GPC-DH and OH (Class F precursor fly ash). The accelerated carbonation treatment led to a reduction in pH value below 8 for GPC-MN, while GPC-DH and OH maintained their alkalinity and had a pH value above 12. The drop in pH led to the breakdown of the passive layer and corrosion of GPC-MN, which was observed in the corrosion of reinforced concretes prepared with Class C fly ash. XRF analysis showed that a higher content of Al_2O_3 and SiO_2 at the rebar/concrete interface in the case of GPC-DH and OH, which was related to the formation of N-A-S-H/C-A-S-H geopolymeric gels. Visual analysis of the rebars after 450 days of exposure indicate that the reinforcement inside GPC-MN was completely corroded (99% surface corrosion), while the reinforcement of GPC-DH and OH exhibited 9 % and 4 % surface corrosion, respectively. SEM/EDS analysis showed

that the rebar interface had higher contents of Fe (24.09%) and O (43.4%) for the case of GPC-MN, which could be related to the formation of ferrous hydroxide.

In addition, the microstructure analysis indicates the presence of akaganeite (corrosion product) at the rebar/concrete interface in the case of GPC-MN, while no forms of corrosion products were detected at the rebar/concrete interface of GPC-DH and OH specimens. Accelerated carbonation treatment led to 28% porosity in GPC-MN, while GPC-OH and DH showed 10% and 12% porosity, respectively. Furthermore, the average of GPC-OH and DH indicates a reduction in threshold pore diameter by a factor of 10, as compared with GPC-MN. This could be attributed to a dense cementitious matrix that was formed in GPC-DH and OH, which inhibited the ingress of CO_2 and thus protected the reinforcement. XRD analysis indicates higher content formation of carbonation phases such as calcite (12%), vaterite (7.2%) and natron (6.3%) and the corrosion product phase of Akaganeite (7.23%) for the GPC-MN specimen. The carbonation treatment led to a decrease in the amorphous content of GPC-MN (44%), compared with GPC-DH (75.17%) and OH (63.95%).

Higher amorphous content can be associated with the greater dense pore structure of GPC prepared with Class F fly ashes. The dense cement matrix inhibits the ingress of CO_2 [162]. This indicates that C-A-S-H gel may have been depleted under accelerated carbonation conditions leading to the breakdown of the protective layer, which caused the corrosion in geopolymer concrete prepared from Class C fly ash.

6.2 Elevated Temperature

Geopolymer concrete prepared using eleven different types of fly ashes obtained from three countries were subjected to thermal shock treatment. The specimens prepared with alumina filler as fine aggregate, exhibited superior performance as compared with specimens made with silica sand. This could be partially explained by the fact that thermal shock

treatment leads to additional formation of N-A-S-H phase, which is responsible for higher strength and durability of geopolymer concrete. Thermally stable phases such as sodalite and analcime were detected after thermal shock treatment. The formation of the amorphous phase of geopolymerization as initiated by crystallization of the zeolite precursor plays a crucial role in the formation of stable phases. Additional alumina is required to form the amorphous zone of N-A-S-H, which plays a vital role in durability, resistance and mechanical performance of the binder at elevated temperatures.

6.3 Microbial Induced Corrosion

6.3.1 pH

After the test began in all three pipe specimens, the pH dropped gradually. However, pipe specimens 2 (control) and 3 (Geospray AMS^{TM}) started decreasing more quickly after week 5 until the pH reached 6.65. This indicates that the activity of bacteria, or organic compound, is greater in pipe specimens 2 and 3. The Chemical Oxygen Demand (COD) of pipe specimens 2 and 3 also confirms that bacterial activity or total organic compound, is more in these two pipes. The pH of all three pipe specimens increases from week 14 to 16. This may be due to a scarcity of nutrient solution. SRB reduces the amount of sulfates, which are present in the nutrient solution. This process produces $H_2 S$ and CO_2. CO_2 forms carbonic acid in the presence of moisture, which lowers the pH of the nutrient solution.

6.3.2 Bacterial concentration

The bacterial concentration increased until week 5 in all three pipe specimens. The bacterial concentration gradually increases from weeks 8 to 13 for pipe 2 (control) and the same trend occurs for pipe 3 from weeks 8 to 11. Initially, the concentration of bacteria was greater in pipe 2 compared to the other two pipes. Bacterial concentration was greater in pipe

2 and pipe 3 from week 8 to 13 and week 8 to 11, respectively. The pH values also validated the bacterial concentration of these two pipes.

6.3.3 Chemical Oxygen Demand (COD)

The Chemical Oxygen Demand (COD) shows the amount of bacterial concentration or organic compound in the solution. COD levels were greater in pipe specimen 2 from weeks 1 to 8 compared to specimens 1 and 3. This suggests that pipe 2 has higher bacterial concentration or organic compound compared to the other two pipes.

6.3.4 Slime layer

The slime layer of each pipe specimen was measured at three different positions. The average depth of the slime layer in pipe 1 (Geospray^{TM}) and pipe 3 (Geospray AMS^{TM}) are around one millimeter. However, the average depth of the slime layer in pipe 2 (control) was around 4 mm. COD, Chemical Oxygen Demand, shows the amount of organic compound is greater in pipe 2 when compared to the other two pipe specimens. The pH in pipe 2 also decreased and reached a value of 6.5 faster than pipe specimens 1 and 3. The concentration of bacteria initially shows an increase in pipe 2; however, results were shown to be inconsistent. The depth of the slime layer indicates that organic compounds or activities of bacteria were significantly higher in pipe 2 compared to pipe specimens 1 and 3.

The relatively thin slime layer in pipe 1 and pipe 3 shows that the coatings reduce the activities of bacteria. These results also show that the coating in pipe specimen 1 (Geospray^{TM}) is more effective than pipe specimen 2 (control). These conclusions are validated through COD, pH, and slime layer results.

BIBLIOGRAPHY

[1] Davidovits, J., Geopolymer Chemistry and Applications2011: Institut Gopolymre.

[2] Duxson, P., *et al.*, Geopolymer technology: the current state of the art. *Journal of Materials Science*, 2007. 42(9): p.2917-2933.

[3] Provis, J.L. and J.S.J. Van Deventer, Geopolymers: Structure, Processing, Properties and Industrial Applications 2009: Woodhead Publishing Limited.

[4] Mehta, P.K. and P.J.M. Monteiro, Concrete: microstructure, properties, and materials 2006: McGraw-Hill.

[5] Neville, A.M., Properties of Concrete 2011: Prentice Hall PTR.

[6] Neville, A.M., Properties of Concrete, 2012, Pearson Education.

[7] Mindess, S., J.F. Young, and D. Darwin, Concrete2003: Prentice Hall.

[8] Emmons, P.H.a.A.M.V., Factors affecting the durability of concrete repair: the contractor's viewpoint. *Construction and Building Materials*, 1994(8(1)): p. 5-16

[9] Purdon, A.O., The action of alkalis on blast-furnace slag. *J. Soc. Chem. Ind.*, 1940(59): p. 191 - 202.

[10] Glukhovsky, V.D., Soil Silicate Articles and Structures, 1967: Kiev, Ukrain. p. 156.

[11] Forss, B., F-cement, a new low-porosity slag cement, in Sil. Ind. 1983. p. 79 - 82.

[12] Forss, B., Experiences from the use of F-cementa binder based on alkali-activated blastfurnace slag. 1983.

[13] Idorn, G.M., Alkalis in Concrete, in Danish Concrete Association, R.S. (Eds.), Editor 1983: Copenhagen, Denmark. p. 101 - 104.

[14] Roy, D.M., Silsbee, M.R., Novel cements and cement products for applications, in the 21st century, in Malhotra Symposium on Concrete Technology, Past, Present and Future1994. p. 349 - 382.

[15] Roy, D.M., Silsbee, M. R. , Alkali-activated cementitious materials: an overview. Materials Research Society Symposium, 1992(245): p. 153 - 164.

[16] Davidovits, J., Synthetic Mineral Polymer Compound of the Silicoaluminates, 1984.

[17] Talling, B., Brandstetr, J. Present and future of alkali-activated slag concrete. in Proceedings of the 3 rd International Conference on the Use of Fly Ash, Silica Fume, Slag & Natural Pozzolans in Concrete. 1989. Norway.

[18] Palomo, A., Grutzeck, M.W., Blanco, M. T., Alkali-activated fly ashes. A cement for the future. Cem. Concr. Res., 1999(29): p. 1323 - 1329.

[19] Fernndez-Jimnez, A., Palomo, J.G. and F. Puertas, Alkali-activated slag mortars: Mechanical strength behaviour. Cement and Concrete Research, 1999. 29(8): p. 1313-1321.

[20] Fernndez-Jimnez, A., Palomo, A., Lpez-Hombrados, C., Engineering properties of alkali activated fly ash concrete. ACI Mater. J., 2006(103 (2)): p. 106-112.

[21] Duxson, P., et al., Understanding the relationship between geopolymer composition, microstructure and mechanical properties. Colloids and Surfaces A: Physicochemical and Engineering Aspects, 2005. 269(13): p. 47-58.

[22] Hakkinen, T., Durability of alkali-activated slag concrete. Nordic. Concr. Res., 1987(6): p. 81-94.

[23] Douglas, E., Bilodeau, A., Malhotra, V. M. , Properties and durability of alkaliactivated slag concrete. ACI Mater. J., 1992. 89((5)): p. 509516.

[24] Puertas, F., Amat, T., Fernndez-Jimnez, A., Vazquez, T., Mechanical and durable behaviour of alkaline cement mortars reinforced with polypropylene fibres. Cem. Concr. Res., 2003(33): p. 20312036.

[25] Fernandez-Jimenez, A., Garcia-Lodeiro, I. and Palomo, A., Durability of alkali activated fly ash cementitious materials. Journal of Material Science, 2007(42): p. 3055-3065.

[26] Allahverdi, A. and Skvara, F., Sulfuric acid attack on hardened paste of geopolymer cements-Part 1. Mechanism of corrosion at relatively high concentrations. Ceramics Silikaty, 2005. 49(4): p. 225.

[27] Fernndez-Jimnez, A., Palomo, A., Pastor, J. Y., Martn, A. , New cementitious materials based on alkali-activated fly ash: performance at high temperature. *Journal of American Ceramic Society*. 2008. 91(10): p. 33083314.

[28] Duxson, P., *et al.*, Geopolymer technology: the current state of the art. *Journal of Materials Science*, 2007. 42(9): p. 2917-2933.

[29] Xu, H., Provis, J. L., van Deventer, J. S. J., Krivenko, P. V., Characterization of aged slag concretes. *ACI Mater. J.*, 2008. 105(2): p. 131-139.

[30] Davidovits, J., Geopolymer Chemistry and Applications, in second ed. Institut Geopolymere2008: 19 Saint-Quentin, France.

[31] Malinowski, R. and Y. Garfinkel, Prehistory of concrete. Concrete International, 1991. 13(3). p. 62-68.

[32] Larew, H.G., *et al.*, Instrumentation of Culvert Pipe Under Deep Fill1975: Virginia Highway & Transportation Research Council.

[33] Palomo, A., Glasser, F. P. , Chemically-bonded cementitious materials based on metakaolin. *Br. Ceram. Trans. J.*, 1992(91): p. 107-112.

[34] Provis, J.L., Lukey, G.C. and J.S.J. van Deventer, Do Geopolymers Actually Contain Nanocrystalline Zeolites? A Reexamination of Existing Results. *Chemistry of Materials*, 2005. 17(12): p. 3075-3085.

[35] Wcng, L., Sagoc-Crentsil, K., Brown, T., Song, S., Effects of aluminates on the formation of geopolymers. Mater. Sci. Eng. B-Solid State Mater. Adv. Technol. , 2005. 117((2)): p. 163168.

[36] Palomo, A., *et al.*, Alkaline Activation of Fly Ashes: NMR Study of the Reaction Products. *Journal of the American Ceramic Society*, 2004. 87(6): p. 1141-1145.

[37] Fernandez-Jimnez, A., *et al.*, The role played by the reactive alumina content in the alkaline activation of fly ashes. Microporous and Mesoporous Materials, 2006. 91(13): p. 111-119.

[38] Duxson, P., Lukey, G. C., Separovic, F., van Deventer, J. S. J. , The effect of alkali cations on aluminum incorporation in geopolymeric gels. Ind. Eng. Chem. Res., 2005. 44 ((4)): p. 832839.

[39] Roy, D.M. and Langton, C.A., Studies of ancient concretes as analogs of cementitious sealing material for repository in Tuff. LA-11527 - MS 1989, Los Alamos National Laboratory.

[40] Degryse, P., Elsen, J. and Waelkens, M. Study of ancient mortars from Sagalassos (Turkey) in view of their conservation. *Cement and Concrete Research*, 2002. 32(9): p. 1457-1463.

[41] Sbordoni-Mora and Mortars, L. Les. cements and Grouts used in the Conservation of Historic Buildings2. in matereaux des enduits traditionnels, Proceedings of the ICCROM Symposium. 1981. Rome.

[42] Lea, F.M., The chemistry of cement, 3rd ed., , 1970: London.

[43] Bogue, R.H. The chemistry of Portland cement. in Reinhold Publication Corp. 1955. New York.

[44] Glukhovsky, V.D. Soil Silicates. in Gostroiizdat Publish 1959. Kiev, USSR.

[45] Contenson, H. and Courtois, L. A propos des vases de chaux. in Recherches sur leur fabrication et leur origine., 1979. Paleorient.

[46] Perinet, G., Contenson, H. and Courtois, L. Etude mineralgique de vaisselles blanches de Ras-Shamra et Tell Ramad (Syrie). in Compte Rendu Acad. Sci. 1980. Paris.

[47] Davidovits, J. and L. Courtois. D. T. A. detection of intra-ceramic geopolymeric setting in archaeological ceramics and mortars. in 21st Symposium on Archaeometry. 1981. New York.

[48] Campbell, D.H. and Folk, R.L. The ancient Egyptian pyramids-concrete or rock Concrete International 1991: p. 29 - 44.

[49] Buchwald, A., Kaps, C. and Hohmann, M. Alkali-activated binders and pozzolan cement binders - compete reaction or two sames of the same story. in Procedings of the 11th International Congress on the Chemistry of Cement (ICC). 2003. Durban, South Africa.

[50] Pinto, A.T., Alkali-activated metakaolin based binders, PhD Thesis, 2004, University of Minho: Portugal.

[51] Davidovits, J., Inorganic polymers and methods of making them, 1982, US Patent 4349386.

[52] Davidovits, J., Geopolymer chemistry and applications 2008.

[53] Taylor, H.F.W., Cement Chemistry, Second Edition1997: Thomas Telford.

[54] Taylor, H.F.W., Proposed Structure for Calcium Silicate Hydrate Gel. *J. Amer. Ceram. SOC.*, 1986(69): p. 464-467.

[55] G., I.R., The nature of the hydration products in hardened cement pastes. *Cem. Concr. Composites*, 2000(22): p. 97-113.

[56] Glasser, F.P., Hong, S. Y., Thermal Treatmnt of C-S-H Gel at 1 Bar Pressure up to 200C. *Cem. Concr. Res.*, 2003. 33, (32): p. 271-279.

[57] Cong, X, Kirkpatrick, R.J. , *Cem. Concr. Res.*, 1995. 25: p. 1237.

[58] Sharara, F.I., Seifer, D. B., and Flaws, J. A. (1998). Fertil. Steril. Shiau, C. Y., Wang, J. D., and Chen, P. C. (2004). Shields, L. M., Wiese, W. H., Skipper, B. J., *et al.* (1994). Placenta 8, 1. Takahashi, Y., Tsuruta, S., Arimoto, M., *et al.*, Handbook on the Toxicology of Metals1998.

[59] Shiau, C.Y., Wang, J. D., Chen, P. C., Occup. Environ. Med, 2004: p. 915-923.

[60] Davidovits, J., Proceedings of 1st International, Conference on Alkaline Cements and Concretes, 131-149, VIPOL Stock Company,, and U. Kiev, (1994). Properties of Geopolymer Cements, Proceedings of 1st International Conference on Alkaline Cements and Concretes. 1994.

[61] Criado, M., Fernamdez-Jimenez, A., Palomo, A., Sobrados, I., Sanz, J. , Effect of the SiO_2/Na_2O ratio on the alkali activation of fly ash. Part 11: 29Si MAS-NMR Survey., Microp. Mesop. Mat., 2007b(109): p. 525-534.

[62] Duxson, P., *et al.*, The role of inorganic polymer technology in the development of green concrete. *Cement and Concrete Research*, 2007. 37(12): p. 1590-1597.

[63] Shi, C., Krivenko, P.V. and Roy, D. Alkali-activated cements and concretes, 2006, Taylor and Francis: London.

[64] Palomo, A., Glasser, F. P., Chemicallybonded cementitious materials based on metakaolin. *Br. Ceram. Trans. J.*, 1992(91): p. 107112.

[65] Fernandez-Jimmez, A., Palomo, A., Sobrados, I., Sanz, J., The role played by the reactive alumina content in the alkaline activation of fly ashes. Microp. Mesop, Muter., 2006a(91): p. 111-119.

[66] Barbosa, V.F.F., Mackenzie, K. J. D., Synthesis and thermal behaviour of potassium silicate geopolymers. Mut. Lett., 2003(57): p. 1477-1482.

[67] Barbosa, V.F.F., MacKenzie, K. J. D. C., Thaumaturgo, C., Synthesis and characterisation of materials based on inorganic polymers of alumina and silica: sodium polysialate polymers. *Inter. J. Inorganic Mut.*, 2000(2): p. 309-317.

[68] Ikeda, K., Preparation of fly ash monoliths consolidated with a sodium silicate binder at ambient temperature. *Cem. Concr. Res.*, 1997(27): p. 657-663.

[69] Fernndez-Jimnez, A. and A. Palomo, Composition and microstructure of alkali activated fly ash binder: Effect of the activator. *Cement and Concrete Research*, 2005. 35(10): p. 1984-1992.

[70] Criado, M., Fernandez-Jimenez, A., Palomo, A., Alkali Activation of fly ash. Effect of the SiO_2/Na_2O ratio. Part I: FTIR study. Microp. Mesop. Mat., 2007a(106): p. 180-191.

[71] Criado, M., Fernandez-Jimenez, G., de laTorreA., G., Aranda M.A., A., Palomo A, An XRD study of the effect of the SiO_2/Na_2O ratio on the alkali activation of fly ash. *Cem. Concr. Res.*, 2007c(37): p. 671-679.

[72] Fernandez-Jimenez, A., , Palomo, A. and Criado, M. , Alkali activated fly ash binders. A comparative study between sodium and potassium activators. *Materiales de Construccidn*, 2006d(56): p. 51-65.

[73] Palomo, A., Fernandez-Jimenez, A., Criado, M., Alonso, M., The alkali activation of fly ashes: from macro to nanoscale, in 2nd International Symposium on Nanotechnology in Construction2005a: Bilbao, Spain.

[74] Palomo, A., Fernandez-Jimenez, Kovalchuk, G., Some key factors affecting the alkali activation of fly ash. in 2nd Inter. Symposium Non-Traditional Cement & Concrete. 2005b. Brno, Czech Republic.

[75] Duxson, P., Mallicoat, S. W., Lukey, G. C., Kriven, W. M. and Van Deventer, J. S. J., The effect of alkali and SilAl ratio on the development of mechanical properties of metakaolin-based geopolymers. Colloids and Surfaces A: Physicochemical and Engineering Aspects, 2007(292): p. 8-20.

[76] Fernandez-Jimenez, A., R., Vallepu, T., Terai, A., Palomo, K., Ikeda (2006b) Synthesis and thermal behaviour of different aluminosilicates. *J. Non-Cryst. Sol*, 2006b(352): p. 2061-2066.

[77] Phair, W., J., Smith, D., J., Van Deventer J.S.J., Characteristics of aluminosilicate hydrogels related to commercial Geopolymers. Material Letters, 2003(57): p. 4356-4367.

[78] Fernandez-Jimenez, A., Palomo, A., Characterization of fly ashes. Potential reactivity as alkaline cements Fuel 2003(82): p. 2259-2265.

[79] Ejaz, T., Jones, A.G., Graham, P., (1999) Solubility of ZeoliteA and its amorphous precursor and J.C.E.D. under synthesis conditions, 44, p. 574- 576.

[80] Patra, A., Ganguli, D., Role of dopant cations in the gelation behaviour of silica sols Bull. *Mater. Sci.*, 1994(17): p. 999-1004.

[81] Silva, P.D., Sagoe-Crenstil, K., Sirivivatnanon, V., Kinetics of geopolymerization: Role of $Al_2O_3SiO_2$. *Cem. Concr. Res.*, 2007(37): p. 512-518.

[82] Sabir, B.B., Wild, S. and Bai, J., Metakaolin and calcined clays as pozzolans for concrete: a review. *Cement and Concrete Composites*, 2001(23): p. 441-454.

[83] Kriven, W. M., Bell, J. L. and Gordon, M. , Microstructure and microchemistry of fully-reacted geopolymers and geopolymer matrix composites. Ceramic Transactions, 2003(153): p. 227-250.

[84] Tsuyuki, N., and Koizumi, Koshiro, Granularity and Surface Structure of Ground Granulated Blast-Furnace Slags, *Journal of the American Ceramic Society*, 1999(82.8): p. 2188-192.

[85] Shimoda, K., Tobu, Y., Kanehashi, K., Nemoto, T. and Saito, K. , Total understanding of the local structures of an amorphous slag: Perspective from multi-nuclear (29Si, 27Al, 170, 25Mg, and 43Ca) solid-state NMR. *Journal of Non-Crystalline Solids*, 2008(354): p. 1036-1043.

[86] Wan, H., Shui, Z. and Lin, Z., Analysis of geometric characteristics of GGBS particles and their influences on cement properties. *Cement and Concrete Research*, 2004(34): p. 133-137.

[87] Wang, F.Z., Trettin, R. and Rudert, V., Effect of fineness and particle size distribution of granulated blast-furnace slag on the hydraulic reactivity in cement systems. Advances in Cement Research, 2005(17): p. 161-166.

[88] Hemmings, R.T, Berry, E. E., On the glass in coal fly ashes: Recent advances. Fly Ash and Coal Conversion By-products: Characterization, Utilization, and Disposal IV, Warrendale, PA, Mccarthy. G. J. (Ed.), 1988: p. 3-38.

[89] Hower, J.C., Rathbone, R. F., Robertson, J. D., Peterson, G. and Trimble, S. , Petrology, mineralogy, and chemistry of magnetically separated sized fly ash. *Fuel,* 1999(78): p. 197-203.

[90] Nugteren, H.W., Coal fly ash: From waste to industrial product. Particle and Particle Systems Characterisation. 2007(24): p. 49-55.

[91] Duxson, P. and Provis, J.L., Designing Precursors for Geopolymer Cements. *Journal of the American Ceramic Society,* 2008. 91(12): p. 3864-3869.

[92] Roy, A., , Schilling, F. J. and Eaton, H. C. , Alkali activated class C fly ash cement. U. S. Patent 5,565,028, 1996.

[93] Perera, D.S., Nicholson, C. L., Blackford, M. G., Fletcher, R. A. and Trautman, R. A., Geopolymers made using New Zealand flyash. *Journal of the Ceramic Society of Japan,* 2004(112): p. S108-S111.

[94] Xu, H., Lukey, G. C. and van Deventer, J. S. J. . The activation of Class C, Class F-fly ash and blast furnace slag using geopolymerisation. Proceedings of 8th CANMETI ACI International Conference on Fly Ash, Silica Fume, Slag and Natural Pozzolans in Concrete, Las Vegas, NV, Malhotra, V. M. (Ed.), 797-819. in Proceedings of 8th CANMETI ACI International Conference on Fly Ash, Silica Fume, Slag and Natural Pozzolans in Concrete, Las Vegas, NV, Malhotra, V. M. (Ed.), 797-819. 2004. Las Vegas, NV: Malhotra, V. M. (Ed.).

[95] Keyte, L.M., Lukey, G. C. and van Deventer, *J. S. J.*. The effect of coal ash glass chemistry on the tailored design of waste-based geopolymeric products. 2005. Albi, France, Nzihou: (Ed.), CD-ROM proceedings.

[96] Chindaprasirt, P., Chareerat, T. and Sirivivatnanon, V. , Workability and strength of coarse high calcium fly ash geopolymer. *Cement and Concrete Composites,* 2007(29): p. 224-229.

[97] Lukey, G.C., Mendis, F. A,, van Deventer, J. S. J. and Sofi, M., Advances in inorganic polymer concrete technology. *Concrete Mix Design,* Quality Control and Speczjication, 3rd Edition. London, Routledge., 2006.

[98] Puertas, F., Martinez-Ramirez, S., Alonso, S. and Vazquez, E. , Alkali-activated fly ash/lslag cement. Strength behaviour and hydration products. *Cement and Concrete Research* 2000(30): p. 625-1632

[99] Goretta, K.C., Chen, N., Gutierrez-Mora, F., Routbort, J. L., Lukey, G. C. and van and J.S.J. Deventer, Solid-particle erosion of a geopolymer containing fly ash and blast-furnace slag. Wear, 2004(256): p. 714-719.

[100] Li, Z., Lui, S., Influence of slag as additive on compressive strength of fly ash-based geopolymer. Journal of Materials in Civil Engineering, 2007(19): p. 470-474.

[101] Weng, L., et al., Effects of aluminates on the formation of geopolymers. Materials Science and Engineering: B, 2005. 117(2): p. 163-168.

[102] Provis, J.L. and van Deventer, J.S.J., Geopolymerisation kinetics. 2. Reaction kinetic modelling. Chemical Engineering Science, 2007. 62(9): p. 2318-2329.

[103] Rees, C.A., , Provis, J. L., Lukey, G. C. and van Deventer, J. S. J. , Geopolymer gel formation with seeded nucleation. Colloids and Surfaces A - Physicochemical and Engineering Aspects, 2008(318): p. 97-105.

[104] van-Jaarsveld, J.G.S.a.v., J. S. J., Effect of the alkali metal activator on the properties of fly ash-based geopolymers. Industrial and Engineering Chemistry Research, 1999(38): p. 3932-3941.

[105] Lee, W.K.W., Van Deventer, J.S.J., Structural reorganisation of class F fly ash in alkaline silicate solutions. Colloids and Surfaces A - Physicochemical and Engineering Aspects, 2002(211): p. 49-66.

[106] de-Jong, B.H.W.S., Brown, G. E., Polymerization of silicate and aluminate tetrahedra in glasses, melts, and aqueous solutions -I. Electronic structure of $H_6Si_2O_7$ $H_6AlSiO_7^{1-}$, and $H_6Al_2O_7^{2-}$. Geochimica et Cosmochimica Acta, 1980(44): p. 491-511.

[107] Hamilton, J.F., Brantley, S. L., Pantano, C. G., Criscenti, L. J. and Kubicki, J. D., Dissolution of nepheline, jadeite and albite glasses: Toward better models for aluminosilicate dissolution. Geochimica et Cosmochimica Acta, 2001(65): p. 3683-3702.

[108] Blum, A.E., Lasaga, A.C., The role of surface speciation in the dissolution of albite. Geochimica et Cosmochimica Acta, 1991(55): p. 2193-2201.

[109] Oelkers, E.H., GGislason, S. R., The mechanism, rates and consequences of basaltic glass dissolution: I. An experimental study of the dissolution rates of basaltic glass as a function of aqueous Al, Si and oxalic acid concentration at 25C and pH = 3 and 11. Geochimica et Cosmochimica Acta, 2001(65): p. 3671-3681.

[110] Stebbins, J.F., Xu, Z. , NMR evidence for excess non-bridging oxygen in an aluminosilicate glass. Nature, 1997(390): p. 60-62.

[111] Lee, S.K., Stebbins, J. F., Disorder and the extent of polymerization in calcium silicate and aluminosilicate glasses: 0-17 NMR results and quantum chemical molecular orbital calculations. Geochimica et Cosmochimica Acta, 2006(70): p. 4275-4286.

[112] Simonson, J.M., Mesmer, R. E. and Rogers, F. S. Z., The enthalpy of dilution and apparent molar heat capacity of NaOH(aq) to 523 K and 40 MPa. *Journal of Chemical Thermodynamics*, 1989(21): p. 561-584.

[113] Pickering, S.U., The hydrates of sodium, potassium and lithium hydroxides. *Journal of the Chemical Society*, Transactions, 1893(63): p. 890-909.

[114] Kurt, C.a.B., J. , Ullmanns Encyclopedia of Industrial Chemistry. Wiley-VCH Verlag, 2006.

[115] Vail, J.G., Soluble Silicates: Their Properties and Uses. New York, Reinhold 1952.

[116] Iler, R.K., The Chemistry of Silica: Solubility, Polymerization, Colloid and Surface Properties, and Biochemistry. New York, Wiley, 1979.

[117] Taylor, H.F.W., Cement Chemistry, ed. U. Academic Press London 1990.

[118] Taylor, H.E.W., Tobermorite, jennite, and cement gel. Zeitschrzfijkr Kristallographie, 1992. 966-974(202): p. 41-50.

[119] Richardson, I.G., Brough, A.R., Brydson, R., Groves, G.W., Dobson, C.M., Location of aluminium in substituted calcium silicate hydrate (C-S-H) gels as determined by 29Si and 27Al NMR and EELS. *J. Am. Ceram. SOC.*7 1993(6): p. 2285-2288.

[120] Richardson, I.G., The nature of the hydration products in hardened cement pastes. *Cem. Concr. Composites*, 2000(22): p. 97-113.

[121] Cong, X., Kirkpatrick, R.J., Effects of the temperature and relative humidity on the structure of C-S-H gel. *Cem. Concr. Research*, 1995(25): p. 1237-1245.

[122] Sharara, A.M., El-Didamony, H., Ebied, E., Abd, El-Aleem, Hydration characteristics of p-C2S in the presence of some pozzolanic materials. *Cem. Concr. Research*, 1994(24): p. 966-974.

[123] Chen, J.J., Thomas, J.J., Taylor, H.F.W., Jennings, H.M., Solubility and structure of calcium silicate hydrate. *Cem. Concr. Res.*, 2004(34): p. 1499-1519.

[124] Davidovits, J. Properties of Geopolymer Cements. in Proceedings of 1st International Conference on Alkaline Cements and Concretes. 1994. VIPOL Stock Company, Kiev, Ukraine

[125] Palomo, A., Alonso, S., Fernandez-Jimenez, A., Sobrados, I., Sanz, J., Alkali activated of fly ashes. A NMR study of the reaction products. *J. Am. Ceramic. SOC.*, 2004a(87): p. 1141-1145.

[126] Duxson, P., Fernandez-Jimenez, A., Provis, J.L., Lukey, G.C., Palomo, A. Van-Deventer, J.S.J., Geopolymer technology: the current state of the art. *J. Mat. Sci.*, 2007a. (9)(42): p. 2917-2933.

[127] Fernandez-Jimenez, A., Vallepu, R., Terai, T., Palomo, A,, Ikeda, K., Synthesis and thermal behaviour of different aluminosilicates. *J. Non-Cryst. Sol.*, 2006b(352): p. 2061-2066.

[128] Taylor, H.F.W., Delayed Ettringite Formation, in Advances in Cement and Concrete (M.W. Gruzzek & S.L. Sarkar, Eds.). *American Society of Civil Engineers*, 1994. (194)(40): p. 61-78

[129] Taylor, H.F. W., Some chemical and microstructural aspects of, i.K.L.S. concrete durability, J.F. Young (Eds), Mechanisms of Chemical, and E.a.F.S. Degradation of Cement-Based Systems, London, 177-184., Some chemical and microstructural aspects of concrete durability, in: K.L. Scrivener, J.F. Young (Eds). Mechanisms of Chemical Degradation of Cement-Based Systems, E. and FN Spon, London, 1997(177-184).

[130] Neville, A.M., Properties of Concrete 1995, Longman, Essex.

[131] Palomo, A., Blanco-Valera, M.T., Granizo, M.L., Puertas, F., Vazquez, T., and Grutzeck, and M. W., Chemical stability of cementitious materials based on metakaolin. *Cem. Concr. Res.*, 1999b(29): p. 997-1004.

[132] Bakharev, T., Durability of geopolymer materials in sodium and magnesium sulfate solutions. *Cem. Concr. Res.*, 2005a(35): p. 1233-1246.

[133] Fernandez-Jimenez, A., Garca-Lodeiro, I., and Palomo, A., Durability of alkali-activated fly ash cementitious materials. *Journal of Materials Science*, 2007. 42(9): p. 3055-3065.

[134] Engelhardt, G., and Michel, D., High-Resolution Solid-state NMR of Silicates and Zeolites. John Wiley and Sons, 1987.

[135] Klinowski, J., Nuclear magnetic resonance studies of zeolites. Progress in NMR Spectroscopy, 1984(16, (3-4)): p. 237-309.

[136] Li, K. L., Huang, G. H., Chen, J., Wang, D. andTang, X.-S. Early Mechanical Propertyand Durability of Geopolymer. in Geopolymer 2005, Proceedings. 2005.

[137] Diamond, S., A review of alkali-silica reaction and expansion mechanisms 1. Alkalies in cements and in concrete pore solutions. *Cement and Concrete Research*, 1975. 5(4): p. 329-345.

[138] Kupwade-Patil, K. and Allouche, E., Impact of Alkali Silica Reaction on Fly Ash Based Geopolymer Concrete. *Journal of Materials in Civil Engineering*, 2012.

[139] Gourley, G., Johnson, G.B. Developments in geopolymer precast concrete World Congress Geopolymer 2005. in Green chemistry and sustainable development solution. 2005. France.

[140] Garcia-Lodeiro, I., Palomo, A., and Fernandez-Jimenez, A., The alkali-aggregate reactions in alkali activated fly ash mortars. *Cem. Concr. Res.*, 2007(37, (2)): p. 175-183.

[141] Palomo, A., Alonso, S., Fernandez-Jimnez, A., Sobrados, I., Sanz, J., Alkaline activation of fly ashes. A 29Si NMR study of the reaction products. *J. Am. Ceram. Soc.*, 2004. 87((6)): p. 11411145.

[142] Virmani, Y. P., Clemena, G.G., Corrosion Protection: Concrete Bridges. Report No. FHWA-RD-98-088, 1998, Federal Highway Administration. Washington: Washington, DC.

[143] Miranda, J.M., Fernandez-Jimenez, A., Gonzalez, J.A., Palomo, A., Corrosion resistance in activated fly-ash mortars. *Cem. Concr. Res.*, 2005(35): p. 1210-1217.

[144] Bastidas, D.M., Fernandez-Jimenez, A., Palomo, A., Gonzalez, J.A., A study on the passive state stability of steel embedded in activated fly ash mortars. *Corrosion Science*, (50(4)): p. 1058-1065.

[145] Page, C.L., Treadaway, K. W.J. and Bamforth, P.B., (eds) Corrosion of Reinforcement in Concrete. Society of Chemical Industry, published by Elsevier Applied Science, London, 1990.

[146] Slater, J.E., Corrosion of Metals in Association with Concrete, 1983, ASTM STP 818: Philadelphia, PA.

[147] Kovalchuk, G., Palomo, A., and Fernandez-Jimenez, A., Alkali activated fly ashes. Effect of thermal curing conditions on mechanical and microstructural development - Part 11. *Fuel*, 2007(86): p. 315-322.

[148] Criado, M., Fernandez-Jimenez, A., and Palomo, A., Alkali activation of fly ashes. Part 1: Effect of curing conditions on the carbonation of the reaction products. *Fuel*, 2005(84): p. 2048-2054.

[149] Yodmunee, S., Yodsudjai, W. Study on corrosion of steel bar in fly ash-based geopolymer concrete. in International conference on Pozzolan, *Concrete and Geopolymer*. 2006. Khon Kaen, Thailand.

[150] Koch, Gerhardus H., Brongers, Michiel P.H., & Thompson, Neil G., Corrosion Costs and Preventive Strategies in the United States. NACE International, Publication No. FHWA-RD-01-156, Houston, Texas, USA (2002)

[151] Parande, A.K., Ramsamy, P. L., Ethirajan, S., Rao, C. R., & Palanisamy, N. (2006). Deterioration of reinforced concrete in sewer environments. Proc. Inst. Civ. Eng.-Municipal Eng., , 159, pp. 11-20., Deterioration of reinforced concrete in sewer environments. Proc. Inst. Civ. Eng.-Municipal Eng, 2006(159): p. 11 - 20.

[152] Parker, C.D., The function of Thiobacillus concretivorus (nov. spec.) in the corrosion of concrete exposed to atmospheres containing hydrogen sulphide. *Australian Journal of Experimental Biology and Medical Sciences*, 23, 1945(23): p. 91 - 98.

[153] Thokchom, S., Ghosh, P., & Ghosh, S. , Resistance of fly ash based geopolymer mortars in sulfuric acid. *ARPN Journal of Engineering and Applied Sciences*, 2009. 4(1): p. 65 - 70.

[154] Song, X. J., Marosszeky, M., Brungs, M., & Munn, R., Durability of fly ash based geopolymer concrete against sulphuric acid attack. DBMC International Conference on Durability of Building Materials and Components, Lyon, France (2005)17 - 20

[155] Broomfield, J.P., Corrosion of Steel in Concrete: Understanding, Investigation And Repair 2007: Taylor & Francis.

[156] Poursaee, A. and Hansson, C.M., Potential pitfalls in assessing chloride-induced corrosion of steel in concrete. *Cement and Concrete Research*, 2009. 39(5): p. 391-400.

[157] Soleymani, H.R. and Ismail, M.E., Comparing corrosion measurement methods to assess the corrosion activity of laboratory OPC and HPC concrete specimens. *Cement and Concrete Research*, 2004. 34(11): p. 2037-2044.

[158] Kupwade-Patil, K. and Allouche, E., Examination of Chloride Induced Corrosion in Reinforced Geopolymer Concretes. *Journal of Materials in Civil Engineering*.

[159] Kupwade-Patil, K. and Allouche, E., Impact of Alkali Silica Reaction on Fly Ash-Based Geopolymer Concrete. *Journal of Materials in Civil Engineering*, 2013. 25(1): p. 131-139.

[160] Kupwade-Patil, K., *et al.*, Corrosion analysis of reinforced geopolymer concretes, in Concrete Solutions 20112011, CRC Press.25(10), p. 14651476, 2013

[161] Bernal, S.A., R. Meja de Gutirrez, and J.L. Provis, Engineering and durability properties of concretes based on alkali-activated granulated blast furnace slag/metakaolin blends. *Construction and Building Materials*, 2012. 33(0): p. 99-108.

[162] Bernal, S.A., *et al.*, Accelerated carbonation testing of alkali-activated binders significantly underestimates service life: The role of pore solution chemistry. *Cement and Concrete Research*, 2012. 42(10): p. 1317-1326.

[163] Bernal, S.A., *et al.*, Gel nanostructure in alkali-activated binders based on slag and fly ash, and effects of accelerated carbonation. *Cement and Concrete Research*, 2013. 53(0): p. 127-144.

[164] Garcia-Lodeiro, I., *et al.*, Compatibility studies between N-A-S-H and C-A-S-H gels. Study in the ternary diagram Na2OCaOAl2O3SiO2H2O. *Cement and Concrete Research*, 2011. 41(9): p. 923-931.

[165] Aligizaki, K., Pore Structure of Cement-Based Materials: Testing Interpretation and Requirements 2005: Taylor & Francis.

[166] Skalny, J. and F. Young, Materials science of concrete 2005: *American Ceramic Society*.

[167] Bernal, S.A., *et al.*, Effect of silicate modulus and metakaolin incorporation on the carbonation of alkali silicate-activated slags. *Cement and Concrete Research*, 2010. 40(6): p. 898-907.

[168] Hajimohammadi, A., J.L. Provis, and J.S.J. van Deventer, Time-resolved and spatially-resolved infrared spectroscopic observation of seeded nucleation controlling geopolymer gel formation. *Journal of Colloid and Interface Science*, 2011. 357(2): p. 384-392.

[169] Duxson, P., *et al.*, 29Si NMR Study of Structural Ordering in Aluminosilicate Geopolymer Gels. Langmuir, 2005. 21(7): p. 3028-3036.

[170] Shi, C., Fanandez-Jimenez, A., and Palomo, A., New cements for the 21st century: The pursuit of an alternative to Portland cement. *Cement and Concrete Research*, 2011. 41(7): p. 750-763.

[171] Fernandez-Jimenez, A., *et al.*, Quantitative determination of phases in the alkali activation of fly ash. Part I. Potential ash reactivity. *Fuel*, 2006. 85(56): p. 625-634.

[172] Kovalchuk, G., Fanandez-Jimenez, A., and Palomo, A., Alkali-activated fly ash: Effect of thermal curing conditions on mechanical and microstructural development Part II. *Fuel*, 2007. 86(3): p. 315-322.

[173] Rickard, W.D.A., Temuujin, J. and van Riessen, A., Thermal analysis of geopolymer pastes synthesised from five fly ashes of variable composition. *Journal of Non-Crystalline Solids*, 2012. 358(15): p. 1830-1839.

[174] Temuujin, J., *et al.*, Preparation and thermal properties of fire resistant metakaolin-based geopolymer-type coatings. *Journal of Non-Crystalline Solids*, 2011. 357(5): p. 1399-1404.

[175] Hobbs, D. W., Concrete deterioration: causes, diagnosis, and minimising risk. International Materials Reviews. 2001, 46(3):117-44.

[176] Juenger, M. C. G., Winnefeld, F., Provis, J.L., Ideker, J. H.. Advances in alternative cementitious binders. *Cement and Concrete Research*. 2011, 41(12):1232-43.

[177] Glasser, F. P., Marchand, J., Samson. E., Durability of concrete Degradation phenomena involving detrimental chemical reactions. *Cement and Concrete Research*. 2008, 38(2):226-46.

[178] Zhang, L., Glasser, F. P., Investigation of the microstructure and carbonation of CSA-based concretes removed from service. *Cement and Concrete Research*. 2005, 35(12):2252-60.

[179] Haque, M. N., Al-Khaiat, H., Carbonation of concrete structures in hot dry coastal regions. *Cement and Concrete Composites*. 1997, 19(2):123-9.

[180] Torgal, F., Miraldo, P. S., Labrincha, J. A., De Brito, J., An overview on concrete carbonation in the context of eco-efficient construction: Evaluation, use of SCMs and/or RAC. *Construction and Building Materials*. 2012, 36(0):141-50.

[181] Villain, G., Thiery, M., Platret, G., Measurement methods of carbonation profiles in concrete: Thermogravimetry, chemical analysis and gammadensimetry. *Cement and Concrete Research*. 2007, 37(8):1182-92.

[182] Bernal, S. A., de Gutierrez, R. M., Provis, J. L., Rose, V., Effect of silicate modulus and metakaolin incorporation on the carbonation of alkali silicate-activated slags. *Cement and Concrete Research*. 2010, 40(6):898-907.

[183] Bernal, S. A., Meja de Gutirrez, R., Provis, J. L., Engineering and durability properties of concretes based on alkali-activated granulated blast furnace slag/metakaolin blends. *Construction and Building Materials.* 2012, 33(0):99-108.

[184] Bernal, S. A., Provis, J. L., Brice, D. G., Kilcullen, A., Duxson, P., van Deventer, J. S. J., Accelerated carbonation testing of alkali-activated binders significantly underestimates service life: The role of pore solution chemistry. *Cement and Concrete Research.* 2012, 42(10):1317-26.

[185] Bernal, S. A., Provis, J. L., Walkley, B., San Nicolas, R., Gehman, J. D., Brice, D. G., *et al.* Gel nanostructure in alkali-activated binders based on slag and fly ash, and effects of accelerated carbonation. *Cement and Concrete Research.* 2013, 53(0):127-44.

[186] Davidovits, J., Geopolymer Chemistry and Applications: Institut Gopolymre; 2011.

[187] Provis, J. L., Van Deventer, J. S. J., Geopolymers: Structure, Processing, Properties and Industrial Applications: Woodhead Publishing Limited; 2009.

[188] Kupwade-Patil, K., Soto, F., Kunjumon, A., Allouche, E. N., Mainardi, D. S., Multi-scale modeling and experimental investigations of geopolymeric gels at elevated temperatures. Computers & Structures. 2013, 122(0):164-77.

[189] Juenger, M. C. G., Winnefeld, F., Provis, J. L., Ideker, J. H., Advances in alternative cementitious binders, *Cement and Concrete Research*, 41 (2011) 1232-1243.

[190] Rashad, A. M., Bai, Y., Basheer, P. A. M., Collier, N. C., Milestone, N. B., Chemical and mechanical stability of sodium sulfate activated slag after exposure to elevated temperature, *Cement and Concrete Research*, 42 (2012) 333-343.

[191] Khaliq, W., Kodur, V., Behavior of high strength fly ash concrete columns under fire conditions, Materials and Structures/Materiaux et Constructions, 46 (2013) 857-867.

[192] Khaliq, W., Kodur, V., Effect of high temperature on tensile strength of different types of high-strength concrete, *ACI Materials Journal*, 108 (2011) 394-402.

[193] DeJong, M. J., Ulm, F-J., The nanogranular behavior of C-S-H at elevated temperatures (up to 700 °C), *Cement and Concrete Research*, 37 (2007) 1-12.

[194] Fernandez-Jimnez, A., Pastor, J. Y., Martn, A., Palomo, A., High-Temperature Resistance in Alkali-Activated Cement, *Journal of the American Ceramic Society*, 93 (2010) 3411-3417.

[195] Bakharev, T., Sanjayan, J.G., Cheng, Y.B., Effect of elevated temperature curing on properties of alkali-activated slag concrete, *Cement and Concrete Research*, 29 (1999) 1619-1625.

[196] Davidovits, J., Geopolymer Chemistry and Applications, Institut Gopolymre, 2011.

[197] Provis, J., L., Van Deventer, J.S.J., Geopolymers: Structure, Processing, Properties and Industrial Applications, Woodhead Publishing Limited, 2009.

[198] Duxson, P., Provis, J. L., Lukey, G.C., van Deventer, J.S.J., The role of inorganic polymer technology in the development of green concrete, *Cement and Concrete Research*, 37 (2007) 1590-1597.

[199] Duxson, P., Fernndez-Jimnez, A., Provis, J., Lukey, G., Palomo, A., van Deventer, J., Geopolymer technology: the current state of the art, *Journal of Materials Science*, 42 (2007) 2917-2933.

[200] Diaz-Loya, E. I., Allouche, E. N., Vaidya, S., Mechanical properties of fly-ash-based geopolymer concrete, *ACI Materials Journal*, 108 (2011) 300-306.

[201] Shi, C., Jimnez, A.F., Palomo, A., New cements for the 21st century: The pursuit of an alternative to Portland cement, *Cement and Concrete Research*, 41 (2011) 750-763.